VOLUME 49, NUMBER 1, MARCH 2026

HADRONIC JOURNAL Volume 49, Number 1, March 2026

HADRONIC JOURNAL

Founded in 1978 by Prof. R. M. Santilli at Harvard University. Some of the past Editors include Professors S. L. Adler, A. 0. Barut, L. C. Biedenharn, N. N. Bogoliubov, M. Froissart, J.Lohmus, S. Okubo, Nobel Laureate Ilya Prigogine, M. L. Tomber, J. P.Vigier, J. Wess, Nobel Laureate Chen Ning Yang.

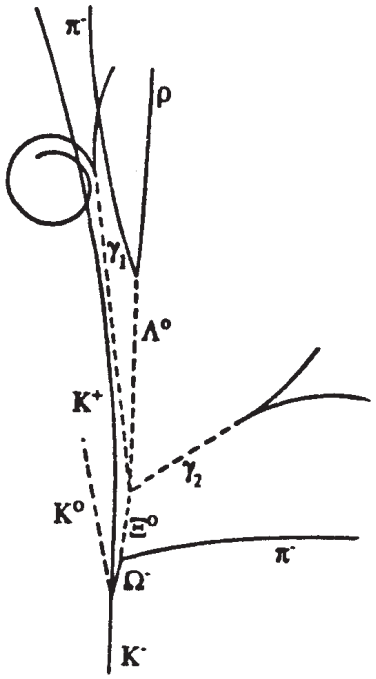

EDITORIAL BOARD

A.O.ANIMALU
A. K. ARINGAZIN
A. A. BHALEKAR
S. J. DHOBLE
J. DUNNING-DAVIES
T. L. GILL
L. P. HORWITZ
S. L. KALLA
S. I. KRUGLOV
J. LISSNER
M. NISHIOKA
R. F. O'CONNELL
Z. OZIEWICZ*
E. RECAMI*
M. SALEEM
S. SILVESTROV
H. M. SRIVASTAVA
E. TRELL
R.I. TSONCHEV
QI-REN ZHANG
C.A.WOLF
YI-ZHONG ZHUO

*In memoriam

FOUNDER and Editor In Chief
R. M. SANTILLI

HADRONIC PRESS, INC.

HADRONIC JOURNAL

Established in 1978 by Prof. R. M. Santilli at Harvard University Hadronic Journal and Algebras, Groups and Geometries have been regularly published since 1978 without publication charges and are among the few remaining independent refereed journals.

This Journal publishes advances research papers and Ph. D. theses in any field of mathematics without publication charges.

For subscription, format and any other information please visit the website
http://www.hadronicpress.com

HADRONIC PRESS INC.
35246 U. S. 19 North Suite 215
Palm Harbor, FL 34684, U.S.A.
http://www.hadronicpress.com
Email: info@hadronicpress.com
Phone: +1-727-946-0427

HADRONIC JOURNAL

Founder and Editor in Chief
RUGGERO MARIA SANTILLI
The Institute for Basic Research
35246 U. S. 19 North Suite 215, Palm Harbor, FL 34684, U.S.A.
Email: resarch@i-b-r.org; TEL: +1-727-688-3992

A. O. ANIMALU, University of Nigeria, Department of Physics, Nsukka, Nigeria animalu@nmc.edu.ng
A.K. ARINGAZIN, Department of Theoretical Physics, Institute for Basic Research Eurasian National University Astana 010008, Kazakhstan aringazin@mail.kz
A.A. BHALEKAR, Department of Chemistry, R.T.M. Nagpur University, Nagpur, 440033 India anabha@hotmail.com
S.J. DHOBLE, Department of Physics R.T.M. Nagpur University Nagpur, 440033 India sjdhoble@rediffmail.com
J. DUNNING-DAVIES, Department of Physics (Retired) University of Hull Hull, HU6 7RX England j.dunning-davies@hull.ac.uk
T. L. GILL, Howard University Research Center ComSERC Washington, DC 20059, USA tgill@howard.edu
L. P. HORWITZ, Department of Physics Tel Aviv Univ., Ramat Aviv, Israel horwitz@taunivm.tau.ac.il
S.L. KALLA, Department of Mathematics Vyas Institute of Higher Education Jodhpur, 342008, India shyamkalla@gmail.com
S.I. KRUGLOV, University of Toronto at Scarborough, Physical and Environmental Sciences Dept., 1265 Military Trail, Toronto, Ontario, Canada M1C 1A4 skrouglo@utm.utoronto.ca
J. LISSNER, Alumnus Foukzon Laboratory Center for Mathematical Sciences Technion-Israel Institute of Technology Haifa, 3200003, Israel
M. NISHIOKA, Yamaguchi University Department of Physics, Yamaguchi 753, Japan
R. F. O'CONNELL, Louisiana State University Department of Physics, Baton Rouge, LA 70803
Z.OZIEWICZ,* Universidad National Autonoma de Mexico, Faculdad de Estudios Superiores C.P. 54714, Cuautitlan Izcalli Aparto Postal # 25, Mexico **** In memoriam***
E. RECAMI, Universita' de Bergamo, Facolta' di Ingeneria, Viale Marconi 5, 1-24044 Dalmine (BG) Italy **** In memoriam***
M. SALEEM, University of the Punjab Center for High Energy Phys., Lahore, Pakistan dms@lhr.paknet.com.pk
S. SILVESTROV, School of Education, Culture and Communication (UKK) Malardalen University Box 883, 71610 Västerås, Sweden sergei.silvestrov@mdh.se
H. M. SRIVASTAVA, Department of Mathematics and Statistics, University of Victoria, Victoria, B. C. V8W 3P4, Canada, hmsri@uvvm.uvic.ca
E. TRELL, Faculty of Health Sciences, University of Linkoping, Se-581 83, Linkoping, Sweden erik.trell@gmail.com
R.I. TSONCHEV, Facultad de Fisica, Universidad Autonoma de Zacatecas, P. O. C-580, Zacatecas 98068, zac, Mexico rumen@ahobon.reduaz.ms
QI-REN ZHANG, Peking University, Department of Technical Phys., Beijing 100871, China zhangqr@sun.ihep.ac.cn
C.A. WOLF, Department of Physics, Massachusetts College of Liberal Arts, North Adams, Ma 01247 cwolf@mcla.mass.edu
YI-ZHONG ZHUO, Institute of Atomic Energy P.O. Box 275 (18) Beijing 102413, China zhuoyz@mipsa.ciae.ac.cn

HADRONIC JOURNAL

VOLUME 49, NUMBER 1, MARCH 2026

THE QUANTUM THEORY OF THE PSEUDOSCALAR MESON,1
Simon Davis
Research Foundation of Southern California
8861 Villa La Jolla Drive #13595
La Jolla, CA 92039

NEW PERSPECTIVES AS REGARDS THE BLACK HOLE INFORMATION AND FIREWALL PARADOXES IN A THREE-DIMENSIONAL DYNAMICAL QUANTUM VACUUM, 27
Davide Fiscaletti
SpaceLife Institute – Via Roncaglia 35 - 61047
San Lorenzo in Campo (PU), Italy

PREDICTED STABILITY OF Z=119 SYSTEMS, 65
J. J. Bevelacqua
Bevelacqua Resources
7531 Flint Crossing Circle SE
Owens Cross Roads, AL 35763

SOLUTION TO THE FINE STRUCTURE CONSTANT 137.036, 77
Francis V. Fernandes
Independent Researcher
137 Bethany, Kodaikanal, TN, India

ON A LOGARITHMIC NONLINEAR SCHRÖDINGER EQUATION COMPATIBLE WITH HADRONIC MECHANICS AND ITS CONNECTION WITH OTHER APPROACHES FOR THE DESCRIPTION OF DISSIPATIVE SYSTEMS, 95
Dieter Schuch
Institut für Theoretische Physik, J. W. Goethe-Univeristät
Robert-Mayer-Str. 8-10, D-60054 Frankfurt am Main, Germany
and Istituto per la Ricerca di Base, Castello Principe Pignatelli
I-86075 Monteroduni (IS), Molise, Italy

EXPERIMENTAL VERIFICATION OF SANTILLI'S CLEAN, SUBNUCLEAR, HADRONIC ENERGY, 113
N. F. Tsagas, A. Mystakidis, G. Bakos, L. Seftelis, D. Koukoulis and S. Trassanidis
Laboratory of Nuclear Technology, Department of Electrical Engineering
Democritus University of Thrace, GR-67100 Xanthi, Greece

HADRONIC JOURNAL 49, 1 - 25 (2026)
DOI 10.29083/HJ.49.01.2026/SCl

THE QUANTUM THEORY OF THE PSEUDOSCALAR MESON

Simon Davis
Research Foundation of Southern California
8861 Villa La Joli.a Drive #13595
La Jolla, CA 92039
sbdavis@resfdnsca.org

Received October 17, 2025
Revised January 14, 2026

Abstract

The quantum theory of a generalized theory of psuedoscalar mesons is studied. Renormalizability is demonstrated by cancelling the divergences in the momentum regulator Λ through renormalization of the coupling and the mass. The quantum corrections to the pseudoscalar mass are computed by adding the finite parts of the two-point fermion loop amplitudes. It is established that the quantum corrected mass m_q, equal to $m_{\eta'}$, can be generated from a classical mass $m = m_\eta$ for a specific value of the coupling.

Keywords: *semiclassical scales, generalized action, mass renormalization, eta prime meson, pseudoscalar meson coupling*

PACS: 12.38.Bx, 12.39.Fe, 12.39.Mk, 12.40.Yx

Copyright © 2026 by Hadronic Press, Inc., Palm Harbor, FL 34684, USA

1 Introduction

The common occurrence of couplings of pseudoscalar mesons to quarks is represented by terms such as $g\bar{\psi}i\gamma^5\phi\psi$. The action may be modified at semiclassical scales, however, as a result of the generalization of the equations for the spin-0 and spin-$\frac{1}{2}$ fields when the energy and momentum operators include another term for a real component of the canonical commutation relations. Since the new free field equations derived from the relativistic relation between energy and momentum are known under these conditions, the alteration to the kinetic terms can be given. The renormalizability of this theory will be studied with a momentum space propagator resulting from the modification of the field equations derived from the relativistic energy conservation rule.

It shall be demonstrated that there is an alternative physical interpretation of diagrams in the pseudoscalar theory. The integrals representing the diagrams are identical to those for the scalar Yukawa term except for the occurrence of the γ_5 matrix. It can be moved through the integrand until it has a similar form to the scalar theory. The only differences are a reversal of the sign of the momentum in the fermion propagator and a change of the chirality.

The superficial degree of divergence of the two-point pseudoscalar amplitude is 2 at all orders in perturbation theory. This infinity can be cancelled by a renormalization of the coupling g. The non-Lorentz invariant propagator and the difference between the limits of the energy and momentum integrals does not affect the power counting in the diagrammatic expansion of the scattering matrix. These features of the calculation do tend to introduce new functional dependences at lower orders in momentum cut-off Λ. There is a logarithmic subleading dependence on Λ in the

two-point amplitude, which can be absorbed into a renormalization of the pseudoscalar mass m_1. The self-energy graphs all have linear divergences that can be removed through a renormalization of the fermion mass m_2.

The finite quantum corrections to the pseudoscalar mass are evaluated by summing over the fermion loop diagrams with two pseudoscalar external lines. The number of diagrams of this type at n^{th} order in the perturbation series is known, and, when the amplitudes have magnitudes that are approximately equal, the correction can be computed. The mass m_1 can be set equal to the η meson mass. Then, the quantum corrected mass m_{1q} can be compared to the η' mass. An equality between m_{1q} and $m_{\eta'}$ is valid for a phenomenologically realistic value of the coupling in the pseudoscalar meson theory.

2 The Perturbative Diagrams of the Pseudoscalar Meson Theory

The Lagrangian of the Lorentz invariant pseudoscalar meson theory is

$$L = \frac{1}{2}(\partial^\mu \phi)(\partial_\mu \phi) + \frac{1}{2}m_1^2\phi^2 + i\bar{\psi}(i\partial\!\!\!/ - m_2)\psi + ig\bar{\psi}\gamma_5\psi\phi. \tag{1}$$

At semiclassical scales, when a real component of the canonical commutation relations of the position and momenta may occur, a generalization of the Hermitian operators

$$\tilde{p}_i = \kappa_0\gamma^i\frac{\partial}{\partial x^2} - i\hbar\frac{\partial}{\partial x^i}$$
$$\tilde{E} = \kappa_0\gamma_5\frac{\partial}{\partial t} - i\hbar\frac{\partial}{\partial t}. \tag{2}$$

Tracing the relativistic formula for the energy, the wave equation of a free scalar field φ is

$$-3\frac{\partial^2\phi}{\partial t^2} - 5\sum_i \frac{\partial^2\varphi}{\partial x_i^2} + m^2\varphi = 0. \tag{3}$$

after setting $\kappa_0 = \hbar = 1$, and the momentum-space propagator is

$$i\Delta_F(E,\vec{p}) = \frac{15i}{5E^2 + 3|\vec{p}|^2 + 15m^2}. \tag{4}$$

Similarly, the new equation of the free spin-$\frac{1}{2}$ field is

$$(\sqrt{3}\gamma^0\partial_0 - \sqrt{5}i\gamma^i\partial_i - m)\psi = 0. \tag{5}$$

and the fermion propagator is generalized to

$$iS_{\alpha\beta}(E.\vec{p}) = \frac{5i\left(-\kappa_0\gamma_5 + i\hbar\mathbb{I}\right)(\gamma\cdot p + m))_{\alpha\beta}}{5E^2 + 3|\vec{p}|^2 + 14m^2}. \tag{6}$$

The pseudoscalar meson action then would be

(7)

$$S_{semiclassical} = \int d^4x \left[\frac{1}{2}\left(\frac{\partial\phi}{\partial t}\right)^2 + \frac{5}{6}\sum_i\left(\frac{\partial\phi}{\partial x_i}\right)^2 + \frac{1}{6}m_1^2\phi^2 + \sqrt{3}\bar{\psi}\left(\gamma^0\partial_0 - \sqrt{5}i\gamma^i\partial_i - m_2\right)\psi + ig\bar{\psi}\gamma_5\psi\phi\right].$$

Given that there is an interaction term $g\bar{\psi}i\gamma_5\psi\phi$, the diagram at first order in perturbation theory with two vertices and one fermion loop may be evaluated. There are two such amplitudes, related by reflecting the internal fermion lines about the central axis of the diagram. It is necessary to multiply by this factor of 2 and -1, required for a fermion loop, to evaluate the entire two-point pseudoscalar amplitude at this order

(8)

$$I_1(p) =$$

$$-2g^2 \int \frac{d^4k}{(2\pi)^4} Tr \left[\frac{5i(-\kappa_0\gamma_5 + i\hbar\mathbb{I})(\gamma\cdot k + m_2)i\gamma_5 \; 5i(-\kappa_0\gamma_5 + i\hbar\mathbb{I})(\gamma\cdot(p-k)+m_2)i\gamma_5}{5E_k^2 + 3|\vec{k}|^2 + 15m_2^2 \qquad 5E_{p-k}^2 + 3|\vec{p}-\vec{k}|^2 + 15m_2^2} \right]$$

$$\delta(p_i - p_f)$$

$$= -50g^2 \int \frac{d^4k}{(2\pi)^4} Tr \left[\frac{(-\kappa_0\gamma_5 + i\hbar\mathbb{I})(\gamma\cdot k + m)\gamma_5 \; (-\kappa_0\gamma_5 + i\hbar\mathbb{I})(\gamma\cdot(p-k)+m)\gamma_5}{5E_k^2 + 3|\vec{k}|^2 + 15m_2^2 \qquad 5E_{p-k}^2 + 3|\vec{p}-\vec{k}|^2 + 15m_2^2} \right]$$

$$\delta(p_i - p_f).$$

The number of powers in the numerator is four and the number in the denominator is two. Therefore, the amplitude is quadratically divergent. Since the momentum space propagators have the same dimension in this field theory, the renormalization procedure would be similar.

The γ_5 factors occur four times in the integral. The second γ_5 matrix from the interaction term can be moved to the beginning of the product until it multiplies the $(-\kappa_0\gamma_5 + i\hbar\mathbb{I})$ matrix by a cyclic permutation. The momentum will be reversed in the propagator, while the product of the matrices is $(-\kappa_0\gamma_5 + i\hbar\mathbb{I})i\gamma_5 = -i\kappa_0 I - \hbar\gamma_5$ which equals $-i\mathbb{I} - \gamma_5$ in units with κ_0 and $\hbar$ equated to one. It follows that, if κ_0 is set equal to $\hbar$ and the fermions have one chirality in the pseudoscalar theory, the diagrams could be evaluated identically to that of the scalar model with the fermions having the opposite chirality. Then

(9) $$Tr\ [(-\gamma_5 + i\mathbb{I})\,(\gamma\cdot k + m_2)\gamma_5\,(-\gamma_5 + i\mathbb{I})\,(\gamma\cdot(p-k)+m_2)\gamma_5]$$

$$= Tr\ [(-\mathbb{I} + i\gamma_5)\,(\gamma\cdot k + m_2)\,(-\mathbb{I} + i\gamma_5)\,(\gamma\cdot(p-k)+m_2)]$$

$$= 2\,Tr\ ((\gamma\cdot k)(\gamma\cdot(p-k))) = 8k\cdot(p-k)$$

and the amplitude is

(10)

$$-\frac{5^2g^2}{2^2\pi^4}\int dE_k|\vec{k}|^2d|\vec{k}|\int_0^{2\pi}d\phi$$

$$\int_0^{\pi}d\theta\ sin\ \theta\frac{4(E_kE_{p-k}-|\vec{k}||\vec{p}|cos\ \theta+|\vec{k}|^2)}{(5E_k^2+3|\vec{k}|^2+15m_2^2)(5E_{p-k}^2+3(|\vec{k}|^2+|\vec{p}|^2-2|\vec{k}||\vec{p}|cos\ \theta))}$$

$$=-\frac{5^2g^2}{2\pi^3}\int dE_k|\vec{k}|^2d|\vec{k}|$$

$$\int_{-1}^{1}d(cos\ \theta)\frac{4(E_kE_{p-k}+|\vec{k}|^2)-4|\vec{k}||\vec{p}|cos\ \theta}{(5E_k^2+3|\vec{k}|^2+15m_2^2)[5E_{p-k}^2+3(|\vec{k}|^2+|\vec{p}|^2)+15m_2^2-6|\vec{k}||\vec{p}|cos\ \theta]}$$

Since

$$\int dx\ \frac{a_1+b_1x}{a_2+b_2x}=\frac{b_1}{b_2}x+\frac{1}{b_2}\left(a_1-\frac{b_1}{b_2}a_2\right)ln(a_2+b_2x), \tag{11}$$

(12)

$$\int_{-1}^{1}d(cos\ \theta)\frac{[4(E_kE_{p-k}+|\vec{k}|^2)]-4|\vec{k}||\vec{p}|cos\ \theta}{(5E_k^2+3|\vec{k}|^2+15m_2^2)[5E_{p-k}^2+3(|\vec{k}|^2+|\vec{p}|^2+15m_2^2-6|\vec{k}||\vec{p}|cos\ \theta]}$$

$$=\frac{1}{5E_k^2+3|\vec{k}|^2+15m_2^2}\left[\frac{4}{3}-\frac{1}{6|\vec{k}||\vec{p}|}\left(4(E_kE_{p-k}+|\vec{k}|^2)\right.\right.$$

$$\left.\left.-\frac{2}{3}(5E_{p-k}^2+3(|\vec{k}|^2+|\vec{p}|^2)+15m_2^2)\right)\ ln\left(\frac{5E_{p-k}^2+3(|\vec{k}|+|\vec{p}|)^2+15m_2^2}{5E_{p-k}^2+3(|\vec{k}|-|\vec{p}|)^2+15m_2^2}\right)\right].$$

The integral of the first term is

$$-\frac{2\cdot5^2g^2}{3^2\pi^3}\int_0^{\sqrt{\Lambda^2+m_2^2}}dE_k\int_0^{\Lambda}d|\vec{k}|\left(1-\frac{\frac{5}{3}E_k^2+5m_2^2}{\frac{5}{3}E_k^2+|\vec{k}|^2+5m_2^2}\right)$$

$$=-\frac{2\cdot5^2g^2}{3^2\pi^3}\left[\Lambda\sqrt{\Lambda^2+m_2^2}-\int_0^{\sqrt{\Lambda^2+m_2^2}}dE_k\sqrt{\frac{5}{3}E_k^2+5m_2^2}\ arc\ tan\ \frac{\Lambda}{\sqrt{\frac{5}{3}E_k^2+5m_2^2}}\right)\right].$$

The range $[0, \sqrt{\Lambda^2+m^2}]$ can be divided into $\left[0, \sqrt{\frac{3}{5}\Lambda^2-3m^2}\right]$ and $\left[\sqrt{\frac{3}{5}\Lambda^2-3m^2}, \sqrt{\Lambda^2+m^2}\right]$ such that

(13)

$$\frac{2\cdot 5^2 g^2}{3^2\pi^3}\int_0^{\sqrt{\Lambda^2+m^2}} dE_k \sqrt{\frac{5}{3}E_k^2+5m^2}\; arc\,tan\left(\frac{\Lambda}{\sqrt{\frac{5}{3}E_k^2+5m^2}}\right)$$

$$= \frac{2\cdot 5^2 g^2}{3^2\pi^3}\int_0^{\sqrt{\frac{3}{5}\Lambda^2-3m^2}} dE_k \sqrt{\frac{5}{3}E_k^2+5m^2}\left[\frac{\pi}{2} - \frac{\sqrt{\frac{5}{3}E_k^2+5m^2}}{\Lambda} + \frac{\left(\frac{5}{3}E_k^2+5m^2\right)^{\frac{3}{2}}}{3\Lambda^3}+\ldots\right]$$

$$+ \frac{2\cdot 5^2 g^2}{3^2\pi^3}\int_{\sqrt{\frac{3}{5}\Lambda^2-3m^2}}^{\sqrt{\Lambda^2+m^2}} dE_k\, \sqrt{\frac{5}{3}E_k^2+5m^2}\left[-\frac{\Lambda}{\sqrt{\frac{5}{3}E_k^2+5m^2}} - \frac{1}{3}\frac{\Lambda^3}{\left(\frac{5}{3}E_k^2+5m^2\right)^{\frac{3}{2}}}+\ldots\right]$$

$$= \frac{2\cdot 5^2 g^2}{3^2\pi^3}\left\{\left[\frac{\pi}{2}\sqrt{\frac{5}{3}}\frac{\left(\frac{3}{5}\Lambda^2-3m^2\right)}{2} - \frac{5}{9}\frac{\left(\frac{3}{5}\Lambda^2-3m^2\right)^{\frac{3}{2}}}{\Lambda} + \frac{5}{27}\frac{\left(\frac{3}{5}\Lambda^2-3m^2\right)^{\frac{5}{2}}}{\Lambda^3} - \ldots.\right]\right.$$

$$\left. + \left[\Lambda^2+m^2-\left(\frac{3}{5}\Lambda^2-3m^2\right) - \frac{1}{5}\Lambda^3\left(\frac{1}{\sqrt{\frac{3}{5}\Lambda^2-3m^2}} - \frac{1}{\sqrt{\Lambda^2+m^2}}\right)+\ldots\right]\right\} + O(ln\;\Lambda)$$

$$= \frac{2\cdot 5^2 g^2}{3^2\pi^3}\left\{\left[\frac{\pi}{4}\sqrt{\frac{3}{5}} - \frac{1}{5}\sqrt{\frac{3}{5}} + \frac{1}{15}\sqrt{\frac{3}{5}} - \ldots\right] - \left[\frac{2}{5} - \frac{1}{5}\left(\sqrt{\frac{5}{3}}-1\right)+\ldots\right]\right\}\Lambda^2 + O(ln\;\Lambda)$$

In the limit $p^\mu \to 0$,

$$I_1(0) = -\frac{2\cdot 5^2 g^2}{3^2\pi^3}\left\{\left[1 - \left[\frac{\pi}{4}\sqrt{\frac{3}{5}} - \frac{1}{5}\sqrt{\frac{3}{5}} + \frac{1}{15}\sqrt{\frac{3}{5}} - \ldots\right] + \left[\frac{2}{5} - \frac{1}{5}\left(\sqrt{\frac{5}{3}}-1\right)+\ldots\right]\right]\Lambda^2\right.$$

$$\left. + O(ln\;\Lambda)\right.$$

$$lim_{p\to 0}\frac{1}{8|\vec{p}|}\int_0^{\sqrt{\Lambda^2+m_2^2}} dE_k \int_0^{\Lambda} d|\vec{k}|\; \frac{|\vec{k}|}{5E_k^2+3|\vec{k}|^2+15m^2}$$

$$\left[\left(4E_kE_{p-k}+2|\vec{k}|^2 - \frac{10}{3}E_{p-k}^2 - 2|\vec{p}|^2 - 10m_2^2\right)\right.$$

$$\left.\left. ln\left(\frac{5E_{p-k}^2+3(|\vec{k}|+|\vec{p}|)^2+15m_2^2}{5E_{p-k}^2+3(|\vec{k}|-|\vec{p}|)^2+15m_2^2}\right)\right]\right\}$$

$$= \frac{2\cdot 5^2 g^2}{3^2\pi^3}\left\{\left[1-\left[\frac{\pi}{4}\sqrt{\frac{3}{5}}-\frac{1}{5}\sqrt{\frac{3}{5}}+\frac{1}{15}\sqrt{\frac{3}{5}}-\ldots\right]+\left[\frac{2}{5}-\frac{1}{5}\left(\sqrt{\frac{5}{3}}-1\right)+\ldots\right]\right]\Lambda^2\right.$$

$$\left.+\frac{3}{2}\int_0^{\sqrt{\Lambda^2+m_2^2}} dE_k \int_0^{\Lambda} d|\vec{k}| \frac{|\vec{k}|^2}{(5E_k^2+3|\vec{k}|^2+15m_2^2)^2}\left(-\frac{22}{3}E_k^2+2|\vec{k}|^2-10m_2^2\right)\right\}$$

$$+O(ln\ \Lambda).$$

Since

$$\int_0^{\Lambda} d|\vec{k}| \frac{|\vec{k}|^2}{(5E_k^2+3|\vec{k}|^2+12m_2^2)^2}\left(-\frac{22}{3}E_k^2+2|\vec{k}|^2-10m_2^2\right)$$

$$= \frac{1}{9}\left(-\frac{22}{3}E_k^2-10m_2^2\right)\int_0^{\Lambda} d|\vec{k}|\ \frac{1}{|\vec{k}|^2}\frac{1}{\left(1+\frac{\frac{5}{3}E_k^2+5m_2^2}{|\vec{k}|^2}\right)^2}$$

$$+\frac{2}{9}\int_0^{\Lambda} d|\vec{k}| \frac{|\vec{k}|^4}{\left(\frac{5}{3}E_k^2+|\vec{k}|^2+5m_2^2\right)^2}$$

$$= \frac{2}{9}\Lambda+\left(\frac{14}{9}E_k^2+\frac{30}{9}m_2^2\right)1\Lambda+O\left(\frac{1}{\Lambda^3}\right),$$

(14)

$$I_1(0) = -\frac{2\cdot 5^2 g^2}{3^2\pi^3}\left\{\left[1-\left[\frac{\pi}{4}\sqrt{\frac{3}{5}}-\frac{1}{5}\sqrt{\frac{3}{5}}+\frac{1}{15}\sqrt{\frac{3}{5}}-\ldots\right]+\left[\frac{2}{5}-\frac{1}{5}\left(\sqrt{\frac{5}{3}}-1\right)+\ldots\right]\right.\right.$$

$$\left.\left.+\frac{3}{2}\left[\left[\frac{2}{9}+\frac{14}{27}+\ldots\right]\right\}\Lambda^2+O(ln\ \Lambda)+O(1).\right.\right.$$

Another conventional method for evaluating integrals of this type may be considered. Given the momentum variable $\hat{p} = (\hat{E}, \vec{p}) = \left(\frac{E}{\sqrt{3i}}, \frac{\vec{p}}{\sqrt{5}}\right)$,

$$(15)\qquad \frac{1}{(5E_{p-k}^2+3|\vec{p}-\vec{k}|^2+15m_2^2)(5E_k^2+3|\vec{k}|^2+15m_2^2)}$$
$$=\frac{225}{\left(\left(\frac{E_{p-k}}{\sqrt{3}i}\right)^2-\left(\frac{|\vec{p}-\vec{k}|}{\sqrt{5}}\right)^2+m_2^2\right)\left(\left(\frac{E_k}{\sqrt{3}i}\right)^2-\left(\frac{|\vec{k}|}{\sqrt{5}}\right)^2+m_2^2\right)}$$
$$=\frac{225}{((\hat{p}-\hat{k})^2-m_2^2)(\hat{k}^2-m_2^2)}$$

Let $q=\hat{k}-x\hat{p}$, $D=x(1-x)\hat{p}^2$ and $\tilde{x}=x\hat{p}(-2\hat{k}+\hat{p})+\hat{k}^2-m_2^2$. Then

$$(16)\qquad \int_0^1 dx\frac{1}{(y^2+D)^2}=\int_0^1\frac{dx}{[x\hat{p}(-2\hat{k}+\hat{p})+\hat{k}^2-m_2^2]^2}$$
$$=\frac{\int_{\hat{k}^2-m_2^2}^{(\hat{p}-\hat{k})^2-m_2^2}\frac{d\tilde{x}/(\hat{p}(-2\hat{k}+\hat{p}))}{}}{[x\hat{p}(-2\hat{k}+\hat{p})+\hat{k}^2-m_2^2]^2}$$
$$=\frac{1}{\hat{p}(-2\hat{k}+\hat{p})}\int_{\hat{k}^2-m_2^2}^{(\hat{p}-\hat{k})^2-m^2}\frac{d\tilde{x}}{\tilde{x}^2}$$
$$=\frac{1}{\hat{p}(-2\hat{k}+\hat{p})}\left[\frac{1}{\hat{k}^2-m_2^2}-\frac{1}{(\hat{p}-\hat{k})^2-m_2^2}\right]$$
$$=\frac{1}{((\hat{p}-\hat{k})^2-m_2^2)(\hat{k}^2-m_2^2)}.$$

It follows that the amplitude is

$$(17)\qquad -2^2 3^2 5^4 g^2\int_0^1 dx\int\frac{d^4k}{(2\pi)^4}\delta(p_i-p_f)\frac{5k\cdot(p-k)-m_2^2}{(q^2+D)^2}$$

Since $(E,\vec{p})=(\sqrt{3}i\hat{E},\sqrt{5}\vec{\hat{p}})$,

$$(18)\qquad 5k\cdot(p-k)-3m^2=-[15E_{\hat{k}}(E_{\hat{p}-\hat{k}})+25\vec{\hat{k}}\cdot(\vec{\hat{p}}-\vec{\hat{k}})+3m_2^2],$$

and the integral is

$$(19)\qquad 2^2 3^2 5^4 g^2\int_0^1 dx\int\frac{d^4q}{(2\pi)^4}\frac{15E_{\hat{k}}(E_{\hat{p}-\hat{k}})+25\vec{\hat{k}}\cdot(\vec{\hat{p}}-\vec{\hat{k}})+3m_2^2}{(q^2+D)^2}.$$

The expression in the numerator also has some dependence on q. Therefore, this technique does not allow an immediate evaluation of the integral. Instead, it is necessary to represent the numerator in terms of partial derivatives of an exponential function of the momenta.

The superficial degree of divergence of all of the two-point pseudoscalar diagrams is 2. At $O(g^4)$, there are three diagrams represented by the insertion of an internal spin-0 line, and a pseudoscalar line attached to the exterior of the fermion loop. Let the amplitudes for the first graph and the other two diagrams be $I_2^{(1)}(p)$ and $I_2^{(2)}(p)$ respectively. Then, the renormalized coupling in the limit of vanishing external momentum is

$$g(\Lambda) = g + A_1\Lambda^2 + A_2\Lambda^2 + ... \tag{20}$$

where $A_1 = lim_{\Lambda\to\infty} - \frac{I_1(0)}{\Lambda^2}$, $A_2 = lim_{\Lambda\to\infty} \frac{-1}{2}(I_2^{(1)}(0) + 2I_2^{(2)}(0))\Lambda^2$, ... after including the inverse factorial factor in the expansion of the scattering matrix. The number of diagrams at each order is estimated from the inclusion of series of spin-0 lines and fermion loops in these graphs or sets of of a minimum of two pseudoscalar propagators connecting different spin-$\frac{1}{2}$ loops. Consequently, A_n is bounded and the renormalization of the coupling is well-defined with counterterms cancelling in the quadratic divergences in the amplitudes. The logarithmic divegences may be absorbed into a renormalization of the pseudosclar mass m_1.

The fermion self-energy diagram has two vertices one pseudoscalar propagator and one fermion propagator. The integral is

(21)

$$i\Sigma_{f1} = -g^2 \int \frac{d^4k}{(2\pi)^4} \bar{u}_r(\vec{p}) \frac{\left[3 \cdot 5^2 i\gamma_5 \left(-\gamma_5 + i\mathbb{I}\right)(\gamma \cdot (p-k) + m_2) i\gamma_5\right]}{(5E^2_{p-k} + 3|\vec{p}-\vec{k}|^2 + m_2^2)(5E_k^2 + 3|\vec{k}|^2 + m_1^2)} u_r(\vec{p})$$

$$= 3 \cdot 5^2 \; i \; g^2 \int \frac{d^4k}{(2\pi)^4} \bar{u}_r(\vec{p}) \frac{\left[\left(\mathbb{I} + \frac{i}{2}\gamma_5\right)(\gamma \cdot (p-k) - m_2)\right]}{(5E^2_{p-k} + 3|\vec{p}-\vec{k}|^2 + m_2^2)(5E_k^2 + 3|\vec{k}|^2 + m_1^2)} u_r(\vec{p}).$$

Since $(\gamma \cdot p - m)u_r(p) = 0$,

(22)

$$i\Sigma_{f1} = -\frac{25}{6} i g^2 \int \frac{d^4k}{(2\pi)^4} \frac{\bar{u}_r(p)(\mathbb{I} + i\gamma_5)\cdot\gamma \cdot k \, u_r(p)}{(5E_k^2 + 3|\vec{k}|^2 + 15m_1^2)(5E^2_{p-k} + 3|\vec{p}-\vec{k}|^2 + 15m + 2^2)}$$

which is linearly divergent. Amongst the one-particle irreducible amplitudes there will be rainbow diagrams and fermion loops in the interior of this self-energy graph. An n-loop rainbow diagram has a superficial degree of divergence equal to $4n - 2n - (2n - 1) = 1$. This infinity may be absorbed into a fermion mass renormalization

(23) $$m_2(\Lambda) = m_2 + (B_1 + B_2 + ...)\Lambda$$

with $B_1 = \Sigma_{f1}(0)$, $B_2 = \frac{1}{2!}\Sigma_{f2}(0)$, ...

3 The Mass of the Pseudoscalar Meson

The mass of the pseudoscalar meson would received contributions from the two-point diagrams at higher orders in perturbation theory. After the cancellation of the quadratic infinities, there remain finite terms which can be added to the momentum-space propagator. Even though the renormalizability analysis does not

required one-particle reducible diagrams, these graphs are still included in the evaluation of the scattering amplitudes. Given the 0^- spin coupling formula and gluon condensate contribution, yielding a mass m_0+m_{gc} [2], the sum of quark-anti-quark annihilation diagrams results in a sum in quadrature of m_0+m_{gc} and the octet mass [3] for $m_{\eta'}$. An evaluation of only a subset of the the diagrams of the pseudoscalar meson theory at higher orders in perturbation results in the quadrature formula for the shift in the massive propagator even though it yields a precise value of the mass of the η' meson. There are 2^n different diagrams with n quark-anti-quark loops, each having a symmetry factor of 2^{n-1}. The coefficient of the amplitude at this order then would be $\frac{2^{2n-1}}{n!}$. Within the context of a conventional quantum field theoretic computation,

(24)

$$\frac{1}{p^2-(m_0+m_{gc})^2} \rightarrow \frac{1}{p^2-(m_0+m_{gc})^2}\left[1+\sum_{n=1}^{\infty}\left(\frac{1}{4}\frac{4m_8^2}{(p^2-(m_0+m_{gc})^2}\right)^n\right]$$
$$= \frac{1}{p^2-(m_0+m_{gc})^2}\frac{1}{1-\frac{m_8^2}{p^2-((m_0+m_{gc})^2+m_8^2)}} = \frac{1}{p^2-((m_0+m_{gc})^2+m_8^2}.$$

The factor of 4 multiplying m_8^2 arises from trace of the identity matrix. It remains to be established if the effect of the gluon condensate and octet mass can be theoretically explained by the pseudoscalar meson theory.

The pseudoscalar propagator is modified to

(25)

$$\Delta_F(p)_{ren} = \frac{15i}{5E_p^2+3|\vec{p}|^2+15m_1^2}\left[1+\widehat{I_1(p)} + \left(\widehat{I_2^{(1)}(p)}+2\widehat{I_2^{(2)}(p)}+\widehat{I_2^{(3)}(p)}\right)+...+...\right]\Big|_{finite}$$

where the normalized amplitude $\widehat{I_1(p)}$ is dimensionless, and therefore, the amplitudes expression must be divided by μ_{QCD}^2, where $\mu_{QCD} \approx 200 MeV/c^2$. and $I_2^{(3)}(p)$ is the one-particle reducible amplitude with two fermion loops in sequence, and

The limit, as the external momentum vanishes, equals

(26)

$$lim_{p\to 0}\Delta_F(0)_{ren} = \frac{3i}{4m_1^2}\left[1+\left(\widehat{I_1(0)}+\left(\widehat{I_2^{(1)}(0)}+2\widehat{I_2^{(2)}(0)}+\widehat{I_2^{(3)}(0)}\right)+...\right)\right]\Bigg|_{finite}$$

The factors multiplying the amplitudes will be given by the product of $\frac{1}{n!}$, and the number of the interchanges of the lines that leave Invariant the one-particle irreducible subgraphs of a diagram. Therefore, the n-loop one-particle, reducible diagram consisting of a sequence of fermion loops, is multiplied by $\frac{2^n}{n!}$, and a set of reducible amplitudes is given by

$$(27)\quad I_{nseq.\ red.}(p)\Big|_{finite} \equiv (-1)^{n+1}\frac{2^{n-1}}{n!}I_1(p)^n_{finite}\left(\frac{15i}{5E_p^2+3|\vec{p}|^2+15m_1^2}\right)^{n-1}$$
$$= -\frac{2^{n-1}}{n!}|I_1(p)_{finite}|^n\left(\frac{15i}{5E_p^2+3|\vec{p}|^2+15m_1^2}\right)^{n-1}$$

Then

$$(28)\quad \sum_{n=1}^{\infty} I_{nseq.\ red.}(p)\Big|_{finite} = \sum_{n=1}\frac{(-2\cdot 15i)^{n-1}}{n!}\frac{I_1(p)^n_{finite}}{(5E_p^2+|\vec{p}|^2+15m_1^2)^{n-1}}$$
$$= \frac{5E_p^2+|\vec{p}|^2+15m_1^2}{2\cdot 15}i\left[e^{\frac{-2\cdot 15iI_1(p)_{finite}}{5E_p^2+3|\vec{p}|^2+15m_1^2}}-1\right]$$

when tends to

$$(29)\quad \frac{2}{3}m_1^2 i\left[e^{\frac{-3iI_1(p)_{finite}}{2m_1^2}}-1\right]$$

as $|\vec{p}| \to 0$ and

(30)

$$\Delta_F(0)_{ren} = \frac{3i}{4m_1^2}\left[1 + \frac{2}{3}\frac{m_1^2}{\mu_{QCD}^2} i\left(e^{\frac{-3iI_1(0)_{finite}}{2m_1^2}} - 1\right)\right.$$
$$\left.\left(\frac{2}{3}\frac{m_1^2}{\mu_{QCD}^2}\left(e^{\frac{-3iI_1(0)_{finite}}{2m_1^2}} - 1\right) + (\widehat{I_2^{(1)}(0)} + 2\widehat{I_2^{(2)}(0)})_{finite} + ...\right)\right)\right].$$

(31)

since one-particle irreducible subgraphs can be included within separate fermion loops in a a one-particle reducible amplitude. Then

(32)

$$Im\ \Delta_F(0)_{ren.} = \frac{3}{4m_1^2}\left[1 + Im\left[\frac{2}{3}\frac{m_1^2}{\mu_{QCD}^2}\left(e^{\frac{-3iI_1(0)_{finite}}{2m_1^2}} - 1\right)\left(\frac{2}{3}\frac{m_1^2}{\mu_{QCD}^2}\left(e^{\frac{-3iI_1(0)_{finite}}{2m_1^2}} - 1\right)\right.\right.\right.$$
$$\left.\left.\left. + \left(\widehat{I_2^{(1)}(0)} + 2\widehat{I_2^{(2)}(0)}\right)_{finite} + ...\right)\right]\right]$$

and

(33)

$$m_{1q}^2 = m_1^2\left[1 + Im\left[\frac{2}{3}\frac{m_1^2}{\mu_{QCD}^2}\left(e^{\frac{-3iI_1(0)_{finite}}{2m_1^2}} - 1\right)\right.\right.$$
$$\left.\left.\left(\frac{2}{3}\frac{m_1^2}{\mu_{QCD}^2}\left(e^{\frac{-3iI_1(0)_{finite}}{2m_1^2}} - 1\right) + \left(\widehat{I_2^{(1)}(0)} + 2\widehat{I_2^{(2)}(0)}\right)_{finite} + ...\right)\right)\right]\right]^{-1}.$$

Since the number of vertices in each pseudoscalar two-point amplitude is even, the trace of the gamma matrices is real in a fermion loop and the pseudoscalar propagator is imaginary, $I_n^{(m_n)}(0)$ is real when there is an even number of internal pseudocalar propagators and imaginary if an odd number is present. The interior of the fermion loop is partitioned into n regions if there are $n-1$ pseudocalar internal

lines. These diagrams constitute a single set of fermion loop diagrams. When an internal pseudoscalar lines generate another fermion loop, two pseudoscalar propagators are introduced, yielding another imaginary unit. Then $I_n(0) = \sum_{m_n} I_n^{(m_n)}(0)$ is real only for odd n and

(34)

$$m_{1q} = m_1 \left[1 + Im \left[\frac{2}{3} \frac{m_1^2}{\mu_{QCD}^2} \left(e^{\frac{-3iI_1(0)_{finite}}{2m_1^2}} - 1 \right) \left(\frac{2}{3} \frac{m_1^2}{\mu_{QCD}^2} \left(e^{\frac{-3iI_1(0)_{finite}}{2m_1^2}} - 1 \right) + \sum_{\substack{n \geq 3 \\ n \ odd}} \widehat{I_n(0)}_{non\ seq.\ red.,\ finite} + \cdots \right) \right] \right]^{-\frac{1}{2}}$$

where $I_n(p)_{non\ seq.\ red.}$ represents amplitudes of all n-loop diagrams excluding those consisting of a sequence of fermion loops with no other internal or attached lines.

There are nearly 2^n different types of one-particle irreducible two-point pseudoscalar diagrams at n^{th} order in perturbation theory. The overall sign depends on the the number of interior fermion loops. The partitioning of the n loops by $n-1$ gluon lines can be subdivided further into $n_k - 1$ lines in the k^{th} loop, with the k^{th} loop being connected to two pseudoscalar lines. When there are one outermost and $\ell - 1$ fermion loops, $\sum_{k=2}^{\ell}(n_k - 1) + 2(\ell - 1) = \sum_{k=1}^{\ell} n_k + \ell - 2 = n - 1$ or $\sum_{k=2}^{\ell} n_k = n - \ell - 1$, and the overall sign is $(-1)^\ell$. The maximum value of ℓ is $1 + \frac{n-1}{2}$ for odd n, and there are $\binom{n}{\ell}$ types of diagrams with ℓ fermion loops. Given an approximate equality of the magnitudes of the higher-order amplitudes, the contribution of the different types receives a factor of $\sum_{\ell=1}^{\frac{n+1}{2}} (-1)^\ell \binom{n-1}{\ell-1} = 2^{\frac{n-1}{2}} cos\left(\frac{(n-1)\pi}{4}\right)$. This estimate is based on the validity of the field theory limit of the eikonal approximation of the string scattering matrix in the evaluation of

the finite part of the amplitude [4][5]. The coefficient of the one-particle irreducible n-loop amplitude, required for equality with $\sum_{m_n} I_n^{m_n}(0)_{1PI}$, then tends to $\frac{2^{n-1}}{n!} \times 2^{\frac{n-1}{2}} cos\left(\frac{(n-1)\pi}{4}\right) = \frac{2^{\frac{3(n-1)}{2}}}{n!} cos\left(\frac{(n-1)\pi}{4}\right)$. Consequently,

$$(35) \quad \sum_{\substack{n\geq 3 \\ n\ odd}} \widehat{I_n(0)}_{non\ seq.\ red.,finite} \approx -\sum_{\substack{n\geq 3 \\ n\ odd}} \frac{2^{\frac{3(n-1)}{2}}}{n!} cos\left(\frac{(n-1)\pi}{4}\right) \frac{|\widehat{I_1(0)}_{finite}|^n}{\mu_{QCD}^2} \cdot \left(\frac{3i}{4m_1^2}\right)^{n-1}$$

$$= -\frac{|I_1(0)_{finite}|}{\mu_{QCD}^2} \sum_{s=1}^{\infty} \frac{1}{(4s+1)!} \left(\frac{3}{\sqrt{2}} \frac{|I_1(0)_{finite}|}{m_1^2}\right)^{4s}$$

$$= -\frac{|I_1(0)_{finite}|}{\mu_{QCD}^2} \left[-1 + \frac{m_1^2}{3\sqrt{2}|I_1(0)_{finite}|} \left(sin\left(\frac{3}{\sqrt{2}} \frac{|I_1(0)_{finite}|}{m_1^2}\right) + sinh\left(\frac{3}{\sqrt{2}} \frac{|I_1(0)_{finite}|}{m_1^2}\right) \right) \right]$$

Therefore,

(36)

$$m_{1q} \approx m_1 \left\{ 1 - \frac{2}{3} \frac{m_1^2}{\mu_{QCD}^2} sin\left(\frac{3|I_1(0)_{finite}|}{2m_1^2}\right) \left[\frac{2}{3} \frac{m_1^2}{\mu_{QCD}^2} sin\left(\frac{3|I_1(0)_{finite}|}{2m_1^2}\right) + \frac{|I_1(0)_{finite}|}{\mu_{QCD}^2} \left[1 - \frac{m_1^2}{3\sqrt{2}|I_1(0)_{finite}|} \left(sin\left(\frac{3}{\sqrt{2}} \frac{|I_1(0)_{finite}|}{m_1^2}\right) + sinh\left(\frac{3}{\sqrt{2}} \frac{|I_1(0)_{finite}|}{m_1^2}\right) \right) \right] \right] \right\}^{-\frac{1}{2}}.$$

The $O(1)$ term in Eq.(10) is given by the expansion of the radicals in Eq.(14)

$$(37) \quad \sqrt{\frac{5}{3}E_k^2 + 5m_2^2} = \sqrt{\frac{5}{3}} E_k \left[1 + \frac{1}{6} \frac{m_2^2}{E_k^2} + ... \right] = \sqrt{\frac{5}{3}} E_k + \frac{1}{6} \sqrt{\frac{5}{3}} \frac{m_2^2}{E_k} - ...$$

$$\sqrt{\frac{3}{5}\Lambda^2 - 3m_2^2} = \sqrt{\frac{3}{5}}\Lambda - \frac{\sqrt{15}}{2} \frac{m_2^2}{\Lambda} + ...$$

and the fractions in Eq.(11)

$$(38)\qquad \frac{|\vec{k}|^2}{(5E_k^2+3|\vec{k}|^2+15m_2^2)^2}=\frac{1}{9|\vec{k}|^2}-\frac{2}{9}\frac{\frac{5}{3}E_k^2+5m_2^2}{|\vec{k}|^4}+\dots$$

$$\frac{|\vec{k}|^4}{(5E_k^2+3|\vec{k}|^2+15m_2^2)^2}=\frac{1}{9}-\frac{2}{9}\frac{\frac{5}{3}E_k^2+5m_2^2}{|\vec{k}|^2}+\dots\,.$$

together with

(39)

$$\int_0^{\sqrt{\Lambda^2+m_2^2}}dE_k\left(-\frac{22}{3}E_k^2-10m_2^2\right)\int_0^{\Lambda}d|\vec{k}|\left[\frac{1}{9|\vec{k}|^2}-\frac{2}{9}\frac{\left(\frac{5}{3}E_k^2+5m_2^2\right)}{|\vec{k}|^4}+\dots\right]$$

$$+\frac{2}{9}\int_0^{\sqrt{\Lambda^2+m_2^2}}dE_k\int_0^{\Lambda}d|\vec{k}|\left[1-2\frac{\left(\frac{5}{3}E_k^2+5m_2^2\right)}{|\vec{k}|^2}+\dots\right]$$

$$=\int_0^{\sqrt{\Lambda^2+m_2^2}}dE_k\left(-\frac{22}{3}E_k^2-10m_2^2\right)\left[-\frac{1}{9\Lambda}+\frac{2}{27\Lambda^3}\left(\frac{5}{3}E_k^2+5m_2^2\right)+\dots\right]$$

$$+\frac{2}{9}\int_0^{\sqrt{\Lambda^2+m_2^2}}dE_k\left[\Lambda+2\left(\frac{5}{3}E_k^2+5m_2^2\right)\frac{1}{\Lambda}-\dots\right].$$

$$=-\frac{1}{9\Lambda}\left[-\frac{22}{3}\left(\Lambda^2+m_2^2\right)^{\frac{3}{2}}-10m_2^2\left(\Lambda^2+m_2^2\right)^{\frac{1}{2}}\right]+\frac{2}{27\Lambda^3}\left[\frac{2\cdot5\cdot11}{9}\left(\Lambda^2+m_2^2\right)^{\frac{5}{2}}\right.$$

$$\left.-\frac{160}{9}m_2^2\left(\Lambda^2+m_2^2\right)^{\frac{3}{2}}-\dots.\right]$$

$$+\frac{2}{9}\Lambda(\Lambda^2+m_2^2)^{\frac{1}{2}}+\frac{4}{9\Lambda}\left(\frac{5}{9}(\Lambda^2+m_2^2)^{\frac{3}{2}}+5m_2^2(\Lambda^2+m_2^2)^{\frac{1}{2}}\right)$$

$$=\left[\frac{1}{9}\frac{22}{3}+\frac{2}{27}\frac{2\cdot5\cdot11}{9}+\dots\frac{2}{9}+\frac{20}{81}+\dots\right]\Lambda^2$$

$$+\left[\frac{1}{9}\frac{22}{3}\frac{3}{2}m_2^2+\frac{5}{9}m_2^2+\frac{2}{27}\frac{2\cdot5\cdot11}{9}\frac{5}{2}m_2^2-\frac{2}{27}\frac{160}{9}m_2^2+\frac{2}{9}\frac{1}{2}m_2^2+\frac{20}{81}\frac{3}{2}+\frac{20}{9}m_2^2+\dots\right]+\dots$$

and the constant in the integral of $\sqrt{\frac{5}{3}\Lambda^2 + 5m_2^2}$. Then

(40)

$$I_1(0)_{finite} = -\frac{2\cdot 5^2 g^2}{3^2\pi^3}\left\{\left[-\frac{\sqrt{15}\pi}{8} + \frac{5}{2}\sqrt{\frac{3}{5}} - \frac{5}{6}\sqrt{\frac{3}{5}} + 2 - \left(\frac{13}{6}\sqrt{\frac{5}{3}} - \frac{1}{2}\right) + ...\right] + ... \right.$$
$$\left. + \frac{3}{2}\left[\frac{1}{9}\frac{22}{3}\frac{3}{2} + \frac{5}{9} + \frac{2}{27}\frac{2\cdot 5\cdot 11}{9}\frac{5}{2} - \frac{2}{27}\frac{160}{9} + \frac{2}{9}\frac{1}{2} + \frac{20}{81}\frac{3}{2} + \frac{20}{9} + ...\right]\right\} m_2^2.$$

The expression of $|\widehat{I_1(0)}|_{finite}$ to the given order is 1.00605044385 $\frac{m_2^2}{\nu_{QCD}^2} g^2$. The coupling in the pseudoscalar meson theory is nearly $g = 0.2$. Setting $g = 0.2 z_g$ and m_2 to be the weighted average of masses of quarks, $\frac{1}{6}m_u + \frac{1}{6}m_d + \frac{2}{3}m_s$, this value equals 0.1833580682 z_g^2. The quantum corrected pseudoscalar mass is

(41)

$$m_{1q} \approx m_1 \left\{1 - 3.0364440741\ sin(0.06038577145\ z_g^2)\right.$$

(42)

$$\left[3.0364440741\ sin(0.06038577145\ z_g^2) + 0.1833580682\ z_g^2\right.$$
$$\left.\cdot\left[1 - 5.85491221095 z_g^{-2}\ \left(sin(0.08539837695 z_g^2) + sinh(0.08539837695 z_g^2)\right)\right]\right]\Bigg\}^{-\frac{1}{2}}.$$

Setting m_1 equal to the η-meson mass $m_\eta = 547.862 \pm 0.018\ MeV/c^2$ and $m_{1q} \doteq m_{\eta'} = 957.78 \pm 0.06\ MeV/c^2$,

(43) $$z_g = 2.127038 \pm 0.000086.$$

This value of z_g yields the coupling

(44) $$g = 0.4254076 \pm 0.0000172.$$

There remains a theoretical uncertainty in the exact value of the series in Eq.(39). This value of g is compatible with the coupling of the η meson to the strange quark within the current margin of error [6].

Several different models have been developed for η' meson. Amongst these are the pion bubble [7] and gluon condensate models [8][9][10]. In the first, the mass is identified with that of seven pion bubbles according to the integer multiple rule [11]. The second introduces a nonperturbative correction to the massive quark propagator, and twice of this mass differential which can be added to the value of the mass for $\frac{1}{\sqrt{3}}(u\bar{u}+d\bar{d}+s\bar{s})$ from the 0^- spin coupling formula. The sum

$$(45)\quad \frac{1}{3}\left(2m_u-\frac{3A}{4m_u^2}\right)+\frac{1}{3}\left(2m_d-\frac{3A}{4m_d^2}\right)+\frac{1}{3}\left(m_s-\frac{3A}{4m-s^2}\right)+\Delta M(p^2)_{q\bar{q}}$$
$$=349.49476\ MeV/c^2+481.58394\ MeV/c^2=831.08154\ MeV/c^2$$

can be combined with a variant of the octet mass, $\bar{m}_8$, which is the average of the masses derived from the linear Gell-Mann-Okubo formula

(46)
$$\bar{m}_8=\frac{1}{2}\left[\frac{1}{2}\left(\frac{m_{K^-}+m_{\bar{K}_0}}{2}+\frac{m_{K^+}+m_{K^{*0}}}{2}\right)+\frac{3m_\eta+m_\pi}{4}\right]=470.534384167\ MeV/c^2,$$

in quadrature to give a value

(47)
$$\sqrt{(831.08154\ MeV/c^2)^2+(470.534384167\ MeV/c^2)^2}=955.038812202\ MeV/c^2$$

nearly equal to $m_{\eta'}$. The quadratic Gell-Mann-Okubo formula [12] yields

(48)
$$\hat{m}_8=\frac{1}{2}\left\{\frac{1}{2}\left[\left(\frac{m_{K^-}+m_{\bar{K}^0}}{2}\right)^2+\left(\frac{m_{K^+}+m_{K^0}}{2}\right)^2\right]\right\}^{\frac{1}{2}}+\frac{1}{2}\left(\frac{3m_\eta^2+m_\pi^2}{4}\right)^{\frac{1}{2}}$$
$$=\frac{1}{2}(495.6625\ MeV/c^2+479.4567247357\ MeV/c^2)=487.559612368\ MeV/c^2$$

and

(49)

$$\sqrt{(831.08154\ MeV/c^2)^2 + (487.559612368\ MeV/c^2)^2} = 963.5407147777\ MeV/c^2,$$

which is larger than $m_{\eta'}$ by $5.76081477697\ MeV/c^2$. Consistency between the two models of the η' meson follows from an annihilation of the quark-anti-quark pairs of the pion bubbles to produce a gluon condensate, which would have an energy that is approximately 40.2% of the $481.58394\ MeV$ energy differential [13], or $193.5967\ MeV$, equal to 20.213% of the $m_{\eta'}c^2$ [14] [15]. This process then produces a fundamental 0^- pseudoscalar core, three quark-anti-quark outer boundary components and gluonic condensate. It may be recalled that the quark boundary components are the ends of surfaces of infinite genus with $m_{u\infty} = 61.85\ MeV/c^2$ and $m_{d\infty} = 64.85\ MeV/c^2$ such the sums with the chiral quark mass of $m_{qc} = 243.15\ MeV/c^2$, resulting from chiral symmetry breaking, are the constituent quark masses $m_u = m_{u\infty} + m_{uc} = 305\ MeV/c^2$ and $m_d = m_{d\infty} + m_{dc} = 308\ MeV/c^2$ [16]. The mass of the quark-anti-quark boundary components then would be

(50)

$$\frac{1}{2}((m_{u\,\infty} + m_{\bar{u}_\infty}) + (m_{d_\infty} + m_{\bar{d}_\infty})) = \frac{1}{2}(2(61.85\ MeV/c^2) + 2(64.85\ MeV/c^2))$$
$$= 126.7\ MeV.c^2.$$

It is known that there are bridges which connect these boundary components. The u and d bridges [17] have masses

(51)

$$m_{ub} = 1.934658\ MeV/c^2$$
$$m_{db} = 4.93509\ MeV/c^2,$$

which coincide with the light quark masses from lattice calculations [18]. With five pairs of both $u-\bar{u}$ and $d-\bar{d}$ bridges, the total mass of the bridges is

(52) $$5m_{ub} + 5m_{db} = 34.34874\ MeV/c^2.$$

The sum of the energies in the gluon condensate model would be

(53)

$$\frac{1}{3}\left(2m_u - \frac{3A}{4m_u^2}\right) + \frac{1}{3}\left(2m_d - \frac{3A}{4m_d^2}\right) + \frac{1}{3}\left(m_s - \frac{3A}{4m - s^2}\right) + \frac{E_{gluon}}{c^2}$$

$$+ 3 \cdot \frac{1}{2}((m_{u\,\infty} + m_{\bar{u}_\infty}) + (m_{d_\infty} + m_{\bar{d}_\infty})) + 5(m_{ub} + m_{db})$$

$$= 349.49476\ MeV/c^2 + 193.5967\ MeV/c^2 + 3(126.7\ MeV/c^2) + 34.34874\ MeV/c^2.$$

$$= 957.539916\ MeV/c^2$$

The method described in this investigation is based similarly on quark-anti-quark loop amplitudes with the coupling reflecting the chirality of the interaction. The pseudoscalar meson theory also introduces a connection between the η and η' meson masses. The decays of the η' meson through $\eta' \to \eta\pi\pi$, which can be predicted by chiral perturbation theory [19],

(54)
$$\eta' \to \eta\pi^0\pi^0 \to \gamma\gamma\pi^0\pi^0 \to 6\gamma$$

$$\eta' \to \eta\pi^0\pi^0 \to 4\pi^0 \to 8\gamma$$

$$\eta' \to \eta\pi^0\pi^0 \to 5\pi^0 \to 10\gamma$$

over $9.02032 \pm 0.87439 \times 10^{-17}$ *sec* and

(55) $\eta' \to \eta\pi^+\pi^- \to \pi^0\pi^0\pi^+\pi^- \to 4\gamma\mu^+\nu_\mu\mu^-\bar{\nu}_\mu \to 4\gamma e^+e^-2\nu_\mu 2\bar{\nu}_\mu\nu_e\bar{\nu}_e$

$\eta' \to \eta\pi^+\pi^- \to \pi^0\pi^0\pi^0\pi^+\pi^- \to 6\gamma\mu^+\nu_\mu\mu^-\bar{\nu} \to 6\gamma e^+e^-2\nu_\mu 2\bar{\nu}_\mu\nu_e\bar{\nu}_e$

$\eta' \to \eta\pi^+\eta^- \to \pi^0 2\pi^+ 2\pi^- \to 2\gamma 2\mu^+ 2\nu_\mu 2\mu^- 2\bar{\nu}_\mu \to 2\gamma 2e^+ 2e^- 4\nu_\mu 4\bar{\nu}_\mu 2\nu_e 2\bar{\nu}_e$

$\eta' \to \eta\pi^+\pi^- \to 2\gamma\mu^+\nu_\mu\mu^-\bar{\nu}_\mu \to 2\gamma e^+e^-2\nu_\mu 2\bar{\nu}_\mu\nu_e\bar{\nu}_e$

over $2.2230011 \pm 0.0025630 \times 10^{-6}$ *sec*, together with other rarer reactions, belong to semiclassical time scales greater than or equal to 2×10^{-19} *sec*. Furthermore, a pion -induced conversion of an η meson into an η' meson before the decay of the η meson after 5×10^{-19} can occur these time scales. This transformation is essential for the mixing of η and η' mesons. The value of the mixing angle θ_P, consistent with dual models of hadrons is $-19.5°$ [20]. Recent experimental values are $-16.7° \pm 1.0° \pm 2.0°$ [21],-$18.76° \pm 3.4°$ [22] and $-17.2° \pm 0.5°$ [23]. It would be expected that duality is not precisely preserved in a semiclassical theory. However, the pseudoscalar mixing angle can be deduced from an effective field theory with both kinetic and mass matrices [24], which is related to the use of two mixing angles [25] and the chiral Lagrangian [26] and compatible with the change in the coefficients of kinetic terms in the semiclassical action.

4 Conclusion

The pseudoscalar meson octet includes the pion, kaon and the η prime meson A ninth 0^- resonance is the η' meson. The quantum theory of pseudoscalar mesons near semiclassical scales is investigated with regard to the η and η' mesons. There are two masses in the theory, which are designated to be m_1 for the pseudo scalar

field and m_2 for the fermion field. Fermion loop diagram is evaluated with propagators that are constructed for the semiclassical model. Traces of gamma matrices including the γ_5 factor are evaluated and a series expansion of the fermion loop amplitude at zero external momentum has terms quadratic and logarithmic in the momentum cut-off Λ. Renormalizability of the theory is established because the superficial degree of divergence of all of the one-particle irreducible diagrams does not exceed 2. The fermion self-energy energy is linearly divergent. The infinities in this one-loop amplitude, rainbow diagrams and other graphs with internal fermion loops may be absorbed through a renormalization of the fermion mass.

The pseudoscalar momentum-space propagator is modified by perturbative corrections. Even though only one-particle irreducible amplitudes are required for renormalizability, reducible diagrams are relevant for computation of mass shifts in momentum-space propagators. Evaluating the finite parts of the two-point pseudoscalar amplitudes, a theoretical prediction can be made for a summation over all orders of quantum corrections to the η meson mass that coincides with the η' meson mass at a specific value of the coupling of η to the quarks.

References

[1] A. Salam, Overlapping Divergences and the S-Matrix, Phys. Rev. **82** (1951) 217-227.

[2] S. Davis, Nonperturbative Contributions to the Massive Propagator in a Class of Strong Interactions, Bull. Pure Appl. Sci. **37D** (2018) 137-145.

[3] L. Venkataraman and G. Kilcup, The η' Meson with Staggered Fermions, hep-lat/9711006.

[4] C. Schubert, Perturbative Quantum Field Theory in the String Inspired Formalism. Phys. Rep. **355**(2001) 73-234.

[5] Y. Du, S. Ajith, R. Rajagopal and D. Vaman, Worldine Proof of Eikonal Exponentiation, arXiv.2409.12895.

[6] T. A. Lähde and D. O. Riska, The Coupling of η Mesons to Quarks and Baryons from $D_s^* \to D_s\pi^0$ Decay, Nucl Phys. **A710** (2002) 99-116.

[7] E. Elbaz, A Geometrical Approach to Elementary Particles, Il Nuovo Cimento **A63** (1981) 257-320.

[8] G. Veneziano, U(1) without Instantons, Nucl. Phys. **B159** (1979) 213-224.

[9] E. Witten, Current Algebra Theorems for U(1) 'Goldstone Boson', Nucl. Phys. **B156** (1979) 269-283.

[10] D. Blaschke, H. P. Pavel, V. N. Pervushin, G. Ropke and M. V. Volkov, Squeezed Condensate of Gluons and $\eta - \eta'$ Mass Difference, Phys. Lett. **397B** (1997) 129-132.

[11] E. L. Koschmieder, The Masses of the Mesons and Baryons, Part I. The Integer Multiple Rule, Bull. Acad. Roy. Belgique X (1999) 281-287.

[12] J. Gasser and H. Leuwyler, Chiral Perturbation Theory to One Loop, Ann. Phys. **158** (1984) 142-210.

[13] C. Alexandrou et al., Quark and Gluon Momentum Fractions in the Pion and in the Kaon, Phys. Rev. Lett. **134** (2025) 131902:1-8.

[14] C. E. Carlson and T. Hans Hansson, $\eta-\eta'$-Glueball Mixing, Nucl. Phys. **199** (1982) 441-450.

[15] J. P. Singh and A. B. Patel, Quark Distributions and Gluon Contents of η and η', J. Phys. G **39** (2012) 015006:1-14.

[16] S. Davis, Theoretical Foundations of the Particle Spectrum, Hadr. J. **47** (2024) 295-312.

[17] S. Davis, Stable Black Holes in Anti-de Sitter Space and Particle Models, RFSC-20-46.

[18] J. Komijani, Precise Determinations of of Quark Masses, 36th Annual International Symposium on Lattice Field Theory 22-28 July 2018, Michigan State University, East Lansing, Michigan, Proc. of Science **334** (2019) 007.

[19] N. Beisert and B. Borasoy, The $\eta' \to \eta\pi\pi$ Decay in U(3) Chiral Perturbation theory, Nucl. Phys. **A705** (2002) 433-454.

[20] A. Bramón, The $\eta - \eta'$ Mixing Angle from Duality and Quark Model, Phys. Lett. **51B** (1974) 87-89.

[21] T. Huang and X.-G. Wu, Determination of the η and η' Mixing Angle from the Pseudoscalr Transition Form Factors, Eur. Phys. J. C **50** (2007) 771-779.

[22] T. N. Pham, $\eta - \eta'$ Mixing Angle from Vector Meson Radiative Decays, Phys. Lett. **694B** (2011) 129-133.

[23] F.-G. Cao, Determination of the $\eta - \eta'$ Mixing Angle, Phys. Rev. **D85** (2012) 057501:1-4.

[24] E. Gedalin, A. Moalem and L. Razdolskaya, Pseudoscalar Meson Mixing in Effective Field Theory, Phys. Rev. **D64** (2001) 076007:1-5.

[25] R. Escribano and J.-M. Frere, Study of the $\eta - \eta'$ System in the Two Mixing Angle Scheme, J. High Energy Phys. **0506** (2005) 029:1-15.

[26] M. Benayoun, L. DelBuono and H. B. O'Connell, VMD, the WZW Lagrangian and ChPT: The Third Mixing Angle, Eur. Phys. J. C **17** (2000) 593-610.

HADRONIC JOURNAL 49, 27 - 64 (2026)
DOI 10.29083/HJ.49 .01 .2026/SC27

NEW PERSPECTIVES AS REGARDS THE BLACK HOLE INFORMATION AND FIREWALL PARADOXES IN A THREE-DIMENSIONAL DYNAMICAL QUANTUM VACUUM

Davide Fiscaletti
SpaceLife Institute – Via Roncaglia 35 - 61047
San Lorenzo in Campo (PU), Italy
spacelife.institute@gmail.com

Received January 13, 2026
Revised January 26, 2026

Abstract

New perspectives to address the black hole information and firewall paradoxes are introduced in the model of a three-dimensional dynamical quantum vacuum defined by a variable energy density and by dissipative processes at a generalized Compton wavelength that provides a unified treatment of macroscopic regime of black holes and quantum regime of elementary particles in terms of sub-Planckian black holes of the variable energy density. The information paradox is treated without invoking a firewall. Finally, it is shown how the dissipative features of the vacuum allow a new re-reading of the connection between the information contained in the effective interior of the black hole and the modes outside the apparent horizon, avoiding the paradoxes present in current theories.

Key words: three-dimensional dynamical quantum vacuum, generalized Compton wavelength, black holes, dissipative features of the vacuum, apparent horizon, entanglement effect of the apparent horizon.

Copyright © 2026 by Hadronic Press, Inc., Palm Harbor, FL 34684, USA

1. Introduction

In the exploration of the properties of black holes, Stephen Hawking originally suggested that the information encoded by things that fall into a black hole is lost [1], while the laws of quantum physics imply that information cannot be destroyed and gauge/gravity duality demonstrates that this information is carried away by the Hawking radiation. Despite the progresses obtained by current theories, today there is yet the problem whether the Hawking radiation carries information about matter that falls in the black hole and whether the quantum information encoded by the matter that collapsed to originate the black hole is destroyed and lost forever. The conflicts between quantum mechanics and general relativity as regards the treatment of black holes can be summarized in the two famous information paradox and firewall paradox.

In order to face the information paradox, in some famous works Susskind et. al. [2-4] suggested the so-called black hole complementarity, namely the idea that the information is both emitted at the horizon and passes through the horizon in such a way that a freely falling observer crossing the horizon would detect nothing out of the ordinary, while an external fixed observer sees this information emitted by complicated dynamics at or very near the horizon, detecting a significant feature known as the "stretched horizon". In this picture, quantum mechanics is saved at the cost of locality because the location of information in the Hilbert space cannot be found. According to the Susskind model, an observer who falls into a black hole after extracting information from the Hawking radiation would not be able to detect the same information inside the black hole before reaching the spacelike singularity, considering that the information absorbed by the black hole can be recreated after the so-called Page time [5]. In other successive works, Hayden and Preskill [6] suggested that, if information is thrown into a black hole after the Page time, it is possible to evade the duplication of information because that it can still be reconstructed after the so-called scrambling time, which is usually less than the Page time.

An alternative way to handle the black hole information paradox could be the consideration of creation of particle–antiparticle pairs on the event horizon and of the escape of a particle when black hole captures its antimatter partner. However, this path does not allow a satisfactory solution, because of the quantum entanglement property named monogamy (i.e. the fact that double entanglement is not permitted to particles simultaneously). In order to avoid a multiple entanglement among particles, antiparticles and Hawking radiation,

Almheiri, Marolf, Polchinski and Sully (AMPS) proposed the idea of a breaking of the particle-antiparticle entanglement at the horizon. In the AMPS model, the release of energy corresponding with this broken entanglement generates the formation of a "firewall" at the black hole boundary, which avoids any act of penetrating the interior of the black hole horizon [7-9], by burning up any infalling observer. AMPS argued that the three assumptions of black hole complementarity, i.e.:

1. Hawking radiation is pure (in the sense that is kept in pure states);
2. Effective field theory is valid outside a stretched horizon;
3. infalling observers encounter nothing unusual as they cross the horizon (i.e. any low-energy dynamics these observers can probe near their worldlines is well-described by familiar Lorentz-invariant effective field theory)

cannot be simultaneously self-consistent. Assuming then that effective field theory is valid and that Hawking radiation is pure, the AMPS work showed that the paradox regarding the simultaneous considerations of these three assumptions of black hole complementarity can be avoided only if photons, emitted with the Hawking radiation, which is traced backward in its path, and modes behind the horizon are not entangled (because a possible entanglement would provoke violations of semiclassical physics at macroscopic distances from the horizon). A crucial point of the AMPS model lies in the fact that equivalence principle, Hawking radiation and quantum entanglement cannot be considered together all, i.e. that one assumption must be removed in order to make the theory self-consistent. In particular, if the entanglement is eliminated, it means that Hawking radiation will no longer be linked to particles that have passed the event horizon, and we cannot predict the information which fell into the horizon through Hawking radiation: in this way, a loss of information and consequently a violation of the conservation of information occur. On the basis of the AMPS work, the information is saved if one considers the formation of a firewall built of a set of high-energy particles near the horizon of the original black hole and that stores the information contained inside the black hole.

However, the implications of the firewall are someway problematic. In the light of Hawking's results [10], the action of the horizon as a "firewall" proposed by AMPS violates the equivalence principle predicted by general relativity and breaks the CPT invariance of quantum gravity. As an alternative proposal, Hawking suggested that, in the formation of a black hole, no real event horizon is formed behind which information is lost and somehow the gravitational

collapse generates only apparent horizons and does not continue beyond them. In this picture, therefore, there would be no black holes, in the sense of regimes from which light cannot escape to infinity and black holes should be only defined as metastable bound states of the gravitational field. Recently, Vaz [11] developed the Hawking idea of the apparent horizon as final result of the gravitational collapse by considering a quantum gravitational model of dust collapse, which implies that a nonstop collapse towards a singularity emerges only if one considers a combination of two independent solutions of the Wheeler-DeWitt equation in terms of shell wave functions:

$$\psi_i = \psi_i^{(1)} + A_i \psi_i^{(2)} \quad (1)$$

where $\psi_i^{(1)}$ represents dust shells condensing to the apparent horizon on both sides of it and $\psi_i^{(2)}$ represents dust shells that move away from the apparent horizon on either side of it where the exterior, outgoing wave is suppressed by the Boltzmann factor at the Hawking temperature for the shell. In this picture, the AMPS firewall paradox is avoided if A_i tends to zero, thus making $\psi_i^{(1)}$ the complete description of the quantum collapse till the apparent horizon.

In this paper, we want to throw new light as regards the explanation of the information loss paradox and firewall paradox of black holes, which go beyond the results obtained by Vaz, on the basis of some interesting insights that can be found in the current literature on the subject.

Before all, as regards the effects associated with matter approaching a black hole horizon within the framework of quantum physics, some recent developments have been performed which do not require additional bizarre assumptions about spacetime structure or modifications to quantum mechanics. In particular, the problem of an information paradox has recently received a new re-reading on the basis of the observation that, close to the event horizon of a black hole, there is a modification of the homotopy class of particle trajectories, and this topological property causes a local alteration of quantum statistics in any collective system of indistinguishable identical particles that pass internally from the rim of the photon sphere (at a distance of $1.5r_S$ from a central singularity of a Schwarzschild black hole, where r_S is the event horizon radius) [12]. A release of energy is associated with this quantum collective statistics transition, compatibly with unitary evolution in quantum mechanics. This release of energy implies the generation of some kind of firewall located at the photon sphere rim instead of a hypothetical one on the event horizon.

According to the author of the present paper, the idea of the formation of a firewall positioned at the photon sphere rim seems compatible with the idea of the gravitational collapse of the black hole till an apparent horizon (as the one invoked by Vaz in [11]), where the photon sphere expands from the photon rim to the apparent horizon. On the basis of the results obtained in [13], an important feature of the photon sphere rim lies in the fact that, if a particle was passing the photon sphere rim inward, an inevitable falling occurs toward the apparent horizon: in the region $r_S < r < 1.5r_S$, the trajectories are spirals directed towards the horizon for particles that overcome the photon sphere rim. As a consequence of the fact that the particles devoid of quantum statistics create a pure quantum state of individual particles which cannot interchange their positions, the entropy or information connected to quantum statistics are not carried by the matter that next crosses the apparent horizon, and this constraint modifies premises for the information paradox [14, 15], in that the role of some kind of firewall is taken by the radiation burst released during the passing by the falling matter of the photon sphere rim relatively distantly from the apparent horizon.

Moreover, according to the author, another important line of research that is worth to be followed is represented by the so-called "Generalized Uncertainty Principle", which extends the usual Heisenberg's Uncertainty Principle in the quantum-gravity regime [16] and has the merit to introduce new scenarios in the exploration of the thermodynamics of black holes as well as the duality between elementary particles and black holes [17-24]. There are several facts that evidence the potential of the generalized uncertainty principle in providing new keys of understanding of the issues connected to black holes. For example, it has been demonstrated that the parameter appearing in the generalized uncertainty principle is proportional to the number of fields [25] and that the generalized uncertainty principle may provide a natural picture in order to reconcile unitarity as perceived by an exterior observer who remains coherent with [macroscopic] superpositions of black hole states, and the infalling observer who does not experience anything special at the horizon, fully in agreement with quantum field theory on curved spacetime in its regime of validity [26]. Moreover, despite the implications of generalized uncertainty principle for information loss problem have not yet been well-studied, the generalized uncertainty principle can throw new light also on the black hole information paradox by suggesting that there is not a loss of information when a black hole evaporates, but instead is encoded and retrieved through quantum effects near the black hole. In

particular, in [27], two distinct generalized uncertainty principle models have been considered, the first which embeds minimal length, the second which embeds both minimal length and maximal momentum where, through rigorous calculation of emission correlations and remnant entropy, it was found that the total entropy remains conserved, ensuring unitary evolution without information loss, thus providing a reconciliation between black hole thermodynamics and quantum mechanics principles and critical insights into resolving the information paradox through quantum gravity frameworks.

Now, in this paper, taking account of these recent results, we want to propose new alternative paths in order to fuel the debate about the treatment of the black hole information and firewall paradoxes. In this regard, we consider a model of a three-dimensional dynamical quantum vacuum (3D DQV), proposed by the author in recent papers [28-36], which postulates the existence of an underlying variable quantum vacuum energy density and, by starting from a peculiar specific form of generalized uncertainty relations, leads to define a universal scale that provides a unified treatment of macroscopic regime of black holes and quantum regime of elementary particles.

The paper is organized as follows. In section 2, we review the fundamental features of the background space invoked by our model of the 3D DQV. In section 3 we explore our interpretation of time as a sequential numerical order of material change ultimately emerging from the dissipative features of the 3D DQV. In section 4, we show how the dissipative features of the vacuum allow us to avoid the concept of firewall at the boundary of a black hole, leading directly to new perspectives of solution of the paradoxes connected to the three assumptions of black hole complementarity. In section 5 we explore how the information loss in black holes can be treated in our model. In section 6 we analyse the relation between interior evolution and exterior evolution of a black hole. Finally, in section 7 we recap the main results of the paper.

2. The geometrodynamic picture of the three-dimensional dynamical quantum vacuum and the sub-Planckian black holes of the variable energy density

In the model of the 3D DQV, the geometric features of the background are associated with the following peculiar specific form of generalized uncertainty relations, which are valid at the Planck scale:

$$\Delta x \Delta p \geq \frac{\hbar}{2}\left(1+\beta l_p^2 \frac{\Delta \rho_{qvE}^2 V^2}{\hbar^2 c^2}\right) \quad (2).$$

In equation (2) $\Delta\rho_{qvE}$ is the variable energy density of the vacuum corresponding to the appearance of a material particle of mass m in a volume V, defined as

$$\Delta\rho_{qvE} \equiv \rho_{pE} - \rho_{qvE} = \frac{mc^2}{V} \quad (3),$$

where

$$\rho_{pE} = \frac{M_{Pl}c^2}{l_p^3} \quad (4)$$

is Planck's energy density (M_{Pl} being Planck's mass, c the light speed and l_p Planck's length) intended as the ground state of the 3D DQV, β is a fluctuating dimensionless parameter which expresses the fact that here one deals with quantum vacuum fluctuations, associated with virtual particles, that fix the minimal length scale only on average, $\hbar$ is Planck's reduced constant and the term $\frac{\hbar}{2}\beta l_p^2 \frac{\Delta\rho_{qvE}^2 V^2}{\hbar^2 c^2}$ measures the degree of violations of the Heisenberg uncertainty relations at scales that approach the Planck scale. The generalized uncertainty relations (14) is directly derived by starting from the operators

$$\hat{P}_k^2 = \left(1 + \beta l_p^2 \frac{\Delta\rho_{qvE}^2 V^2}{\hbar^2 c^2}\right)\hat{p}_k \quad (5)$$

$$\hat{X}_j = \hat{x}_j + O(\beta^2) \quad (6)$$

where $\hat{x}_j$ and $\hat{p}_k$ satisfy the ordinary Heisenberg uncertainty relations, which obey the commutator

$$[\hat{X}, \hat{P}] = i\hbar\left(1 + \beta l_p^2 \frac{\Delta\rho_{qvE}^2 V^2}{\hbar^2 c^2}\right) \quad (7).$$

By starting from the generalized uncertainty relations (2), one obtains a suggestive unification of the quantum regime of elementary particles and the macroscopic regime of black holes in terms of a generalized Compton wavelength which provides a unified expression for the Compton wavelength and Schwarzschild radius, given by relation

$$R'_C = R'_S = \sqrt{\left(\frac{\beta\hbar c}{\Delta\rho_{qvE}V}\right)^2 + \left(\beta l_p^2 \frac{\Delta\rho_{qvE}V}{\hbar c}\right)^2} \quad (8).$$

On the basis of the generalized Compton wavelength (8), one recovers the standard value of the Schwarzschild radius for $\frac{\Delta\rho_{qvE}V}{c^2} \gg M_{Pl}$ where M_{Pl} is the Planck mass, and the standard value of the Compton wavelength associated to an elementary particle for $\frac{\Delta\rho_{qvE}V}{c^2} \ll M_{Pl}$. The physical meaning of equation (8) is that the origin of elementary particles of the quantum world and of material objects and black holes of macroscopic regime is represented by elementary objects of the

Planck scale, namely sub-Planckian black holes with a size of order of their Compton wavelength, i.e. opportune aggregates of one or more virtual particles of the 3D DQV corresponding to the geometrodynamic properties of the variable quantum vacuum energy density.

In the model of the 3D DQV, the generalized Compton wavelength can be considered as the universal scale where quantum regime and general relativity can be unified. The activity of the sub-Planckian black holes of the underlying variable energy density at the scale (8), generates a deformation of the geometrical properties of the background expressed by a quantum-modified Schwarzschild metric which has the following form

$$ds^2 = F(r)c^2dt^2 - F(r)^{-1}dr^2 - r^2d\Omega^2 \quad (9)$$

where

$$F(r) = 1 - \frac{\sqrt{\left(\frac{\beta\hbar c}{\Delta\rho_{qvE^V}}\right)^2 + \left(\beta l_p^2 \frac{\Delta\rho_{qvE^V}}{\hbar c}\right)^2}}{r} + \varepsilon \frac{\left(\frac{\beta\hbar c}{\Delta\rho_{qvE^V}}\right)^2 + \left(\beta l_p^2 \frac{\Delta\rho_{qvE^V}}{\hbar c}\right)^2}{4r^2} \quad (10)$$

and $d\Omega^2 = d\theta^2 + sin^2\theta d\phi^2$ is the metric on the 3-sphere and ε is a dimensionless deformation parameter of the metric that, in analogy to the treatment made in [37], satisfies the constraint $|\varepsilon| \leq 1$. The standard Schwarzschild metric of general relativity can be considered as a special case of the more general quantum-modified metric (10), in the sense that the quantum-modified metric (10) determines corrections in the values of the global deflection angle of light, the total precession of the orbit of a planet, the time dilation and the gravitational red-shift with respect to the corresponding formulations predicted by standard general relativity, leading to general formulas which allow the standard corresponding general relativistic relations to be recovered under appropriate limits [38]. Moreover, the impact of the deformation parameter ε in the Hawking temperature of black holes has been explored, showing reduced quantum evaporation rates for positive values of ε and enhanced Hawking radiation for negative values of ε [39].

The generalized Compton wavelength (8) plays an important role also as regards cosmology. In fact, in our theory each micro-region of the universe here can be described by a wave-function Ψ (which is a function of the scale factor a and of the scalar fields φ associated with the quantum vacuum energy density fluctuations as well as the polarization of the vacuum), that satisfies a peculiar form of Wheeler-DeWitt (WDW) equation, intended as an equation of background, a real "equation of everything" where all the possibilities of the physical world are written in timeless form:

$$\ddot{\Psi} + \frac{k\left(\left(\frac{\beta\hbar c}{\Delta\rho_{qvE}V}\right)^2 + \left(\beta l_p^2 \frac{\Delta\rho_{qvE}V}{\hbar c}\right)^2\right)^{3/2}\Delta\rho_{qvE}}{ac^2\sqrt{\alpha}}\Psi + \omega^2(a)\Psi = 0 \quad (11).$$

In equation (11), $\dot{\Psi} = \frac{\partial\Psi}{\partial a}$, α is the fine-structure constant, ω is the mode frequency linked with the scale factor and, finally, k is an adimensional parameter corresponding to the size of the condensate of virtual sub-particles of the 3D DQV, namely represents a sort of effective parameter of density of the virtual particles of the medium [40]. By invoking the third quantization formalism, the wave function Ψ of the universe satisfying WDW equation (11) is promoted to the role of operator, which can be expressed as

$$\hat{\Psi}_{\pm} = \frac{V\Delta\rho_{qvE}}{\sqrt{2\pi}\hbar l_p^2}\int d\rho\left(e^{\pm i\frac{V\Delta\rho_{qvE}}{\hbar l_p^2}\varphi}\Psi_{\Delta\rho_{qvE}}(a)\hat{b}_{\Delta\rho_{qvE}} + e^{\mp i\frac{V\Delta\rho_{qvE}}{\hbar l_p^2}\varphi}\Psi^*_{\Delta\rho_{qvE}}(a)\hat{b}^{\dagger}_{\Delta\rho_{qvE}}\right) \quad (12)$$

where $\hat{b}_{\Delta\rho_{qvE}}$ and $\hat{b}^{\dagger}_{\Delta\rho_{qvE}}$ are the annihilation and creation operators which annihilate and create respectively micro-universes, associated with corresponding changes of the quantum vacuum energy density, and satisfy the "quantum Boltzmann statistics" that consists of a q deformation of the commutation relations of the oscillators, given by the following relation

$$\hat{b}_k\hat{b}_l^{\dagger} - q\hat{b}_l^{\dagger}\hat{b}_k = \delta_{kl} \quad (13)$$

where the cases $q = \pm 1$ correspond to bosons and fermions. Here, the quantum operators $\hat{b}_{\Delta\rho_{qvE}}$ and $\hat{b}^{\dagger}_{\Delta\rho_{qvE}}$ are embedded in the mathematical formalism in relation to space-time in the sense that their properties are intrinsically connected to the symmetries of space-time and the way micro-universes (that can give origin to bosons or fermions) behave under transformations in the background.

The generalized Compton wavelength defines a granular structure of the 3D DQV background in the sense that one deals here with elementary cells that contain the information

$$I = \frac{A}{l_p^2} \quad (14)$$

where

$$A = k\left[\left(\frac{\beta\hbar c}{\Delta\rho_{qvE}V}\right)^2 + \left(\beta l_p^2\frac{\Delta\rho_{qvE}V}{\hbar c}\right)^2\right] \quad (15)$$

is the area of the cell. The information (14) of the elementary cells of the 3D DQV is the fundamental element that gives rise to the appearance of a particle. In particular, the wave function (12) of a micro-universe satisfying the generalized WDW equation (11) gives

origin to the manifestation of a corresponding particle characterized by the chronon scale if the information (14) satisfies relation $I^3 l_p \approx 10^{-13} cm$, namely

$$\frac{k^3}{l_p^5}\left[\left(\frac{\beta\hbar c}{\Delta\rho_{qvE}V}\right)^2+\left(\beta l_p^2\frac{\Delta\rho_{qvE}V}{\hbar c}\right)^2\right]^3 \approx 10^{-13} cm \quad (16).$$

On the basis of equation (16), an interesting aspect of the interpretation of elementary particles in the model of the 3D DQV ruled by the generalized Compton wavelength lies in the possibility of choosing opportunely the parameter k that defines the size of the condensate of the virtual sub-particles of the medium in order to obtain the appearance of the desired particle of the Standard Model with its usual properties. As a consequence, here the chronon scale of ordinary Standard Model particles can be interpreted as the emergence scale of processes of collective organization of opportune condensates of the virtual sub-particles of the 3D DQV which take place at the generalized Compton wavelength.

3. Time and dissipative features of the vacuum

In the model of the 3D DQV, the variable quantum vacuum energy density ultimately corresponding to the foam of the virtual particles of the vacuum give origin to elementary objects, namely sub-Planckian black holes, with a size of order of their generalized Compton wavelength, which can be considered as the common matrix that can give origin to elementary particles or black holes. In this picture, an ultimate quantum nature characterizes all black holes, and each subatomic particle, at the deepest level, derives from something which has similar properties of a black hole. Moreover, by following [41, 42], we consider that sub-Planckian black holes of the variable quantum vacuum energy density can be described by a cyclic intrinsic Compton periodicity, intended as the fundamental connecting element between the particle aspect and the black hole aspect of these elementary objects. In particular, here we assume that the intrinsic Compton periodicity of the sub-Planckian black holes of the variable energy density is generated, at a fundamental level, by the dissipative features of the vacuum at the generalized Compton wavelength, expressed by an opportune dispersion relation of the form

$$\omega^2 = c^2k^2 - \frac{c^4\hbar^2}{\Delta\rho_{qvE}{}^2V^2}k^4 \quad (17)$$

where the wave number k is assimilated just to the inverse of the generalized Compton wavelength (8), yielding

$$\omega^2 = \frac{c^2}{\left(\frac{\beta\hbar c}{\Delta\rho_{qvE^V}}\right)^2 + \left(\beta l_p^2 \frac{\Delta\rho_{qvE^V}}{\hbar c}\right)^2} - \frac{c^4\hbar^2}{\Delta\rho_{qvE}{}^2 V^2\left[\left(\frac{\beta\hbar c}{\Delta\rho_{qvE^V}}\right)^2 + \left(\beta l_p^2 \frac{\Delta\rho_{qvE^V}}{\hbar c}\right)^2\right]^2} \quad (18) \quad [43].$$

The dissipative features of the 3D DQV described by the dispersion relation (18) imply that time/clock is described by states that are ruled by a non-linear Schrödinger equation, a peculiar version of the Gross–Pitaevskij equation of the form

$$i\hbar\frac{\partial\psi}{\partial t} = \frac{-\hbar^2}{2m}\nabla^2\psi + \frac{a^2}{2\pi}\left(\sqrt{\frac{c^2}{\left(\frac{\beta\hbar c}{\Delta\rho_{qvE^V}}\right)^2 + \left(\beta l_p^2 \frac{\Delta\rho_{qvE^V}}{\hbar c}\right)^2} - \frac{c^4\hbar^2}{\Delta\rho_{qvE}{}^2 V^2\left[\left(\frac{\beta\hbar c}{\Delta\rho_{qvE^V}}\right)^2 + \left(\beta l_p^2 \frac{\Delta\rho_{qvE^V}}{\hbar c}\right)^2\right]^2}}\right) m|\psi|^2\psi + U\psi \quad (19).$$

In this equation, m is the mass of each sub-planckian black hole of the physical vacuum, U is the potential energy relating to the single virtual particle and ν is a viscosity coefficient having the dimensions $\frac{length^2}{time}$ which can be expressed as $\nu = \frac{a^2\omega}{2\pi}$ where a is the scattering length between the virtual particles. As a consequence of the dissipative hydrodynamics described by the Gross-Pitaevskij equation (19), the time marked by the clock has the physical meaning of sequential numerical order of material change associated with the dynamics of the system into consideration, that can be associated to the inverse of the frequency defined by the dispersion relation (17), namely

$$t = \frac{1}{\sqrt{\frac{c^2}{\left(\frac{\beta\hbar c}{\Delta\rho_{qvE^V}}\right)^2 + \left(\beta l_p^2 \frac{\Delta\rho_{qvE^V}}{\hbar\ c}\right)^2} - \frac{c^4\hbar^2}{\Delta\rho_{qvE}{}^2 V^2\left[\left(\frac{\beta\hbar c}{\Delta\rho_{qvE^V}}\right)^2 + \left(\beta l_p^2 \frac{\Delta\rho_{qvE^V}}{\hbar\ c}\right)^2\right]^2}}} \quad (20)$$

The physical meaning of equation (20) is just that the entanglement between the evolving system and the clock generates a counter function labelled by the hands of the clock which is linked with the frequency modes of the 3D DQV, namely with the variations of the quantum vacuum energy density, that are ultimately determined by the dissipative features of the vacuum at the generalized Compton wavelength. Therefore, in summary, we can consider that the intrinsic Compton periodicity characterizing the proto-particles of the vacuum, i.e. the sub-planckian black holes of the variable quantum vacuum energy density, is ultimately associated with the dissipative features of the vacuum at the generalized Compton wavelength and is expressed by equation (20).

4. Gravitational collapse and the apparent horizon

The dissipative features of the vacuum at the generalized Compton wavelength, by determining the intrinsic periodicity (20) of the sub-planckian black holes of the variable quantum vacuum energy density, introduce new suggestive perspectives of treatment of the paradoxes connected with the physics of black holes.

The frequency modes of the 3D DQV associated with the variations of the quantum vacuum energy density at the generalized Compton wavelength lead to sub-Planckian black holes characterizing by an intrinsic periodicity which allows us to avoid the paradoxes connected with the simultaneous consideration of the three fundamental assumptions underlying black hole complementarity invoked by AMPS. In other words, the model of sub-Planckian black holes of the 3D DQV where the dissipative features at the generalized Compton wavelength lead to an intrinsic periodicity expressed by equation (20), implies that the three fundamental assumptions underlying black hole complementarity are not necessarily incompatible. This derives from the fact that, in the light of the dissipative features of the 3D DQV at the generalized Compton wavelength, the result of the gravitational collapse is represented by extremely compact quantum objects that are ruled by quantum gravity processes and that lead to the formation of an apparent horizon whose area acts as a coarse-grained entropy.

The model based on the dissipative features of the 3D DQV can go beyond the results of Vaz's quantum gravitational model of dust collapse based on the wave function (1). By replacing the standard Wheeler-DeWitt equation with the equation of background (11) whose general solutions are the wave functions (12), the gravitational collapse involving the birth of black holes can be described by means of a lattice of collapsing dust shells, namely micro-universes, determined by the elementary sub-Planckian black holes of the variable energy density, defined by the following wave functions

$$\Phi_{\pm} = \begin{cases} \frac{V\Delta\rho_{qvE}}{\sqrt{2\pi}\hbar l_p{}^2}\, e^{\hbar\sqrt{\left(\frac{\beta hc}{\Delta\rho_{qvE}V}\right)^2+\left(\beta l_p^2\frac{\Delta\rho_{qvE}V}{\hbar\ c}\right)^2}\ \Delta\rho_{qvE}{}^2V^2\left[\left(\frac{\beta hc}{\Delta\rho_{qvE}V}\right)^2+\left(\beta l_p^2\frac{\Delta\rho_{qvE}V}{\hbar\ c}\right)^2\right]^{\frac{1}{2}}d} \int d\rho\left(e^{\pm i\frac{V\Delta\rho_{qvE}}{\hbar l_p{}^2}\varphi}\Psi_{\Delta\rho_{qvE}}(a)\hat{b}_{\Delta\rho_{qvE}}+e^{\mp i\frac{V\Delta\rho_{qvE}}{\hbar l_p{}^2}\varphi}\Psi^*_{\Delta\rho_{qvE}}(a)\hat{b}^{\dagger}_{\Delta\rho_{qvE}}\right) \\ \frac{V\Delta\rho_{qvE}}{\sqrt{2\pi}\hbar l_p{}^2}\, e^{\hbar\sqrt{\left(\frac{\beta hc}{\Delta\rho_{qvE}V}\right)^2+\left(\beta l_p^2\frac{\Delta\rho_{qvE}V}{\hbar\ c}\right)^2}\ \Delta\rho_{qvE}{}^2V^2\left[\left(\frac{\beta hc}{\Delta\rho_{qvE}V}\right)^2+\left(\beta l_p^2\frac{\Delta\rho_{qvE}V}{\hbar\ c}\right)^2\right]^{\frac{1}{2}}\left(d-\frac{\pi}{\hbar g_h}\right)} \int d\rho\left(e^{\pm i\frac{V\Delta\rho_{qvE}}{\hbar l_p{}^2}\varphi}\Psi_{\Delta\rho_{qvE}}(a)\hat{b}_{\Delta\rho_{qvE}}+e^{\mp i\frac{V\Delta\rho_{qvE}}{\hbar l_p{}^2}\varphi}\Psi^*_{\Delta\rho_{qvE}}(a)\hat{b}^{\dagger}_{\Delta\rho_{qvE}}\right) \end{cases} \quad (21).$$

The micro-universes described by equation (21) represent dust shells condensing to an apparent horizon, where g_h is the surface gravity at the apparent horizon and d is an opportune parameter $d = d(\Delta\rho_{qvE})$ that depends of the variable energy density corresponding to the formation of the shells. These dust shells have bound states of energy that can be determined by considering the following potential of interaction between the fluctuations of the quantum vacuum energy density and the quantum compact object

$$V(r) = -G\frac{\Delta\rho_{qvE}Vm}{2Rc^2} \quad (22)$$

where m is the mass of the dark compact object associated with the spherical massive shell and R is the radius of the shell. In analogy to what happens in the hydrogen atom, on the basis of the potential of interaction (22), one obtains the following bound states of energy of the dust shells:

$$E_n = -\frac{1}{n^2}\frac{G^2m^3\Delta\rho_{qvE}^2V^2}{2\hbar^2c^4} \quad (23)$$

that lead to the following mass spectrum of the shells:

$$m_n = \frac{2}{n^2}\frac{G^2\Delta\rho_{qvE}^4V^4}{\hbar^2c^4} \quad (24).$$

As a consequence of the intrinsic non-locality associated with the quantum Boltzmann statistics satisfied by the creation and annihilation operators appearing in the wave functions (21), the position of the physical quantum shells generated during the gravitational collapse cannot be exactly localized but can be defined through an average radius expressed by relation

$$\langle R_n\rangle = \frac{3}{2}\frac{m_nc^2}{\Delta\rho_{qvE}V}\sqrt{\left(\frac{\beta\hbar c}{\Delta\rho_{qvE}V}\right)^2 + \left(\beta l_p^2\frac{\Delta\rho_{qvE}V}{\hbar c}\right)^2} \quad (25).$$

The minimum value of the radius of these shells, in Planck units, can be computed as the difference between the volume of the sphere having radius $\langle R_n\rangle + \frac{1}{2}l_p$ and the volume of the sphere having radius $\langle R_n\rangle - \frac{1}{2}l_p$:

$$V_{min} = \frac{4}{3}\pi\left[\left(\langle R_n\rangle + \frac{1}{2}l_p\right)^3 - \left(\langle R_n\rangle - \frac{1}{2}l_p\right)^3\right] = \frac{4}{3}\pi\left[3\langle R_n\rangle^2l_p + \frac{1}{4}l_p^3\right] = 4\pi\langle R_n\rangle^2l_p + \frac{\pi}{3}l_p^3 \quad (26).$$

Therefore, taking account of the mass spectrum (24), one finds the following expression for the maximum value of the density of the shells:

$$\sigma_{max} = \frac{2G^2\Delta\rho_{qvE}^4V^4}{n^2\hbar^2c^4\left(4\pi\langle R_n\rangle^2l_p + \frac{\pi}{3}l_p^3\right)} \quad (27)$$

This result is in agreement with the results obtained by Corda in [44] and, at the same time, shows how the maximum value of the density of

the shells generated during the gravitational collapse of the black hole is determined by variable energy density and, above all, taking account of relation (25), by the processes at the generalized Compton wavelength. In other words, we can say that the evolution of the collapsing dust shells described by the wave functions (21) leads to the formation of an apparent horizon if the density of the shells is characterized by a maximum density (27) that is directly fixed by the fluctuations of the variable energy density at the generalized Compton wavelength.

Moreover, the process of gravitational collapse of the dust shells can be associated to a corresponding behaviour of the entropy of the collapsing matter. In this regard, taking account the results obtained in [45], the formation of a black hole involves processes where the entropy of collapsing matter is converted into that of the vacuum and, during these processes, because of the entanglement between the vacuum and the arising Hawking radiation, which leads, as a consequence of the evaporation process, to the entanglement among the final-state Hawking quanta, the horizon is soft and no firewall develops. As a consequence, during the gravitational collapse of the dust shells that leads to the formation of an apparent horizon, we can consider that the black hole entropy is generated by the interaction between the virtual particles associated with the fluctuations of the 3D DQV and the black hole's apparent horizon, as well as by the entanglement between the virtual particles of the vacuum and the arising Hawking radiation. These processes of interaction imply, on the basis of the results obtained in [46], that the area of the apparent horizon μ acts as a sort of coarse-grained entropy:

$$S^{coarse} = \frac{Area\,[\mu]}{4G\hbar} \quad (28),$$

in a picture where the area of the apparent horizon can be interpreted statistically as the maximum boundary entropy that is compatible with the geometry of its exterior and therefore with the maximum density of the shells (27). Now, if the coarse-grained entropy of the apparent horizon is constrained by the maximum density of the shells (27), as a consequence of this fact, the area of the apparent horizon appearing in equation (28) derives from the geometry of the shells on the basis of relation

$$Area\,[\mu] = \frac{m_n \langle R_n \rangle}{\sigma_{max}} \quad (29)$$

namely

$$Area\,[\mu] = \frac{3}{2}\frac{m_n c^2}{\Delta\rho_{qvE} V}\sqrt{\left(\frac{\beta\hbar c}{\Delta\rho_{qvE} V}\right)^2 + \left(\beta l_p^2 \frac{\Delta\rho_{qvE} V}{\hbar c}\right)^2}\,.$$

$$\cdot\left(9\pi\frac{m_n{}^2c^4}{\Delta\rho_{qvE}{}^2V^2}\left[\left(\frac{\beta\hbar c}{\Delta\rho_{qvE}V}\right)^2+\left(\beta l_p^2\frac{\Delta\rho_{qvE}V}{\hbar c}\right)^2\right]l_p{}^2+\frac{\pi}{3}l_p^3\right) \quad (30).$$

By substituting equation (30) inside equation (28) and taking account of relations (25) and (24), one finds the final expression of the coarse-grained entropy (29):

$$S^{coarse}=\frac{3}{8}\frac{m_nc^2}{G\hbar\Delta\rho_{qvE}V}\sqrt{\left(\frac{\beta\hbar c}{\Delta\rho_{qvE}V}\right)^2+\left(\beta l_p^2\frac{\Delta\rho_{qvE}V}{\hbar c}\right)^2}\cdot$$

$$\cdot\left(9\frac{m_n{}^2c^4}{\Delta\rho_{qvE}{}^2V^2}\left[\left(\frac{\beta\hbar c}{\Delta\rho_{qvE}V}\right)^2+\left(\beta l_p^2\frac{\Delta\rho_{qvE}V}{\hbar c}\right)^2\right]l_p{}^2+\frac{1}{3}l_p^3\right) \quad (31).$$

On the basis of equation (31), the coarse-grained entropy associated with the apparent horizon – that in current theories is widely accepted to be proportional to the area – here is directly determined by a more fundamental behaviour of the fluctuations of the quantum vacuum energy density that generate the dissipative features of the 3D DQV at the generalized Compton wavelength. According to the author, this is an important clue of the fact that the 3D DQV plays a fundamental role as regards the issues regarding the entropy of black holes.

The model developed in this chapter provides an important lesson as regards the paradoxes connected to the firewall and the AMPS work. The lesson is the following. The physical meaning of the approach based on equations (21)-(31) is that the sub-Planckian black holes of the variable energy density give rise to collapsing dust shells that will condense to an apparent horizon that therefore can be seen as the result of the opportune elementary fluctuations of the quantum vacuum energy density and, in particular, of the dissipative features of the 3D DQV at the generalized Compton wavelength. This means that, in the physics of black holes, there will be no further collapse, namely there will be no tunnelling into the exterior and no firewall as a consequence of the processes associated with the dissipative features of the vacuum at the generalized Compton wavelength, ultimately fixed by opportune behaviours of the variable quantum vacuum energy density. The intrinsic Compton periodicity of the sub-Planckian black holes of the variable energy density – that emerges from the dissipative features of the vacuum at the generalized Compton wavelength – allows us to replace the concept of firewall and central singularity with the idea of the apparent horizon, intended as the final stage of the wave functions (21) of the collapsing dust shells characterized by the maximum density (27). As a consequence of the dissipative features of the vacuum at the generalized Compton wavelength determined by opportune fluctuations of the variable quantum vacuum energy density, the area of the apparent horizon acts as the coarse-grained entropy

(31) and this action allows us to avoid the incompatibility determined by the simultaneous consideration of equivalence principle, Hawking radiation and quantum entanglement of the AMPS argument, that here are not violated, therefore restoring the conservation of information when information reaches the apparent horizon through Hawking radiation.

In this picture, the AMPS paradox is directly avoided without further assumptions, in the sense that, as a consequence of the processes determined by the dissipative features of the vacuum at the generalized Compton wavelength regarding the formation of an apparent horizon whose area acts as a coarse-grained entropy, the three hypotheses invoked by AMPS in [7, 8] are not necessarily incompatible and thus do not lead to paradoxes connected to the black hole complementarity. Our model, by predicting the generation of an apparent horizon characterized by the coarse-grained entropy (31) that is directly fixed by the dissipative features of the 3D DQV at the generalized Compton wavelength, implies that equivalence principle, Hawking radiation and quantum entanglement are not incompatible. By demonstrating in a direct way the impossibility of the formation of a firewall, it allows us to avoid the arguments involved in the AMPS work. In this way, our proposal of solution of the firewall paradoxes allows a new re-reading of the gravitational collapse of dust shells invoked by Vaz in [44], in the sense that here it can be associated to the coarse-grained entropy (31) of the area of the forming apparent horizon that is directly fixed by the dissipative features of the 3D DQV at the generalized Compton wavelength. The background of the sub-Planckian black holes of the variable energy density whose intrinsic periodicity is determined by the dissipative features of the vacuum on the basis of equation (20) and where the gravitational collapse is described by collapsing micro-universes defined by the wave functions (21) and by the maximum density (27), allows us to naturally avoid the idea of firewall and its connected paradoxes as a consequence of the formation of an apparent horizon characterized by a coarse-grained entropy which expresses the dissipative features of the dynamical processes at the generalized Compton wavelength. Moreover, an important consequence of this model lies in the possibility to avoid the existence of singularities, in the sense that – just as a consequence of the appearance of the coarse-grained entropy (31), associated with the maximum density of the collapsing dust shells (27) – the gravitational collapse of black holes do not continue till a central singularity but would terminate at the apparent horizon. We emphasize that this result is in good agreement with Hawking's proposal [10, 6], allowing above all a novel re-reading in terms of fundamental dynamical processes at

the universal scale represented by the generalized Compton wavelength. Finally, we underline that our model of sub-Planckian black holes of the 3D DQV, by considering a coarse-grained entropy (31) associated with the dissipative features of the 3D DQV at the generalized Compton wavelength, which implies a gravitational collapse till the condensation of quantum shells to the apparent horizon, provides a suggestive alternative path with respect Penrose's model regarding infinite space-time curvature in the centre of a black hole [47] and Kerr's model regarding gravitational singularity towards the centre of black hole [48, 49].

5. Entanglement effect of the apparent horizon and consequences regarding information of the black hole

As a consequence of the dissipative features of the 3D DQV at the generalized Compton wavelength and the emerging intrinsic periodicity of the sub-Planckian black holes of the variable energy density, the physics of the black holes is ruled by a gravitational collapse of dust shells that can be interpreted as micro-universes that are defined by the wave functions (21) and have maximum density (27). The final result of these processes of gravitational collapse lies in the generation of an apparent horizon whose area acts as a coarse-grained entropy (31) directly fixed by the fluctuations of the quantum vacuum energy density associated with the dissipative features of the 3D DQV at the generalized Compton wavelength, that has an important role in providing a solution to the paradoxes connected to the firewall. Now, in this section we want to show how our model allows us to make some progresses also as regards the information problem of black holes.

In this regard a key point is that, as a consequence of the creation and annihilation operators of micro-universes that appear in the wave functions (21), that are fixed by opportune quantum vacuum energy density fluctuations and satisfy the quantum Boltzmann statistics (13), and taking account the unavoidable falling toward the apparent horizon for any particle passing the photon sphere rim inward (demonstrated in [15]), the role of the apparent horizon lies in the generation of an entanglement between the information inside the black hole and the information above the photon sphere rim and, therefore, outside the black hole, thus making the interior spacetime of the black hole as an effective description of a given exterior time. In our approach, by using the quantum-modified Schwarzschild metric (10),

the trajectories of particles in various regions near the apparent horizon, on the basis of the treatment in [13, 50], may be expressed as:

$$r = \frac{\varepsilon_0}{mc^2}\int \frac{dr}{\left(1-\frac{\sqrt{\left(\frac{\beta\hbar c}{\Delta\rho_{qvE}V}\right)^2+\left(\beta l_p^2\frac{\Delta\rho_{qvE}V}{\hbar\, c}\right)^2}}{r}+\varepsilon\frac{\left(\frac{\beta\hbar c}{\Delta\rho_{qvE}V}\right)^2+\left(\beta l_p^2\frac{\Delta\rho_{qvE}V}{\hbar c}\right)^2}{4r^2}\right)\sqrt{\left(\frac{\varepsilon_0}{mc^2}\right)^2-\left(1+\frac{\mathcal{L}^2}{m^2c^2r^2}\right)\left(1-\frac{\sqrt{\left(\frac{\beta\hbar c}{\Delta\rho_{qvE}V}\right)^2+\left(\beta l_p^2\frac{\Delta\rho_{qvE}V}{\hbar\, c}\right)^2}}{r}+\varepsilon\frac{\left(\frac{\beta\hbar c}{\Delta\rho_{qvE}V}\right)^2+\left(\beta l_p^2\frac{\Delta\rho_{qvE}V}{\hbar c}\right)^2}{4r^2}\right)}} \tag{32}$$

for the trajectory radius, and

$$\varphi = \int dr\frac{\mathcal{L}}{r^2}\left[\frac{\varepsilon_0}{c^2}-\left(m^2c^2+\frac{\mathcal{L}^2}{r^2}\right)\left(1-\frac{\sqrt{\left(\frac{\beta\hbar c}{\Delta\rho_{qvE}V}\right)^2+\left(\beta l_p^2\frac{\Delta\rho_{qvE}V}{\hbar c}\right)^2}}{r}+\varepsilon\frac{\left(\frac{\beta\hbar c}{\Delta\rho_{qvE}V}\right)^2+\left(\beta l_p^2\frac{\Delta\rho_{qvE}V}{\hbar c}\right)^2}{4r^2}\right)\right] \tag{33}$$

for the azhimutal angle, where m, $\mathcal{L}$ and ε_0 are the particle mass, angular momentum and energy. Equations (32) and (33) imply that, in the region $(1-\varepsilon)\sqrt{\left(\frac{\beta\hbar c}{\Delta\rho_{qvE}V}\right)^2+\left(\beta l_p^2\frac{\Delta\rho_{qvE}V}{\hbar c}\right)^2} < r < 1.5(1-\varepsilon)\sqrt{\left(\frac{\beta\hbar c}{\Delta\rho_{qvE}V}\right)^2+\left(\beta l_p^2\frac{\Delta\rho_{qvE}V}{\hbar c}\right)^2}$, the trajectories regarding particles that pass the photon sphere rim appear as short spirals directed toward the apparent horizon as a consequence of the action of the dissipative features of the 3D DQV at the generalized Compton wavelength determined by opportune fluctuations of the quantum vacuum energy density.

Taking account the results obtained in [13] and the features of the trajectories expressed by equations (32) and (33), because of the quantum Boltzmann statistics that rules the collapsing dust shells determined by the dissipative features of the sub-Planckian black holes of the variable energy density at the generalized Compton wavelength, all particles entering the photon sphere from outside must fall inevitably towards the surface of the apparent horizon, that therefore emerges as source of an entanglement island between the information inside the black hole and the information outside the black hole. In other words, because of the attraction of the apparent horizon on any particle passing the photon sphere rim inward which can be associated to the gravitational collapse determined by the dissipative features of the 3D DQV at the generalized Compton wavelength, the "quantum Boltzmann statistics" that characterizes the creation and annihilation operators $\hat{b}_{\Delta\rho_{qvE}}$ and $\hat{b}^{\dagger}_{\Delta\rho_{qvE}}$ appearing in the wave function (21) of the collapsing shells implies the generation of an entanglement between the information inside the black hole and the information outside the black hole [51].

Now, the fundamental questions are the following. What is the link between the interior evolution and the exterior evolution as a consequence of the entanglement action of the surface of the apparent horizon? And, above all, what conclusions can we draw from the action of the surface of the apparent horizon as entanglement island as regards the perspectives of handling the information paradox? Our idea is the following. The result of the entanglement produced by the apparent horizon, by virtue of the generation of collapsing micro-universes associated with the wave functions (21) that imply the unavoidable falling toward the apparent horizon for any particle passing the photon sphere rim inward, lies in the formation of an effective time evolution that foliates the interior region that is different from the more fundamental, exterior time evolution, which foliates only the spacetime region outside the horizon. The surface of the apparent horizon, in the light of the dissipative features of the 3D DQV at the generalized Compton wavelength, acts as a sort of entanglement island, that indeed generates the connection between the information contained in the effective interior of the black hole and the modes outside the apparent horizon and, therefore, between the effective interior evolution and the fundamental exterior evolution.

By following the ER=EPR approach originally developed by Susskind and Maldacena [52], the action of the surface of the apparent horizon as an entanglement island between the information contained in the interior and the modes outside the apparent horizon can be associated with an opportune entanglement entropy determined by the energetic content of sub-Planckian black holes of the variable energy density at the generalized Compton wavelength on the basis of relation:

$$S_A = \frac{N_k \Delta\rho_{qvE}{}^2 V^3}{k_B \eta c^2} \frac{\left[\left(\frac{\beta\hbar c}{\Delta\rho_{qvE} V}\right)^2 + \left(\beta i \frac{\Delta\rho_{qvE} V}{\hbar c}\right)^2\right]}{4G} \quad (34)$$

where k_B is the Boltzmann constant, N_k is the number of the virtual particles of the vacuum in the volume V and the parameter η plays the role of an inverse temperature, that can be related with the texture of sub-Planckian black holes. The effect of the entanglement entropy (34) of the texture of sub-Planckian black holes is of determining a connection between the information contained in the interior and the modes outside the apparent horizon, in the sense that one deals here with a quantum superposition of the form

$$\psi(\eta) = \sum_k e^{-\frac{\eta N_k \Delta\rho_{qvE} V}{c^2 \; k_B}} |\psi_k\rangle \otimes |\psi_k\rangle \quad (35)$$

where $|\psi_k\rangle$ is the k-th energy eigenstate for a single mode outside the apparent horizon that can be associated with the wave functions (21)

satisfying the WDW equation (11). In other words, we can say that the fluctuations of the variable energy density at the generalized Compton wavelength determine the generation of a sort of quantum wormholes described by an entanglement entropy that is responsible of the connection between the information contained in the interior and the modes outside the apparent horizon and, therefore, between causally disconnected regions of the universe and their corresponding evolutions. The entanglement entropy which encodes the action of the surface of the apparent horizon as entanglement island between the information contained in the effective interior of the black hole and the modes outside the apparent horizon, introduces new perspective of explanation of the black hole information paradox. In fact, we can consider the possibility that the Hawking radiation, during its formation, becomes entangled with the region from the apparent horizon to the photon sphere rim, as a consequence just of the action of the surface of the apparent horizon as entanglement island, thus avoiding information loss during evaporation of the black hole. In other words, the entanglement entropy implies the generation of an entanglement between the forming Hawking radiation and the region between the apparent horizon and the photon sphere rim and, therefore, there is no information loss during evaporation of the black hole. And this action of the entanglement entropy in determining a connection between the Hawking radiation and the region between the apparent horizon and the photon sphere rim is transmitted by quantum wormholes which transmit the information between interior and exterior of the black hole. This means that the entanglement entropy of the apparent horizon allows a promising solution of the information paradox that avoids the violation of quantum mechanics' principle of unitarity.

The entanglement action of the surface of the apparent horizon corresponds to a deformation of the geometry described by the metric

$$ds^2 = -c^2\left(1-\frac{2G\Delta\rho_{qvE}Vr^2}{c^4\left(r^2+\left(\frac{\beta\hbar c}{\Delta\rho_{qvE}V}\right)^2+\left(\beta l_p^2\frac{\Delta\rho_{qvE}V}{\hbar c}\right)^2\right)^{3/2}}\right)dt^2 + \frac{dr^2}{1-\frac{2G\Delta\rho_{qvE}Vr^2}{c^4\left(r^2+\left(\frac{\beta\hbar c}{\Delta\rho_{qvE}V}\right)^2+\left(\beta l_p^2\frac{\Delta\rho_{qvE}V}{\hbar c}\right)^2\right)^{3/2}}} + r^2d\Omega^2 \quad (36)$$

where $d\Omega = \mathrm{d}\theta^2 + \sin^2\theta\mathrm{d}\varphi^2$. The metric (36) means that the entanglement action of the surface of the apparent horizon is associated to the actualization of wormholes that embed non-local

correlations, and therefore cause the generation of entangled states of disconnected regions of the universe in a similar way to the action of an ER bridge. In this way, one obtains in this approach a sort of generalization of the ER=EPR conjecture, in that the wormhole formation transmitting the information between the interior and the exterior of a black hole (i.e. above the photon sphere rim) corresponds to the dissipative features of fluctuations of the texture of sub-Planckian black holes at the generalized Compton wavelength. This means that texture of the sub-Planckian black holes are the real ultimate origin of the peculiar masses that can generate, through a gravitational collapse, a black hole till the apparent horizon. On the basis of the entanglement entropy (34), the metric (36) gives rise to the Bekenstein-Hawking entropy

$$S_A = \frac{N_k \Delta\rho_{qvE}{}^2 V^3}{k_B \eta c^2} \frac{\left[\left(\frac{\beta\hbar c}{\Delta\rho_{qvE}V}\right)^2 + \left(\beta l_p^2 \frac{\Delta\rho_{qvE}V}{\hbar c}\right)^2\right]}{4G} \cdot$$

$$\cdot \left(1 - \frac{8\pi\left[\left(\frac{\beta\hbar c}{\Delta\rho_{qvE}V}\right)^2 + \left(\beta l_p^2 \frac{\Delta\rho_{qvE}V}{\hbar c}\right)^2\right]}{A}\right) \sqrt{1 + \frac{4\pi\left[\left(\frac{\beta\hbar c}{\Delta\rho_{qvE}V}\right)^2 + \left(\beta l_p^2 \frac{\Delta\rho_{qvE}V}{\hbar c}\right)^2\right]}{A}} +$$

$$+ \frac{3\pi N_k \Delta\rho_{qvE}{}^2 V^3}{k_B \eta c^2} \left[\left(\frac{\beta\hbar c}{\Delta\rho_{qvE}V}\right)^2 + \left(\beta l_p^2 \frac{\Delta\rho_{qvE}V}{\hbar c}\right)^2\right] \cdot$$

$$\ln\left(\frac{1}{2l_0}\left(\sqrt{\frac{A}{\pi}} + \sqrt{\frac{A + 4\pi\left[\left(\frac{\beta\hbar c}{\Delta\rho_{qvE}V}\right)^2 + \left(\beta l_p^2 \frac{\Delta\rho_{qvE}V}{\hbar c}\right)^2\right]^2}{\pi}}\right)\right) \quad (37).$$

where A is the area of the wormhole metric, that plays the role of the cut through the ER bridge and is fixed by the generalized Compton wavelength. Now, by defining $A = 8\pi\left[\left(\frac{\beta\hbar c}{\Delta\rho_{qvE}V}\right)^2 + \left(\beta l_p^2 \frac{\Delta\rho_{qvE}V}{\hbar c}\right)^2\right]$, one obtains the following quantum-modified Bekenstein entropy associated with the sub-planckian black holes of the variable energy density acting as quantum wormholes:

$$S_A = \frac{3\pi N_k \Delta\rho_{qvE}{}^2 V^3}{k_B \eta c^2}\left[\left(\frac{\beta\hbar c}{\Delta\rho_{qvE}V}\right)^2 + \left(\beta l_p^2 \frac{\Delta\rho_{qvE}V}{\hbar c}\right)^2\right] \ln\left(\sqrt{2} + \sqrt{3}\right) \quad (38).$$

Therefore, we can say that the entanglement entropy (34) which encodes the action of the surface of the apparent horizon as entanglement island by generating an entanglement between the forming Hawking radiation and the region between the apparent

horizon and the photon sphere rim, therefore avoiding the information loss during evaporation of the black hole, determines a deformation of the metric that corresponds to the actualization of sub-planckian black holes acting as quantum wormholes, that are characterized by the quantum-modified Bekenstein entropy (38). The modified Bekenstein entropy (38) is in agreement with the treatment provided in [53] close to the zero-point (Planck) length. Moreover, the metric (36) and the corresponding quantum-corrected Bekenstein entropy (38) imply that the apparent horizon acting as entanglement channel between interior information and exterior information can be described by the characteristic length

$$r = \sqrt{2}\left[\left(\frac{\beta\hbar c}{\Delta\rho_{qvE^V}}\right)^2 + \left(\beta l_p^2 \frac{\Delta\rho_{qvE^V}}{\hbar c}\right)^2\right] \quad (39)$$

and by the characteristic mass

$$M = 3\sqrt{3}\frac{\sqrt{\left[\left(\frac{\beta\hbar c}{\Delta\rho_{qvE^V}}\right)^2 + \left(\beta l_p^2 \frac{\Delta\rho_{qvE^V}}{\hbar c}\right)^2\right]}}{4G}c^2 \quad (40).$$

Here, it is interesting to remark that, in the domain where the generalized Compton wavelength tends to the Planck length, the mass (40) leads to a numerical value of the mass that is close to the Planck mass.

If, as we have shown above, the entanglement entropy (34) of the surface of the apparent horizon, because of its action in generating an entanglement between the forming Hawking radiation and the region between the apparent horizon and the photon sphere rim, allows us to avoid information loss during evaporation of the black hole, in a similar way the sub-planckian black holes acting as quantum wormholes, described by the quantum-modified Bekenstein entropy (38), which transmit the information between the interior and the modes outside the apparent horizon, imply that there is no information loss after evaporation of the black hole. In the light of the non-local correlations embedded by the quantum wormholes that transmit the information between the interior and the modes outside the apparent horizon, some information about the interior might be detectable on the surface of the apparent horizon, where pairs of virtual particles jump in and out of existence in such a way that there is no paradox if one of these quantum entangled pairs is split up by the apparent horizon and is held in the black hole, while the other flies out as Hawking radiation. In this approach, there is therefore no paradox regarding the fate of the information contained in the black hole after its evaporation, in other words the information paradox is easily resolved also under these constraints.

The entanglement action of the surface of the apparent horizon can provide a new key of reading, at a deeper level, of the results recently obtained by Bousso and Penington, regarding the existence of entanglement surfaces that exist slightly outside the event horizon and that, for a supermassive black hole, could extend as much as an atom's length [54]. In fact, Bousso's and Penington's entanglement surfaces outside the event horizon and extending as an atom's length, can be seen as a result, as an emergent fact, from the more fundamental entanglement action of the surface of the apparent horizon described by the entanglement entropy (34) and the subsequent formation of quantum wormholes, that are characterized by the quantum-modified Bekenstein entropy (38) and transmit the information between the interior of the horizon and the modes outside the horizon. In other words, we consider the possibility that the entanglement islands outside the event horizon invoked by Bousso and Penington are indeed a macroscopic effect of a more fundamental, primordial action of entanglement provided by the surface of the apparent horizon that is described by the entanglement entropy (34), that produces a deformation of the geometry expressed by the metric (36) which in turn corresponds to the actualization of sub-planckian black holes acting as quantum wormholes which are described by the modified Bekenstein entropy (38), where all these processes are ultimately ruled by the dissipative features of the vacuum at the generalized Compton wavelength. Moreover, we underline that the entanglement action of the surface of the apparent horizon and the resulting n on-local action of the quantum wormholes that transmit the information between the effective interior and the modes in the exterior by means of the entanglement entropy (34) and the modified Bekenstein entropy (38) respectively, is compatible with the holographic approach – proposed in [55] – where, after the formation of a black hole from collapse, the information in the black hole interior remains encoded in the boundary, in such a way that the area of the black hole's apparent horizon is precisely the maximum holographic entanglement entropy that reproduces the geometry of the exterior.

6. About the relation between interior evolution and exterior evolution: the perspective effect

The mathematical formalism developed in section 5 shows that the interior spacetime of the black hole emerges as an effective description of a given exterior time. In this regard, on the basis of the treatment provided in [56], the interior of a black hole provides a way of reorganizing the degrees of freedom associated to the transitory

phenomenon of an infalling object dissolving into the (apparent) horizon. Here, the interior of the black hole can be seen as an inner boundary of spacetime, which holographically encodes the information inside, thus implying that the modes outside the horizon contain any information of the effective interior which therefore exists in the causal past of the Hawking radiation. As a consequence, the interior spacetime emerges as an effective description described by an effective theory containing a zone $r_S < r < r_Z$, where r_S is the location of the horizon in the Schwarzschild radial coordinate r, r_Z is the location of the outer edge of the near black-hole region inside the barrier of the effective gravitational potential generated by the black hole, up to a time

$$T_{t_x} = t_x + 2\frac{r_+}{c}\ln\frac{r_+}{l_p} \quad (41)$$

where r_+ is the radius of the apparent horizon of the black hole corresponding to the time $t_x < T_{evap}$.

Now, in the model of the 3D DQV, the treatment based on equation (41) suggested in [57] can receive a new re-reading that leads directly to a compelling solution of the problems connected to Hawking radiation, interior time evolution and exterior time evolution. In our model, because of the origin of the intrinsic periodicity of the sub-Planckian black holes of the 3D DQV from the dissipative features of the 3D DQV at the generalized Compton wavelength and the consequent processes of entanglement between interior information and exterior information of a black hole, that are determined by the apparent horizon and the resulting sub-planckian black holes acting as quantum wormholes, respectively encoded by the entanglement entropy (34) and the modified-Bekenstein entropy (38), the physics characterizing the black hole interior can be associated to a perspective effect ultimately fixed by the variable energy density of the 3D DQV, i.e. to an effective theory regarding a spacetime region K_{t_x} containing a portion of the zone $\sqrt{\left(\frac{\beta\hbar c}{\Delta\rho_{qvEV}}\right)^2 + \left(\beta l_p^2\frac{\Delta\rho_{qvEV}}{\hbar c}\right)^2} < r < r_Z$ where r_Z is the location of the outer edge of the near black-hole region inside the barrier of the effective gravitational potential generated by the black hole, only up to a time

$$T_{t_x} = t_x + 2\frac{r_+}{c}\ln\frac{r_+}{c\sqrt{\frac{c^2}{\left(\frac{\beta\hbar c}{\Delta\rho_{qvEV}}\right)^2 + \left(\beta l_p^2\frac{\Delta\rho_{qvEV}}{\hbar c}\right)^2}\frac{c^4\hbar^2}{\Delta\rho_{qvE}{}^2V^2\left[\left(\frac{\beta\hbar c}{\Delta\rho_{qvEV}}\right)^2 + \left(\beta l_p^2\frac{\Delta\rho_{qvEV}}{\hbar c}\right)^2\right]^2}}} \quad (42).$$

The time (42) is directly fixed by a corresponding behaviour of the variable energy density of the 3D DQV, in the sense that, in equation (42), r_+ is the radius of the apparent horizon of the black hole corresponding to the time t_x given by relation

$$t_x = \frac{\hbar\eta}{S_A} \quad (43)$$

where S_A is the modified Bekenstein entropy given by (38) and therefore

$$t_x = \frac{\hbar k_B \eta^2 c^2}{3\pi N_k \Delta\rho_{qvE}{}^2 V^3 \left[\left(\frac{\beta\hbar c}{\Delta\rho_{qvE} V}\right)^2 + \left(\beta l_p^2 \frac{\Delta\rho_{qvE} V}{\hbar c}\right)^2\right] \ln(\sqrt{2}+\sqrt{3})} \quad (44).$$

In other words, we can say that the time instants defined by (42) and (44) have the physical meaning of numerical orders of the opportune fluctuations of the quantum vacuum energy density, that are associated to opportune networks of sub-planckian black holes of the variable energy density.

On the basis of equations (42)-(44), the physics characterizing the interior portion of K_{t_x} of the black hole describes correlations between the degrees of freedom, that correspond to the time interval

$$t_x < t < T_{t_x} \quad (45)$$

and, therefore, can be interpreted as originating from the infalling time evolution generated by an opportune operator without involving a further exterior time evolution, because of the action of the dissipative features of the 3D DQV at the generalized Compton wavelength, that lead to the action of the apparent horizon as entanglement island and the consequent quantum wormholes, respectively described by the entanglement entropy (34) and the quantum-modified Bekenstein entropy (38), therefore generating the entanglement between interior information and exterior information. Therefore, in the model of the 3D DQV whose elementary constituents are sub-Planckian black holes characterized by dissipative features at the generalized Compton wavelength and that lead to collapsing dust shells described by the wave function (21) and by the maximum density (27), there is no paradox as regards the link between the interior time evolution to the black hole and the exterior time evolution. There is no contradiction between interior description and exterior description. The connection between the interior and the exterior time evolution of the black hole appears as a direct natural consequence of the rearrangement of correlations determined by the action of the surface of the apparent horizon as an entanglement island and transmitted by the non-local action of the resulting sub-planckian black holes acting as quantum wormholes. In other words, we can say that the connection between

the interior and the exterior time evolution of the black hole can be seen as a sort of perspective effect, which is caused by this rearrangement of correlations determined by apparent horizon and corresponding quantum wormholes.

The occurrence of an event x in the interior background is related with exterior modes between $t_{min} = min\{t_x : x \in K_{t_x}\}$ and $T_{t_{max}}$ where $t_{max} = max\{t_x : x \in K_{t_x}\}$ and, for any point in the interior description, $T_{t_{max}} < T_{evap}$ where T_{evap} is the time corresponding to the evaporation of the black hole. This means that, in the exterior description, by virtue of the perspective effect determined by the dissipative features of the vacuum and ultimately derived from the entanglement interaction between interior and exterior produced by the surface of the apparent horizon and transmitted by the non-local action of the quantum wormholes, the physics experienced by an interior observer at a given point x already occurred before the evaporation of the black hole. Thus, whatever are the constraint conditions of the Hawking radiation, the detector cannot influence the actual experience of the interior observer inside the black hole and this occurs ultimately as a result of the dissipative features of the 3D DQV corresponding to opportune fluctuations of the quantum vacuum energy density.

By following [56], one can also extend the analysis to the case in which one deals with operators before the complete evaporation of the black hole, by considering an infalling observer who reaches the apparent horizon at some exterior time t_f. If the effective theory of the interior corresponding to the time t_f describes the experience of the observer shortly after crossing the horizon, this does not necessarily imply that the effective theory describes well all the experiences of this observer. For example, the observer may accelerate towards the horizon, eventually leaving the region K_{t_f} encoding the rearrangement of correlations associated with the entanglement which connects the information contained in the effective interior of the black hole and the modes outside the apparent horizon. In this case, the experience of the infalling observer corresponds to the time

$$t_{comp} = t_f + t_{scr} \quad (46)$$

in the exterior description, where

$$t_{scr} = 4\frac{r_+}{c}\ln\frac{r_+\sqrt{\frac{c^2}{\left(\frac{\beta\hbar c}{\Delta\rho_{qvE}V}\right)^2+\left(\beta l_p^2\frac{\Delta\rho_{qvE}V}{\hbar c}\right)^2}\frac{c^4}{\Delta\rho_{qvE}{}^2V^2\left[\left(\frac{\beta\hbar c}{\Delta\rho_{qvE}V}\right)^2+\left(\beta l_p^2\frac{\Delta\rho_{qvE}V}{\hbar c}\right)^2\right]^2}}}{c} \quad (47)$$

is the scrambling time, which depends logarithmically of the radius r_+ of the apparent horizon of the black hole corresponding to the time t_x as

well as of the intrinsic periodicity of the sub-planckian black holes. On the basis of equation (47), the scrambling time is directly fixed by the behaviour of the variable energy density of the 3D DQV and can be interpreted here as the minimum time needed for quantum information to be extracted by outside observers from the black hole after the apparent horizon has absorbed an infalling observer. The experience of the infalling observer can be associated to the time (44) in the sense that the effective theory leads to a late trajectory of the observer that can be associated with the time

$$t_f^{'} = t_f + 2\frac{r_+}{c}\ln\frac{\sqrt{\left(\frac{\beta\hbar c}{\Delta\rho_{qvE}V}\right)^2+\left(\beta l_p^2\frac{\Delta\rho_{qvE}V}{\hbar c}\right)^2}\ \sqrt{\Delta\rho_{qvE}{}^2V^2\left[\left(\frac{\beta\hbar c}{\Delta\rho_{qvE}V}\right)^2+\left(\beta l_p^2\frac{\Delta\rho_{qvE}V}{\hbar c}\right)^2\right]^2}}{c} \quad (48)$$

even in the worst case of motion of the observer outward at the speed of light crossing the apparent horizon. By following the same route that led to equation (45), any experience of the observer in the interior corresponds to the time

$$T_{t_f^{'}} = t_f + t_{scr} \quad (49).$$

On the other hand, if one uses the general argument provided in [6], one can say that the information about an object that fell into the black hole at t_f emerges in Hawking radiation only after the time $t_f + t_{scr}$ as a consequence of the perspective effect, of the rearrangement of correlations determined by the action of the surface of the apparent horizon as entanglement island between interior and exterior of the black hole. Therefore, as a consequence of the action of the scrambling time intended as a numerical order of material change associated with the dissipative features of the vacuum at the generalized Compton wavelength as well as of the radius of the apparent horizon, it follows that any operation on Hawking radiation — even if it is performed before the time of evaporation — cannot influence the experience of an observer in the interior [57, 58].

The treatment made in this chapter leads to the following interpretation of the black hole's singularity [59]. From an exterior perspective, the immediate thermalization of an object when it encounters the apparent horizon does not occur. Instead, a distinct excitation on the horizon takes place for some duration in the form of a perspective effect generated by the dissipative features of the vacuum at the generalized Compton wavelength. Over the scrambling time t_{scr}, where one deals with gradual dissipation of this excitation into the horizon, the effective description as an object traversing the near-empty interior of the black hole works. After the object's excitation is

fully integrated into the apparent horizon, the perspective effect associated with the rearrangement of correlations determined by the dissipation processes of the vacuum and the corresponding effective theory that describes the connection between the information contained in the effective interior of the black hole and the modes outside the apparent horizon, do not hold anymore. Interior description and exterior description emerge therefore as complementary aspects, that are indeed not contradictory because of the appearance of this fundamental perspective effect of the rearrangement of correlations determined by the entanglement action of the surface of the apparent horizon and the non-local action of the resulting quantum wormholes, that ultimately are originated by the dissipative features of the vacuum at the generalized Compton wavelength.

Since the features of the black hole evolution involve collapsing dust shells which terminate at the apparent horizon as a consequence of the dissipative features of the 3D DQV at the generalized Compton wavelength, an exterior observer cannot recover information about an object which traversed the apparent horizon at an earlier time. Thus, in this picture, there is no problem of cloning if the observer jumps into the horizon. In other words, an observer cannot obtain a second copy of the information and the no-cloning theorem is naturally saved as a consequence of the entanglement action of the surface of the apparent horizon between the information contained in the effective interior of the black hole and the modes outside the apparent horizon. In particular, by substituting the scrambling time (47) inside the generalized energy-time uncertainty relation

$$\Delta E \Delta t \geq \frac{\hbar}{2}\left(1+\beta l_p^2 \frac{\Delta\rho_{qvE}^2 V^2}{\hbar^2 c^2}\right) \quad (50),$$

the duplication of quantum information is avoided (and therefore the information cloning is evaded) if one deals with a scale of energy

$$\Delta E \gg \frac{\hbar c}{r_+ \sqrt{\frac{c^2}{\left(\frac{\beta\hbar c}{\Delta\rho_{qvE}V}\right)^2+\left(\beta l_p^2\frac{\Delta\rho_{qvE}V}{\hbar c}\right)^2}\;\frac{c^4\hbar^2}{\Delta\rho_{qvE}{}^2V^2\left[\left(\frac{\beta\hbar c}{\Delta\rho_{qvE}V}\right)^2+\left(\beta l_p^2\frac{\Delta\rho_{qvE}V}{\hbar c}\right)^2\right]^2}}} \cdot \left(1+\beta l_p^2 \frac{\Delta\rho_{qvE}^2 V^2}{\hbar^2 c^2}\right) \quad (51).$$

$$8r_+ \ln \frac{}{c}$$

We underline here that the result (48) turns out to be compatible with the treatment in [60], if the mass of the black hole satisfies relation

$$Mc = \frac{\hbar}{8r_+ \ln \frac{r_+ \sqrt{\left(\frac{\beta\hbar c}{\Delta\rho_{qvE}V}\right)^2 + \left(\beta l_p^2 \frac{\Delta\rho_{qvE}V}{\hbar c}\right)^2 \; \Delta\rho_{qvE}{}^2V^2\left[\left(\frac{\beta\hbar c}{\Delta\rho_{qvE}V}\right)^2 + \left(\beta l_p^2 \frac{\Delta\rho_{qvE}V}{\hbar c}\right)^2\right]^2}}{c}} \cdot \left(1 + \beta l_p^2 \frac{\Delta\rho_{qvE}^2 V^2}{\hbar^2 c^2}\right) \quad (52).$$

In summary, on the basis of equations (45) and (52), we can conclude that the cloning of information is avoided if one deals with a scale of energy that exceeds the quantity

$$\frac{\hbar c}{8r_+ \ln \frac{r_+ \sqrt{\left(\frac{\beta\hbar c}{\Delta\rho_{qvE}V}\right)^2 + \left(\beta l_p^2 \frac{\Delta\rho_{qvE}V}{\hbar c}\right)^2 \; \Delta\rho_{qvE}{}^2V^2\left[\left(\frac{\beta\hbar c}{\Delta\rho_{qvE}V}\right)^2 + \left(\beta l_p^2 \frac{\Delta\rho_{qvE}V}{\hbar c}\right)^2\right]^2}}{c}} \left(1 + \beta l_p^2 \frac{\Delta\rho_{qvE}^2 V^2}{\hbar^2 c^2}\right)$$

and this occurs when the scrambling time (47) is sufficiently large.

On the other hand, if we explore further the comparison with the Susskind and Maldacena ER=EPR approach, where virtual wormholes determine a connection between the black hole could and Hawking radiation [52], in our approach of 3D DQV ruled by the generalized Compton wavelength, as we have already underlined, the firewall is not present. The intrinsic periodicity of the sub-Planckian black holes of the variable energy density emerging from the dissipative features of the vacuum at the generalized Compton wavelength implies that the interior of a black hole can be considered as a way of reorganizing the degrees of freedom involved in the temporary phenomenon of an infalling object dissipating into the apparent horizon through the entanglement action of the apparent horizon characterized by the entanglement entropy (34) and the non-local action of the quantum wormholes associated with the fluctuations of the texture of the sub-Planckian black holes, described by the modified Bekenstein entropy (38). As a consequence of the entanglement action of the surface of the apparent horizon in generating the connection between the information contained in the effective interior of the black hole and the modes outside the apparent horizon, no operation performed on Hawking radiation can influence the experience of an infalling observer. Finally, we emphasize that, in the processes of gravitational collapse of dust shells determined by the dissipative features of the 3D DQV, the transition to extremely compact quantum objects, ruled by quantum gravity, giving rise to an apparent horizon whose surface acts as an entanglement island between the information inside the black hole and the modes outside the apparent horizon, can be associated (and are compatible) with the creation of baby-universes which will separate

from a plasma of large parent universes. As a consequence of the dissipative features of the vacuum acting at the generalized Compton wavelength, we can say that there is, on one hand, the evaporation of the observable part of the black hole at the time (47) and, on the other hand, a true entanglement between thermal radiation in our universe and a new universe beyond it (which is in the form of an island inside the black hole). These two universes together continue to be indeed in a pure quantum state, but separately they seem to be in a mixed state, thus leading to the result that, in the model of sub-planckian black holes of the variable energy density that are characterized by an intrinsic periodicity that is fixed by the dissipative features of the vacuum at the generalized Compton wavelength, there is no paradox associated to the evaporation of a black hole and there is no problem as regards unitarity of quantum mechanics, that turns out to be saved. As a consequence of the role of entanglement island by the surface of the apparent horizon, the black hole evaporation leads to the result that every black hole in a given universe can be seen as a white-hole source of a new universe, thus providing a model of multiverse where each decoupling bag of gold = black hole for us and a white-hole for some emerging new universe has all the quantum numbers (charges), associated with gauge symmetries, that are vanishing, but can have non-trivial entanglement with the parent universe and also non-trivial values of ungauged charges, like baryon number, thus determining new options to resolve the baryon asymmetry problem [61]. In this way, in the cosmological background determined by the dissipative features of the vacuum, our universe – as well as other baby universes – can be considered as white holes emerging from a black hole in a plasma of large parent universes. Each black hole is surrounded by Hawking radiation, which stays in its own universe, while the other content of the black hole decouples from it at around the Page time (intended as the last numerical order of material change associated with the decoupling of the interior of the black hole) and gives birth to a new baby universe, whose origin, inside the new universe, can be associated to a white hole. Moreover, if one assumes that the end of the black hole evaporation is associated to a mild singularity, the black hole interior can be seen as a closed universe that is separated from the ambient space describing the exterior of the black hole, compatibly with the interpretation provided in [62], according to which, after the black hole evaporates, its microscopic information is encoded in the states of the baby universes arising in the system of replicated black holes associated with the plasma of large parent universes.

5. Conclusions

The approach of 3D DQV whose elementary constituents are sub-planckian black holes of the variable energy density that are characterized by an intrinsic periodicity that is fixed by the dissipative features of the vacuum at the generalized Compton wavelength, leads to relevant perspectives of handling the firewall and information paradoxes connected to black holes.

Before all, as regards the issue of the complementarity of the black holes, the three fundamental assumptions invoked by AMPS in [7, 8], i.e.:

1. Hawking radiation is pure;
2. effective field theory is valid outside a stretched horizon;
3. infalling observers encounter nothing unusual as they cross the horizon

are not necessarily incompatible, in the sense that, in our model, a lattice of collapsing dust shells, namely micro-universes described by the wave functions (21), as a consequence of their maximum density (27), condense to an apparent horizon which is characterized by the coarse-grained entropy (31) that is directly fixed by the dissipative features of the 3D DQV at the generalized Compton wavelength, thus implying that equivalence principle, Hawking radiation and quantum entanglement are not incompatible. Since the dissipative processes of the 3D DQV at the generalized Compton wavelength determine the formation of an apparent horizon, our model demonstrates in a direct way the impossibility of the formation of a firewall, allowing us to avoid the arguments involved in the AMPS work and resolve the firewall paradoxes of black holes.

Moreover, during the gravitational collapse of the black hole till the apparent horizon, because of the dissipative features of the 3D DQV at the generalized Compton wavelength, the surface of the apparent horizon gets the role of entanglement island between interior and exterior. The entanglement action of the apparent horizon is encoded by the entanglement entropy (34) and corresponds to a deformation of the geometry (36) that leads to the formation of the non-local action of quantum wormholes, characterized by the modified Bekenstein entropy (38), that create a connection between the information contained in the effective interior of the black hole and the modes outside the apparent horizon. As a consequence of the perspective effect caused by the rearrangement of correlations which are determined by the apparent horizon and the quantum wormholes, interior description and exterior description emerge as complementary aspects, that are not contradictory. The model based on the

entanglement action of the apparent horizon and the non-local action of the resulting quantum wormholes allows us to provide a compelling solution to the information paradox can both during evaporation of the black hole and after evaporation of the black hole. In fact, on one hand, the entanglement entropy of the surface of the apparent horizon implies the generation of an entanglement between the forming Hawking radiation and the region between the apparent horizon and the photon sphere rim, which is transmitted by non-local quantum wormholes, implying that there is no information loss during evaporation of the black hole. On the other hand, the sub-planckian black holes acting as quantum wormholes, described by the quantum-modified Bekenstein entropy (38), which transmit the information between the interior and the modes outside the apparent horizon, imply that there is no information loss after evaporation of the black hole. In this way, the action of the surface of the apparent horizon described by the entanglement entropy (34) and the generation of quantum wormholes characterized by the modified Bekenstein entropy (38) allow a promising solution of the information paradox that avoids the violation of quantum mechanics' principle of unitarity.

In this picture, the evolution of the system after the formation of the apparent horizon can be seen as a perspective entanglement effect owed to the dissipative features of the vacuum at the generalized Compton wavelength, where correlations between the degrees of freedom associated with the time interval (45) are rearranged in such a way that they can be interpreted as originating from the infalling time evolution generated by an opportune operator without involving a further exterior time evolution. Moreover, the evolution of the collapsing dust shells which terminate at the apparent horizon as a consequence of the dissipative features of the 3D DQV at the generalized Compton wavelength, has also the merit to naturally save the no-cloning theorem.

The attempt to handle the firewall and information paradoxes in the model explored in this paper turns out to be compatible also with the idea of a multiverse. In fact, the processes of gravitational collapse can be associated to the creation of baby-universes which will separate from a plasma of large parent universes where, as a consequence of the dissipative features of the vacuum acting at the generalized Compton wavelength, on one hand, one has the evaporation of the observable part of the black hole and, on the other hand, one has a true entanglement between thermal radiation in our universe and a new universe. The two universes together continue to be indeed in a pure quantum state, but separately they seem to be in a mixed state and

therefore there is no paradox associated to the evaporation of a black hole and there is no problem as regards unitarity of quantum mechanics, that turns out to be saved.

In summary, despite at its germinal stages, we can say that our model of sub-planckian black holes of the variable energy density of the three-dimensional dynamical quantum vacuum suggests a compelling attempt to treat problems and paradoxes connected to black holes.

Finally, our model provides a novel key of re-reading of the non-existence of a central singularity, which is alternative with respect to current approaches, in particular those involving the insertion of an imaginary time through the so-called Wick rotation, which provide ad hoc mechanisms leading to ad hoc solutions [63, 64]. The results obtained in this paper – and, in particular, the perspective effect determined by the action of the surface of the apparent horizon as entanglement island between interior information and exterior information – seem to be compatible with a recent proposal of solution of the problem of singularities of Lorentz-Euclidean black holes, named "atemporality", involving a dynamical mechanism by which an observer pointing towards the event horizon cannot reach the singularity in r=0, in a Lorentz-Euclidean-Schwarzschild metric, because both the time variable and radial velocity become imaginary inside the black hole [65]. In the "atemporality" approach, any massive particle stops at the event horizon because, if entering it, conservation laws would be violated as a consequence of the appearance of an imaginary radial velocity. The possible links between the "atemporality" approach and the model of sub-planckian black holes of the variable energy density of the 3D DQV introduce new scenarios which are all to be explored.

References

[1] X. Dai, "The black holes paradoxes and possible solutions", *Journal of Physics: Conference Series* **1634**, 012088 (2020).

[2] L. Susskind, L. Thorlacius and J. Uglum, "The Stretched horizon and black hole complementarity", *Physical Review D* **48**, 3743 (1993).

[3] L. Susskind, "String theory and the principles of black hole complementarity", *Physical Review Letters* **71**, 2367 (1993).

[4] L. Susskind and L. Thorlacius, "Gedanken experiments involving black holes", *Physical Review D* **49**, 966 (1994).

[5] D.N. Page, "Information in black hole radiation", *Physical Review Letters* **71**, 3743 (1993).
[6] P. Hayden and J. Preskill, "Black holes as mirrors: Quantum information in random subsystems", *Journal of High Energy Physics* **09**, 120 (2007).
[7] A. Almheiri, D. Marolf, J. Polchinski and J. Sully, "Black holes: complementarity or firewalls?", *Journal of High Energy Physics* **62** (2013).
[8] A. Almheiri, D. Marolf, J. Polchinski, D. Stanford and J. Sully, "An Apologia for Firewalls", *Journal of High Energy Physics* **09**, 018 (2013).
[9] S.L. Braunstein, S. Pirandola and K. Życzkowski, "Better Late than Never: Information Retrieval from Black Holes", *Physical Review Letters* **110**, 101301 (2013).
[10] S.W. Hawking, "Information preservation and weather forecasting for black holes", arXiv:1401.5761 (2014).
[11] C. Vaz, "Black holes as gravitational atoms", *International Journal of Modern Physics D* **23**, 1441002 (2014).
[12] J.E. Jacak, "Topology-induced quantum transition in multi-particle systems in vicinity of a black hole", *Classical and Quantum Gravity* **41**, 035006 (2024).
[13] J.E. Jacak, "Modification of premises for the black hole information paradox caused by topological constraints in the event horizon vicinity", *Entropy* **26**, 1035 (2024).
[14] S.W. Hawking, "Black hole explosions?", *Nature* **248**, 30–31 (1974).
[15] A. Bekenstein, "Black holes and the second law", *Lettere Al Nuovo Cimento* **4**, 737–740 (1972).
[16] R.J. Adler and D.I. Santiago, "On gravity and the uncertainty principle", *Modern Physics Letters A* **14**, 1371 (1999).
[17] F. Scardigli, "Generalized uncertainty principle in quantum gravity from micro-black hole gedanken experiment", *Physics Letters B* **452**, 39-44 (1999).
[18] B.J. Carr, "The Black Hole Uncertainty Principle Correspondence", *Springer Proceedings Physics* **170**, 159-167 (2016).
[19] M.J. Lake and B. Carr, "The Compton-Schwarzschild relations in higher dimensions", arXiv:1611.01913 [gr-qc] (2016).
[20] M.J. Lake and B. Carr, "Does Compton/Schwarzschild duality in higher dimensions exclude TeV quantum gravity?", *International Journal of Modern Physics D*, 1930001 (2018).
[21] M.J. Lake and B. Carr, "The Compton-Schwarzschild correspondence from extended de Broglie relations", *Journal of*

High Energy Physics **1511**, 105 (2015) doi:10.1007/JHEP11 (2015).

[22] B.J. Carr, J.R. Mureika and P. Nicolini, "Sub-Planckian black holes and the generalized uncertainty principle", *Journal of High Energy Physics* **2015**, 07052 (2015).

[23] J. Carr, L. Modesto and I. Prémont-Schwarz, "Generalized uncertainty principle and self-dual black holes", arXiv:1107.0708 [gr-qc] (2011).

[24] B.J. Carr, "The generalized uncertainty principle and higher dimensions: linking black holes and elementary particles", arXiv:2302.12609v1 [gr-qc] (2023).

[25] A.F. Ali, S. Das and E.C. Vagenas, "Discreteness of space from the generalized uncertainty principle", *Physics Letters B*, 678, 497-499 (2009).

[26] P. Chen, Y.C. Ong and D.-h. Yeom, "Generalized uncertainty principle: implications for black hole complementarity", *Journal of High Energy Physics* **12**, 021 (2014).

[27] F. Yang, "Generalized uncertainty principles models' multifaceted impact on black hole thermodynamics and entropy conservation during Hawking radiation", *Modern Physics Letters A*, https://doi.org/10.1142/S0217732325501329 (2025).

[28] D. Fiscaletti, The timeless approach. Frontier perspectives in 21st century physics, World Scientific, Singapore (2015).

[29] D. Fiscaletti, "About dark energy and dark matter in a three-dimensional quantum vacuum model", *Foundations of Physics* **46**, 10, 1307-1340 (2016).

[30] D. Fiscaletti and A. Sorli, "About a three-dimensional quantum vacuum as the ultimate origin of gravity, electromagnetic field, dark energy ... and quantum behaviour", *Ukrainian Journal of Physics* **61**, 5, 413-431 (2016).

[31] D. Fiscaletti and A. Sorli, "Dynamical quantum vacuum and relativity", *Annales UMCS Sectio AAA: Physica* **LXXI**, pp. 11-52 (2016).

[32] D. Fiscaletti and A. Sorli, "Quantum vacuum energy density and unifying perspectives between gravity and quantum behaviour of matter", *Annales de la Fondation Louis de Broglie* **42**, 2, 251-297 (2017).

[33] D. Fiscaletti and A. Sorli, "Quantum relativity: variable energy density of quantum vacuum as the origin of mass, gravity and the quantum behaviour", *Ukrainian Journal of Physics* **63**, 7, 623-644 (2018).

[34] D. Fiscaletti, "About dark matter as an emerging entity from elementary energy density fluctuations of a three-dimensional quantum vacuum", *Journal of Theoretical and Applied Physics* **14**, 203-222 (2020).

[35] D. Fiscaletti and A. Sorli, "Generalized uncertainty relations, particles, black holes, and Casimir effect in the three-dimensional quantum vacuum", *Theoretical and Mathematical Physics* **214**, 1, 132-151 (2023).

[36] D. Fiscaletti, "Generalized uncertainty relations, generalized Compton wavelength and particles in a quantum foam described by a variable energy density", *Hadronic Journal* **47**, 183-206 (2024).

[37] F. Scardigli and R. Casadio, "Gravitational tests of the generalized uncertainty principle", *European Physical Journal C* **75**, 425 (2015).

[38] D. Fiscaletti, "Implications of generalized Compton wavelength in the effects of general relativity", *Theoretical and Mathematical Physics*, accepted for publication, 2024.

[39] R.C. Pantig, A. Övgün and G. Lambiase, "Thenomenology of Schwarzschild-like black holes with a generalized Compton wavelength", arXiv:2504.18226v1 [gr-qc] (2025).

[40] D. Fiscaletti, "About the multiverse in the three-dimensional quantum vacuum with variable energy density", *Bulgarian Journal of Physics* **51**, 2, 185-210 (2024).

[41] D. Dolce, "Introduction to the quantum theory of elementary cycles: the emergence of space, time and quantum", in *Beyond Peaceful Coexistence: The Emergence of Space, Time and Quantum*, eds I. Licata and G. 't Hooft, World Scientific (2016), pp. 93-135.

[42] D. Dolce, "New stringy physics beyond quantum mechanics from the Feynman path integral", DOI:10.21203/rs.3.rs-503118/v1 (2022).

[43] D. Fiscaletti and A. Sorli, "Perspectives about scales and hierarchies in a three-dimensional quantum vacuum ruled by generalized uncertainty relations", *Bulgarian Journal of Physics* **50**, 4, 412-438 (2023).

[44] C. Corda, "Black hole spectra from Vaz's quantum gravitational collapse", arXiv:2305.02184v2 [gr-qc] (2023).

[45] Y. Nomura and S.J. Weinberg, "Entropy of a vacuum: what does the covariant entropy count?", *Physical Review D* **90**, 104003 (2014).

[46] N. Engelhardt and A.C. Wall, "Decoding the apparent horizon: a coarse-grained holographic entropy", arXiv:1706.02038v4 [hep-th] (2019).

[47] R. Penrose, "Gravitational collapse and space-time singularities", *Physical Review Letters* **14**, 3, 57 (1965).

[48] R.P. Kerr, "Do black holes have singularities?", arXiv:2312.00841.pdf (2023).

[49] R.P. Kerr, "Gravitational of a spinning mass as an example of algebraically special metrics", *Physical Review Letters* **11**, 237 (1963).

[50] L.D. Landau and E.M. Lifshitz, *The classical theory of fields*, Pergamon Press LTd., Oxford, UK (1971).

[51] I. Licata and D. Fiscaletti, "Holography and nucleation processes from the primeval Wheeler-DeWitt equation in a de Sitter universe", *International Journal of Theoretical Physics* **63**, 122 (2024).

[52] J. Maldacena and L. Susskind, "Cool Horizons for entangled black holes", *Fortschritte der Physik* **61**, 9, 781-811 (2013).

[53] K. Jusufi, E. Moulay, J. Mureika and A.F. Ali, "Einstein-Rosen bridge from the minimal length", *European Physical Journal C* **83**, 282 (2023).

[54] R. Bousso and G. Penington, "Islands far outside the horizon", arXiv:2312.03078v3 [hep-th] (2023).

[55] N. Engelhardt and A.C. Wall, "Decoding the apparent horizon: a coarse-grained holographic entropy", arXiv:1706.02038v4 [hep-th] (2019).

[56] B. Concepcion, Y. Nomura, K. Ritchie and S. Weiss, "Complementarity for a dynamical black hole", *Physical Review D* **110**, 086002 (2024).

[57] W.G. Unruh and R.M. Wald, "Acceleration radiation and generalized second law of thermodynamicals", *Physical Review D* **25**, 942 (1982).

[58] A.R. Brown, "Tensile strength and the mining of black holes", *Physical Review Letters* **111**, 211301 (2013).

[59] Y. Nomura, "Reanalyzing an evaporating black hole", *Physical Review D* **99**, 086004 (2019).

[60] W. Kim and M. Nam, "Investigation of black hole complementarity in ADS_2 black holes", arXiv:2310.13274v2 [hep-th] (2024).

[61] A. Morozov, "On information paradox and the fate of black holes", arXiv:2304.00197v1 [hep-th] (2023).

[62] D. Marolf and H. Maxfield, "Observations of Hawking radiation: The Page curve and baby universes", *Journal of High Energy Physics* **04**, 272 (2021).

[63] A. Zee, *Quantum Field Theory in a Nutshell*, 2nd edn. Princeton University Press, Princeton (2010).

[64] J.B. Hartle, S.W. Hawking and T. Hertog, "The Classical Universes of the No-Boundary Quantum State", *Physical Review D* **77**, 123537 (2008).

[65] S. Capozziello, S. De Bianchi and E. Battista, "Avoiding singularities in Lorentzian-Euclidean black holes: The role of atemporality", *Physical Review D* **109**, 10, 104060 (2024).

HADRONIC JOURNAL 49, 65 - 76 (2026)
DOI 10.29083/HJ.49.01.2026/SC65

PREDICTED STABILITY OF Z=119 SYSTEMS

J. J. Bevelacqua
Bevelacqua Resources
7531 Flint Crossing Circle SE
Owens Cross Roads, AL 35763
bevelresou@aol.com

Received January 18, 2026

Abstract

Single-particle energies of Z=119 nuclei are calculated to determine their decay properties. The Rost interaction is used as the basis for these calculations. A = 290 – 304 systems have predicted stability in the ps – ms range. The most stable isotope occurs at A = 297, and it has an alpha decay half-life of 0.112 s. These model results are consistent with the observed properties of Z = 110 – 118 nuclei.

KEYWORDS: Z=119, superheavy nuclei, alpha and beta decay half-lives, single-particle energies.

Copyright © 2026 by Hadronic Press, Inc., Palm Harbor, FL 34684, USA

1.0 Introduction

Superheavy nuclei and their associated stability have been active experimental and theoretical areas of research [1-28]. Calculations in the superheavy mass region require the selection of an appropriate nuclear interaction. The focus on Z = 119 and neighboring systems has been an area of active investigation as illustrated in [14, 22-28].

Calculations for the Z = 119 system are presented in this paper. These calculations determine the nuclear structure and predict the decay characteristics of the Z = 119 systems.

Z = 119 system stability is evaluated using the methodology Lukasiak and Sobiczewski [3] and Petrovich et al. [4]. The calculations are based on the unmodified Rost interaction [2]. Single-particle model calculations facilitate the investigation of superheavy systems that have yet to be experimentally detected and have received limited theoretical study [22-28]. These studies provide insight into binding energy systematics and nuclear stability beyond the previously established mass regions.

Using a more sophisticated method than the single-particle approach is not warranted in view of the uncertainties encountered in these initial calculations. These uncertainties include extrapolations of the nuclear interaction into the Z > 118 mass region. Since there are no experimental data to guide the calculations, single-particle calculations are a reasonable approach for initial calculations of Z = 119 nuclei [3,5,21].

The stability of Z = 119 systems is determined by evaluating the various decay modes (i.e., alpha decay, beta decay, positron decay, electron capture, and spontaneous fission). Based on previous calculations [1, 3, 5, 21-28], stability in the Z = 119 mass region is expected to be dominated by alpha decay.

2.0 Calculational Methodology

The model used to describe the particle (i) plus core (c) system represents an application of the standard method of Lukasiak and Sobiczewski [3] and Petrovich et al. [4]. The calculational method used to generate the single-particle level spectrum determines the binding energy E_{NLSJ} of a particle in the field of a nuclear core by solving the radial Schrödinger Equation

$$\left[\frac{\hbar^2}{2\mu}\left(\frac{d^2}{dr^2} - \frac{L(L+1)}{r^2}\right) - E_{NLSJ} - V_{LSJ}(r)\right] U_{NLSJ}(r) = 0 \qquad (1)$$

where r is the radial coordinate defining the relative motion of the nuclear core and the particle; $V_{LSJ}(r)$ is the model interaction; E_{NLSJ} is the core plus particle binding energy; $U_{NLSJ}(r)$ is the radial wave function; and L, S, and J are the orbital, spin, and total angular momentum quantum numbers, respectively. N is the radial quantum number and μ is the reduced mass. For the present application, V_{LSJ} is defined as:

$$V_{LSJ}(r) = -\frac{V_0}{1+exp\left(\frac{r-R_o}{a_o}\right)} - V_{so}\left(\frac{\hbar}{m_\pi c}\right)^2 \frac{1}{a_{so}r}\frac{exp\left(\frac{r-R_{so}}{a_{so}}\right)}{\left[1+exp\left(\frac{r-R_{so}}{a_{so}}\right)\right]^2}F(L,S,J) + Z_i Z_C e^2 C(r) \quad (2)$$

where

$$R_0 = r_0 A^{\frac{1}{3}} = R_C \quad (3)$$

and

$$R_{so} = r_{so} A^{1/3} \quad (4)$$

The parameters V_0, r_0, and a_0 are the strength, radius parameter, and diffuseness for the central potential. Similarly, V_{so}, r_{so}, and a_{so} are the corresponding parameters for the spin-orbit potential. To complete the specification of (2), we define:

$$F(L,S,J) = J(J+1) - L(L+1) - S(S+1) \quad (5)$$

and

$$C(r) = \frac{1}{2R_C}\left(3 - \left(\frac{r}{R_C}\right)^2\right) \quad for \quad r < R_C \quad (6)$$

$$C(r) = \frac{1}{r} \quad for \quad r \geq R_C \quad (7)$$

For the Coulomb potential, it is assumed that the particle is a point charge of magnitude $z_i e$. The core has a charge $Z_C e$ uniformly distributed through a sphere of radius R_C. Since the potential is not a function of the spherical coordinates, the

solution of the angular equation is most easily expressed in terms of spherical harmonics $Y_{LM}(\theta,\varphi)$.

The total bound-state wave function $\left(\Psi_{NLSJM}(\vec{r})\right)$ for the relative motion of the core plus particle, interacting through a spherically symmetric potential, is given by the product of space and spin wave functions:

$$\Psi_{NLSJM}(\vec{r}) = \frac{1}{r} U_{NLSJ}(r) \sum_{M_L M_S} C(L, M_L, S, M_S; JM) Y_{LM_L}(\theta,\varphi) \chi_{SM_S} \qquad (8)$$

where M_L and Ms are the projections of angular momentum and spin, and χ is the spin wave function. For the calculation of single-particle energy levels, N, L, S, and J specify the quantum numbers of the single-particle level.

The binding energy of a single-particle level is obtained by rewriting the radial Schrödinger equation in the form

$$\left(\frac{d^2}{dr^2} - k(p,r)\right) U(p,r) = 0 \qquad (9)$$

where

$$U(p,r) = U_{NLSJ} \qquad (10)$$

and

$$k(p,r) = \frac{L(L+1)}{r^2} + \frac{2\mu}{\hbar^2}\left(E_{NLSJ} + V_{LSJ}(r)\right) \qquad (11)$$

The model searches for values of the parameter p in order to obtain the binding energy E_{NLSJ} for a given potential. The method of searching for p is provided by Brown, Gunn, and Gould [29] using the methodology of [30] to obtain a converged solution. [2 - 4, and 21] provide additional details of the model, numerical methods, and associated interactions.

2.1 Determination of Q Values and Half-Lives

Alpha decay Q values are calculated using the relationship

$$\mathbf{Q_\alpha = 28.3\ MeV - 2\ S_n - 2\ S_P} \qquad (12)$$

where S_n and S_p are the binding energies of the last occupied neutron and proton single-particle energy levels, respectively [1]. The alpha decay, positron decay, and electron capture half-lives were determined following the methodology noted in [3]. Spontaneous fission half-lived were qualitatively evaluated using the methodology of [3] and were not limiting [4,21].

The log ft methodology of Wong [1] is used to determine the beta decay half-lives. Allowed (first-forbidden) beta decay half-lives are obtained from the values of log ft = 5 (8) [1]. In view of the uncertainties in the calculated level energies, second and higher forbidden transitions were not determined. The beta half-lives summarized in Table 1 listed as *stable* are either beta stable or decay by these higher order forbidden transitions.

3.0 Nuclear Interaction

The model considers the single-particle spectrum generated by a Woods-Saxon potential with parameters optimized for extrapolation into the region of superheavy nuclei [4]. The parameters of the Rost potential were obtained from a fit to the particle levels in ^{208}Pb and ^{209}Bi [2].

The single-particle level spectrum is generated using a Woods-Saxon potential of the Rost interaction [2]. The Rost central interaction strength is given by the relationship:

$$V_0 = 51.6 \left[1 \pm 0.73 \frac{N-A}{Z}\right] MeV \qquad (13)$$

The potential for protons (neutrons) is given by the upper (lower) sign. The remaining parameters were held constant and are given by Rost [2]: r_0 = 1.262 (1.295) fm, r_{so} = 0.908 (1.194) fm, a = 0.70 (0.70) fm, and λ = 17.5 (28.2) for protons (neutrons). V_{so} is related to λ by the relationship [2]:

$$V_{so} = \frac{\lambda V_0}{180} \qquad (14)$$

The scaling relationship of (13) yields reasonable fits to observed single-particles levels in ^{120}Sn and ^{138}Ba [4]. The pairing correction term of Blomqvist and Wahlborn [31] is used in the calculations presented herein. The pairing correction improves the predicted energies of occupied levels in ^{120}Sn, ^{138}Ba, and ^{208}Pb [4]. A Woods-Saxon potential which reproduces the single-particle levels in the lead region provides the basis for a discussion of the stability properties of Z=119 superheavy nuclei [2,4].

4.0 Results and Discussion

Table 1 summarizes the results of Z = 119 single-particle level calculations. This table provides the alpha decay Q value and the alpha and beta decay half-lives for A = 290 – 304, Z = 119 systems. This mass range is consistent with the calculations summarized in [27] that reviewed the possible reactions that would theoretically produce the various Z = 119 isotopes.

The results suggest that A = 290 – 304 systems have predicted half-lives in the ps – ms range. Alpha emission is predicted to be the limiting decay mode. Table 1 also provide the valance neutron and proton single-particle (sp) levels for each of the calculated Z = 119 systems. The most stable Z = 119 isotope is predicted to occur at A = 297 with an alpha decay half-life of 0.112 s. Following [3], shell corrections are included in the alpha decay half-life and Q-value calculations.

Table 1

Z=119 Q_α and Half Life Values

A (p, n single-particle level)	Q_α (MeV)	$T_{1/2}^{\alpha}$	$T_{1/2}^{\beta}$
290 ($2f_{5/2}$, $2g_{7/2}$)	12.3	0.652 μs	15.7 min[a]
291($2f_{5/2}$, $2g_{7/2}$)	12.0	3.38 μs	17.3 min[b]
292 ($2f_{5/2}$, $3d_{5/2}$)	11.7	12.1 μs	18.9 min[b]
293 ($2f_{5/2}$, $3d_{5/2}$)	11.4	65.7 μs	20.7 min[b]
294 ($2f_{5/2}$, $3d_{5/2}$)	11.1	0.380 ms	22.8 min[b]
295 ($2f_{5/2}$, $3d_{5/2}$)	10.8	2.35 ms	25.1 min[b]
296 ($2f_{5/2}$, $3d_{5/2}$)	10.5	15.6 ms	27.8 min[b]
297 ($2f_{5/2}$, $3d_{5/2}$)	10.2	0.112 s	1.06 h[c]
298 ($2f_{5/2}$, $4s_{1/2}$)	12.1	1.85 μs	1.22 h[c]
299 ($2f_{5/2}$, $4s_{1/2}$)	11.8	9.23 μs	1.41 h[c]
300 ($2f_{5/2}$, $3d_{3/2}$)	11.6	31.1 μs	1.64 h[c]
301 ($2f_{5/2}$, $3d_{3/2}$)	11.3	0.175 ms	1.92 h[c]
302 ($2f_{5/2}$, $3d_{3/2}$)	10.9	1.05 ms	2.27 h[c]
303 ($2f_{5/2}$, $3d_{3/2}$)	10.6	6.79 ms	[d]
304 ($2f_{5/2}$, $2h_{11/2}$)	15.2	2.48 ps	[d]

[a] First forbidden $2f_{5/2}$(p) to $2g_{7/2}$ (n) positron transition.
[b] First forbidden $2f_{5/2}$(p) to $3d_{5/2}$ (n) positron transition.
[c] First forbidden $2f_{5/2}$(p) to $3d_{3/2}$ (n) positron transition.
[d] Beta stable.

The A = 297 single-particle level diagram for Z = 119 is provided in Fig. 1. The last occupied neutron (proton) single-particle level is $3d_{3/2}$ ($2f_{5/2}$). Half-life values for the Z = 119 systems are in the ps – ms range. Nuclear stability rapidly decreases beyond A = 303 as the valence neutron transitions from the $3d_{3/2}$ to $2h_{11/2}$ single-particle level. The decrease in the $2h_{11/2}$ neutron single-particle binding energy increases the Q_α value that leads to a shorter alpha decay half-life.

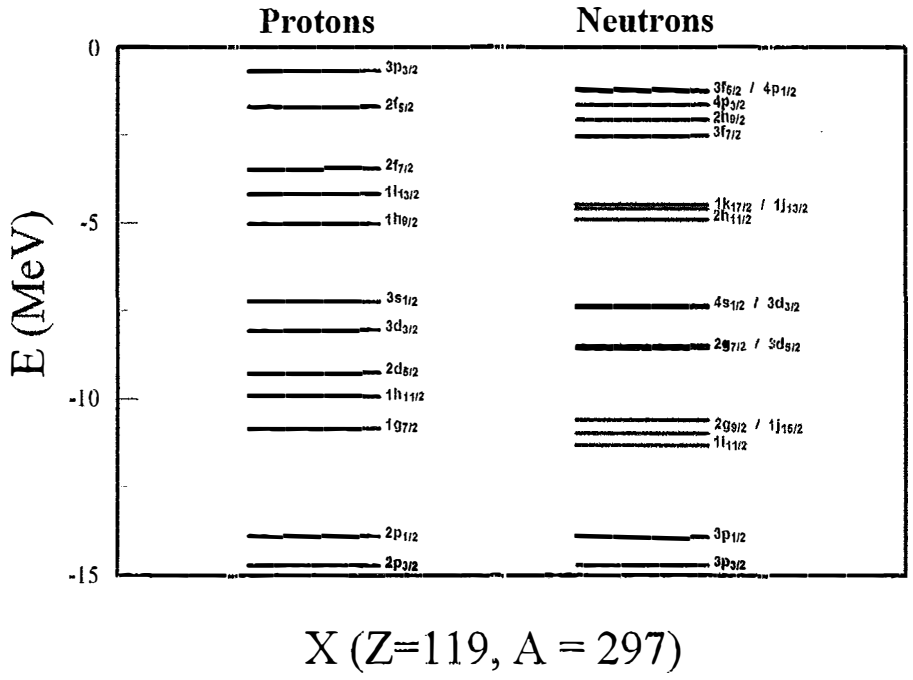

X (Z=119, A = 297)

Fig. 1. Calculated single-particle levels for the most stable Z = 119 nucleus (A = 297). The notation a/b is used to indicate adjacent energy levels with level a more tightly bound than level b.

Qian and Ren [22] provide a set of Z = 119 calculations for A = 290 – 299. [22] predicts the decay mode will be alpha, but only provides a broad range of half-life values. For example, the [22] half-life values are in the range of 1.4×10^{-5} to 2.47×10^{3} s.

Table 2 compares the model results to Z = 110 – 118 systems to the experimental range of isotope masses, half-life range, and most stable system [32]. The Z = 119 model results appear to be consistent with the trends in Z = 110 - 118 mass and half-life values. Alpha decay is the dominant decay mode in most of these systems [32], and that is also consistent with the model results.

Table 2

Comparison of Z = 110 – 118 Data[a] and Z = 119 Model Results[b]

Z	Mass Range	Half-Life Range	Most Stable
110	267 – 282	3.0 μs – 1.1 min	^{282}Ds
111	272 – 282	3.8 ms – 100 s	^{282}Rg
112	277 – 286	0.61 ms – 11.0 min	^{286}Cn
113	282 - 290	70 ms – 9.5 s	^{286}Nh
114	284 – 290	25 ms – 19 s	^{290}Fl
115	287 – 290	37 ms -0.65 s	^{290}Mc
116	290 – 293	8.3 ms – 95 ms	^{293}Lv
117	293 – 294	21 ms – 51 ms	^{294}Tn
118	294	0.58 ms	^{294}Og
119	290 - 304	2.48 ps – 0.112 s	^{297}X

[a]Derived from NuDat3 [32].
[b]This work.

Within the scope of the model, the effective half-life of the Z = 119 systems includes the combined effect of the alpha and positron decay modes, and is defined as

$$T_{1/2}^{eff} = (T^{\alpha}_{1/2}\, T^{\beta}_{1/2}) / (T^{\alpha}_{1/2} + T^{\beta}_{1/2}) \qquad (15)$$

Since the positron decay half-life is much larger than the alpha decay half-life, the effective half-life is essentially the alpha decay half-life.

Based on previous calculations [3,4,21], spontaneous fission stability is expected to be enhanced near closed shells. These spontaneous fission calculations utilized the Wentzel-Kramers-Brillouin (WKB) approximation methodology and the phenomenological parameter values of [3]. The calculations suggest that fission half-lives near closed shells are greater than the effective decay half-lives calculated using (15).

5.0 Model Weaknesses

Model limitations include uncertainties in the nuclear interaction [2], exclusion of nonconventional decay modes that could exist in superheavy systems, and treating all system as spherically symmetric nuclei. In spite of these

uncertainties, the Rost interaction yields results that are consistent with the trends observed in Z = 110 – 118 systems.

The accuracy of the proposed model can be partially addressed by comparing the (Z, A) values of calculated system properties to the predictions of Adler's relationship [33,34]. The Alder relationship provides the most stable nucleus Z value for a given A:

$$\mathbf{Z = (0.487\ A) / (1 + A^{2/3} /166)} \qquad (16)$$

This relationship can be compared to the model predictions for the most stable A = 297 system. The Adler relationship predicts that the most stable A = 297 value occurs at Z = 114. This is about 4% smaller than the Z =119, A = 297 result obtained from the spherical model outlined in this paper. This comparison between the model and predictions of the Adler relationship of (16) suggests at least the qualitative usefulness of the proposed model.

7.0 Conclusions

Single-particle energies of Z=119 nuclei are calculated to determine their decay properties. The Rost interaction is used as the basis for these calculations. A = 290 – 304 systems have predicted stability in the ps – ms range. The most stable isotope Z = 119 is predicted to occur at A = 297 with an alpha decay half-life of 0.112 s. These results are consistent with the observed properties of Z = 110 – 118 nuclei.

References

1) C. Y. Wong, Additional evidence of stability of the superheavy element $^{310}126$ according to the shell model, Phys. Lett. **21**, 688-690 (1966).

2) E. Rost, Proton Shell-Model Potentials for Lead and the Stability of Superheavy Nuclei, Phys. Lett. **26B**, 184-187 (1968).

3) A. Lukasiak and A. Sobiczewski, Estimations of half-lives of far-superheavy nuclei with Z approx. = 154 - 164, Acta Phys. Pol. **B6,** 147-165 (1975).

4) F. Petrovich et al., Comments on Primordial Superheavy Elements, Phys. Rev. Lett. **37**, 558-561 (1976).

5) G. N. Flerov and G. M. Ter-Akopian, Superheavy Nuclei, Rep. Prog. Phys. **46**, 817 -875 (1983).

6) R. Smolańczuk, Properties of the hypothetical spherical superheavy nuclei, Phys. Rev. C **56**, 812 - 824 (1997).

7) M. Bender et al., Potential energy surfaces of superheavy nuclei, Phys. Rev. C **58**, 2126 -2132 (1998).
8) S. Hofmann and G. Münzenberg, The discovery of the heaviest elements, Rev. Mod. Phys. **72**, 733 -767 (2000).
9) S. B. Duarte et al,, Half-life predictions for decay modes of superheavy nuclei, J. Phys. G: Nucl. Part. Phys. **30**, 1487-1494 (2004).
10) H. Koura et al., Nuclidic Mass Formula on a Spherical Basis with an Improved Even-Odd Term, Prog. Theor. Phys. **113**, 305-325 (2005).
11) P. Mohr, α-nucleus potentials, α-decay half-lives, and shell closures for superheavy Nuclei, Phys. Rev. C **73,** 031301(R) to -5(R) (2006).
12) Yu. Ts. Oganessian et al., Synthesis of the isotopes of elements 118 and 116 in the ^{249}Cf and ^{245}Cm + ^{48}Ca fusion reactions, Phys. Rev. C **74**, 044602-1 to -9 (2006).
13) P. R. Chowdhury, C. Samanta, and D. N. Basu, Search for long lived heaviest nuclei beyond the valley of stability, Phys. Rev. C **77,** 044603-1 to -10 (2008).
14) V. Zagrebaev and W. Greiner, Synthesis of superheavy nuclei: A search for new production reactions, Phys. Rev C **78**, 034610-1 to -11 (2008).
15) C. Samanta, Alpha decay chains from superheavy nuclei, Prog. Part. Nucl. Phys. **62**, 344-348 (2009).
16) P. Möller et al., Heavy-element fission barriers, Phys. Rev. C **79**, 064304-1 to -38 (2009).
17) A. Marinov et al., Evidence for the Possible Existence of a Long-Lived Superheavy Nucleus with Atomic Mass Number A = 292 and Atomic Number Z ≅ 122 in Natural Th, Int. J. Mod. Phys. E **19**, 131-140 (2010).
18) D. N. Poenaru, R. A. Gherghescu, and W. Greiner, Heavy-Particle Radioactivity of Superheavy Nuclei, Phys. Rev. Lett. **107**, 062503-1 to -4 (2011).
19) Yu. Ts. Oganessian et *al*, Production and Decay of the Heaviest Nuclei ^{293,294}117 and ^{294}118, Phys. Rev. Lett. **109**, 162501-1 to -5 (2012).
20) K. Morita et *al*, New Result in the Production and Decay of an Isotope, ^{278}113, of the 13th Element, J. Phys. Soc. Japan **81**, 103201-1 to -4 (2012).
21) J. J. Bevelacqua, 570 ≤ A ≤ 620 Superheavy Nuclei, Physics Essays **25**, 475-483 (2012).
22) Y. Qian and Z. Ren, Predictions on properties of α decay and spontaneous fission in superheavy odd-*Z* nuclei, Phys. Rev. C **90**, 064308-1 to -8 (2014).
23) G. G. Adamian et al., Predictions of identification and production of new superheavy nuclei with Z = 119 and 120, Phys. Rev. **C** 101, 034301-1 to -13 (2020).
24) J. Khuyagbaatar et al., Search for elements 119 and 120, Phys. Rev. C **102,** 064602-1 to -9 (2020).

25) M. Tanaka et al., Probing Optimal Reaction Energy for Synthesis of Element 119 from $^{51}V+^{248}Cm$ Reaction with Quasielastic Barrier Distribution Measurement, Journal of the Physical Society of Japan **91**, 084201-1 to -11 (2022).
26) O.R. Smits et al., Pushing the limits of the periodic table — A review on atomic relativistic electronic structure theory and calculations for the superheavy elements, Physics Reports **1035**, 1–57 (2023).
27) R. Zargini and S. A. Seyyedi, Significance of the compound nucleus surface energy coefficients in the synthesis of superheavy nuclei with Z = 112–120, Phys. Rev. C **108**, 034606-1 to -13 (2023).
28) T. Wan, S-L. Tang, Y-B.Qian, α-decay properties of superheavy nuclei with $117 \leq Z \leq 120$ from the systematics of decay chains and isotopic chains, Chinese Physics C **48,** 034103-1 to -8 (2024).
29) G. E. Brown, J. H. Gunn, and P. Gould, Effective mass in nuclei, Nucl. Phys. **46**, 598-606 (1963).
30) L. Fox and E. T. Godwin, Some new methods for the numerical integration of ordinary differential equations, Proc. Cambridge Philos. Soc. **45**, 373-388 (1949).
31) J. Blomqvist and S. Wahlborn, Shell model calculations in the lead region with a diffuse nuclear potential, Ark. Fys. **16**, 545-566 (1959).
32) NuDat3, National Nuclear Data Center, Brookhaven National Laboratory, Upton, NY. https://www.nndc.bnl.gov/nudat3/.
33) K. Adler, Coulomb Interactions with Heavy Ions, CONF-720669, Proceedings of the Heavy Ion Summer School, June 12 – July 1, 1972, Oak Ridge National Laboratory, Oak Ridge, TN (1972).
34) J. J. Bevelacqua, *Contemporary Health Physics: Problems and Solutions*, 2nd ed. (Wiley-VCH, Weinheim, 2009).

HADRONIC JOURNAL 49, 77 - 94 (2026)
DOI 10.29083/HJ.49.01.2026/SC77

SOLUTION TO THE FINE STRUCTURE CONSTANT 137.036

Francis V. Fernandes
Independent Researcher
137 Bethany, Kodaikanal, TN, India
director@magellantherapeutics.org

Received March 31, 2025
Revised September 26, 2025

Abstract

The fine structure constant 137.036 represents radial pulsation limits of Fernandes-186 ether to the Planck ether length and mass respectively. The Fernandes -186 ether represent the unity of gravity and electromagnetism. Moreover, this unity is possible because of a substructure in the Fernandes-186 ether. The Fernandes dogmas define empirically the true nature of mass. A toroid comprised of Fernandes186-Ether tori is the reason for a measure of wavelength and frequency of light. Experimental evidence utilizing NIST data is provided. At the heart of motion and hence every observed phenomenon is 137.036. A solution to the energy crisis is thus in sight.

Keywords: Ether, Planck, Feynman, Fine Structure Constant, Sommerfeld, MM Experiment, Gravity, Electromagnetism, Current, Voltage, Resistance, Hand of God, Wavelength, Frequency, Ohm's Law, Newton, Charge, Mass, Graviton, Aitheron

Copyright © 2026 by Hadronic Press, Inc., Palm Harbor, FL 34684, USA

1. Introduction

The significance of this paper is a near complete theory on the etheric fabric of space that produces every known measurement in terms of electromagnetism, force, field, and gravitational acceleration. A toroid comprised of 186-Ether allows for the measure of wavelength and frequency of light. My school training of utilizing Physics and Chemistry data booklets is invaluable.

2. Literature Review

Arnold Sommerfeld

In physics, the fine-structure constant, also known as the Sommerfeld constant, commonly denoted by α (the Greek letter *alpha*), is a fundamental physical constant which quantifies the strength of the electromagnetic interaction between elementary charged particles.

It is a dimensionless quantity, independent of the system of units used, which is related to the strength of the coupling of an elementary charge e with the electromagnetic field, by the formula $4\pi\varepsilon_0\hbar c\alpha = e^2$.

The constant was named by Arnold Sommerfeld, who introduced it in 1916 when extending the Bohr model of the atom. α quantified the gap in the fine structure of the spectral lines of the hydrogen atom, which had been measured precisely by Michelson and Morley in 1887.

Why the constant should have this value is not understood, but there are a number of ways to measure its value. Fine-structure constant - Wikipedia

Max Planck

Planck stated in his paper about the Planck mass and length to the Prussian Academy of Sciences, "These necessarily retain their meaning for all times and for all civilizations, even extraterrestrial and non-human ones, and can therefore be designated as 'natural units." Fermilab Today (fnal.gov)

Richard Feynman

"There is a most profound and beautiful question associated with the observed coupling constant, e - the amplitude for a real electron to emit or absorb a real

photon. It is a simple number that has been experimentally determined to be close to 0.08542455. (My physicist friends won't recognize this number, because they like to remember it as the inverse of its square: about 137.03597 with about an uncertainty of about 2 in the last decimal place. It has been a mystery ever since it was discovered more than fifty years ago, and all good theoretical physicists put this number up on their wall and worry about it.) Immediately you would like to know where this number for a coupling comes from: is it related to pi or perhaps to the base of natural logarithms? Nobody knows. It's one of the greatest damn mysteries of physics: a magic number that comes to us with no understanding by man. You might say the "hand of God" wrote that number, and "we don't know how He pushed his pencil." We know what kind of a dance to do experimentally to measure this number very accurately, but we don't know what kind of dance to do on the computer to make this number come out, without putting it in secretly!" Richard Feynman, QED: The Strange Theory of Light and Matter.

Figure 1: Nature reviews the appearance of the Fine Structure Constant in this picture below obtained in several experiments. It is a dimensionless constant.

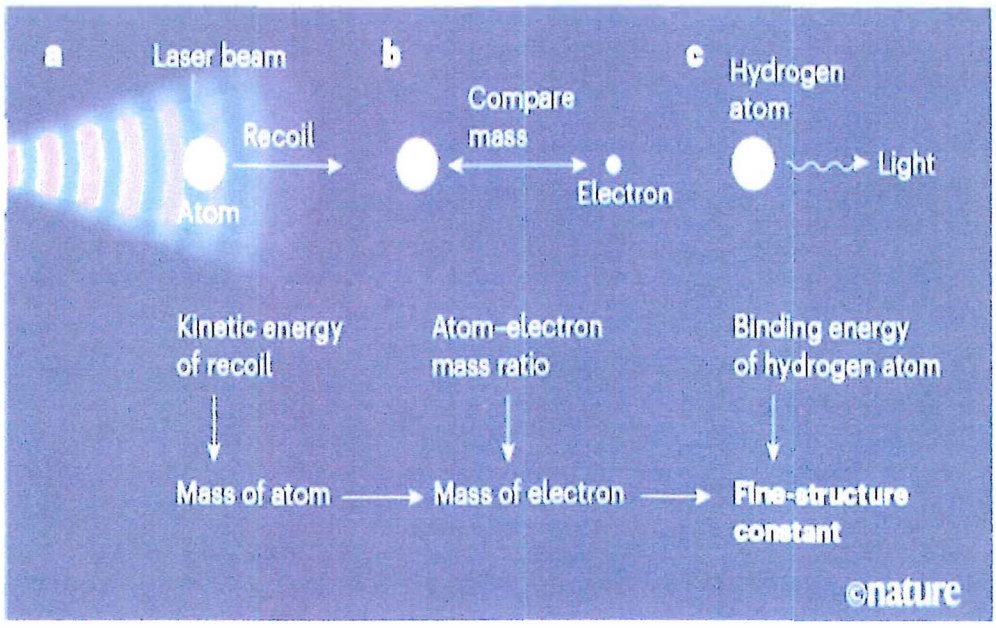

However, in Ref. 1. I have shown the exact reason for the observed Fine Structure Constant depicted above in Nature via the Bohr Model.

3. Method

Employing ratio and proportion where dimensional homogeneity is maintained on both sides of an empirical equation, I present this Fernandes Ether Model utilizing algebraic computation. The ratio of the Fernandes-186 Ether radius to the Planck length is by a factor of 1/137.036 or alpha.

The 186-ether mass, m

$$E = G\frac{mm}{r} = k\frac{ee}{r} \quad (1)$$

$$m = 1.859222909 \times 10^{-9}\ \text{kg} \quad (2)$$

$$G = \frac{1.380668031 \times 10^{-36}}{1.859222909 \times 10^{-9}} \times c^2 \quad (3)$$

4. Data Processing and Analysis

1. Levitation

A simple demonstration of Levitation by an orthogonal magnetic field B on a current carrying conductor. B = I / R

Gravitational force = Electric current squared

Let us consider current generated by the magnetic field, B, of 0.4 T on a 0.5m length of the conductor

$$I = 0.4\ \text{T} \times 0.5\ \text{m} = 0.2\ \text{A} \quad (4)$$

$$F = 0.008\ \text{kg} \times \frac{9.8\ \text{N}}{\text{kg}} = 0.0784\ \text{N} \quad (5)$$

$$F_{grav} = I^2 \quad (6)$$

$$0.0784\ \text{N} = 0.392\ \text{A} \times 0.2\ \text{A} \quad (7)$$

A magnetic field, B, contributes 0.2 A and additional input current of 0.392 A is the reason for levitation.

$$\text{Force} = ma\ \ \frac{eV}{e} = V = a = \frac{c^2}{r}\ \text{The symbol V is acceleration} \quad (8)$$

$$\text{Force} = \text{Current Squared} = ma \quad a = I \times R = I \times \frac{I}{m} \quad R = \frac{I}{m} = \frac{c}{e} \qquad (9)$$

$$\text{Ohms Law} \equiv \text{Newtons Law} \quad a = I \times \frac{I}{m} \qquad (10)$$

2. Magnetic Flux Phi = $\frac{h}{2e}$

Magnetic Flux Quantum – The Magnetic flux quantum is 186-Ether

Electrical Resistance = I/m = c/e where m = ether mass in this context then,

$$I = 3.478898832 \times 10^{18} \text{ amp} \qquad (11)$$

$$\emptyset_0 = \frac{3.478898832 \times 10^{18}}{1.380668031 \times 10^{-36}} \times A \qquad (12)$$

$$\emptyset_0 = 2.519721434 \times 10^{54} \times A \qquad (13)$$

$$A = 8.206596204 \times 10^{-70} \text{ m}^2 \qquad (14)$$

$$A = \pi \times R^2 \times 137.036 \qquad (15)$$

This formula for area, A was arrived at by dividing the area in the above equation by the area of a circle.

$$A = \pi \times (1.380668031 \times 10^{-36})^2 \times 137.036 \times \text{m}^2 \qquad (16)$$

$$\emptyset = I \times \pi \times r \times 10^{-7} \times 137.036 \text{ Wb} \qquad (17)$$

This Area of 186-ether led me to the solution of 137.036 as I spotted the proximity of the Planck dimensions. On checking the ratio, I get 137.036. I connected the B = I / R with the magnetic quantum flux Phi.

3. MM Experiment Revisited – ETHER EXISTS [Ref.1]

Depicted below is a diagram representation of the Michelson & Morley Experiment.

Figure 2: A text book depiction of fringe width and phase shift in the famous MM Experiment about a 100 years ago.

The two beams are waves - let's say that they start in phase. A change in pathlength of one λ corresponds to a shift of one fringe. Let ϕ = the phase shift between the two combined beams:

$$\phi = \frac{\Delta d}{\lambda} = 2\frac{Lv^2}{\lambda c^2}$$

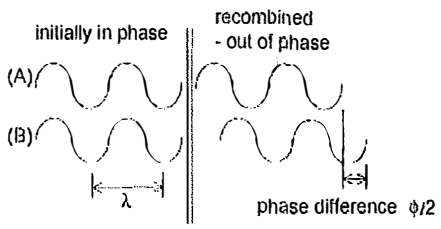

Michelson and Morley predicted $\phi = 0.4$ using their interferometer, with L = 11 m, $\lambda = 5.90 \times 10^{-7}$ m (590 nm), and v = orbital speed of Earth, so that $v/c = 10^{-4}$. They were capable of observing a shift of 0.01. However, they detected no phase shift! Thus, there was no experimental evidence for the ether wind. The results are consistent with the later STR.

I will now show that a fringe shift phi = 2.8×10^{-11} not 0.4 is calculated and therefor was not detected in the experiment. The experimental conclusion of absence of ether is false.

Sun Ether acceleration determines v locally at the arm length of an interferometer

Sun-Earth Distance = 1.471×10^{11} m See (68) for the next step (18)

Ether = $1.346611109 \times 10^{27} \times 1.471 \times 10^{11} = 1.980864941 \times 10^{38}$ kg (19)

Mass of Earth = 5.9748×10^{24} kg (20)

Mass of the Sun = 1.9885×10^{30} kg (21)

Mass of Sun $\times c^2$ = Ether $\times v^2$ Ether from (19) (22)

Mass of every particle and the Sun and Moon is at

the speed of light squared

$v^2 = 902219352.5$ m^2/s^2 (23)

v = 30036.97 m/s Same value as in (26) (24)

$$a = 6.133374 \times 10^{-3}\ m/s^2 \quad (25)$$

Velocity Earth around the Sun = 3×10^4 m/s Data booklet value (26)

Earth $\times c^2$ = Ether $\times v^2$ [RHS represents ether energy] (27)

$v^2 = 2710.8776$ $v \approx 52.0661$ m/s $a = 1.8428 \times 10^{-8}$ m/s^2 (28)

Force of Sun on Earth=Force of Earth on Sun $F = ma$ (29)

$$1.9885 \times 10^{30} \times 1.84288 \times 10^{-8} = 5.9748 \times 10^{24} \times 6.133374 \times 10^{-3} \quad (30)$$

$$a = 6.133374 \times 10^{-3} \approx v^2/11m \quad (31)$$

$v^2 = 0.067467114\ m^2/s^2$ See (34) (32)

L = 11m Ether Model Phi , $\varphi = 2.8 \times 10^{-11}$

[Predicted value by MM phi = 0.4]

An erroneous conclusion by MM - by applying the Earth velocity v around the Sun instead of Ether acceleration caused by the Sun on the arm length of the interferometer.

Delta d is a result of Ether acceleration of 6.133374×10^{-3} m/s^2 by the Sun upon an interferometer of arm length L on Earth. *Ether is the reason for the delta d fringe measurement.* Ether is the fabric in the void of space vibrating with frequency.

$a = 6.133374 \times 10^{-3} = v^2/11m = \boldsymbol{g}$ $v^2 = 0.067467114\ m^2/s^2$

Fits Eqn. (34) (33)

Acceleration, g is key acting locally.

Ether fringe shift $\Delta d = 1.65149 \times 10^{-17}$ m [Ether Model]

$$\varphi = \frac{\Delta d}{\lambda} = 2\frac{L}{\lambda}\frac{v^2}{c^2} \quad (34)$$

Sodium photon mass m* = $3.746133578 \times 10^{-36}$ kg, wavelength 5.9×10^{-7} m

$$\frac{m^*}{m \times 2\pi \times 137.036} = \frac{\varphi}{2} \quad (35)$$

$$m \times 2\pi \times 137.036 = 2.676661 \times 10^{-25}\ \text{Kg} \quad (36)$$

$$m = 3.10689304 \times 10^{-28}\ \text{Kg} \quad (37)$$

$$1/\varphi = m \times 2\pi \times 137.036/2m^* \quad (38)$$

$1/\varphi = 3.572564812 \times 10^{10}$ See (61) Phi , $\varphi = 2.8 \times 10^{-11}$ See (52) (39)

$\varphi/2 = 7.142857143 \times 10^{10}$ (40)

$3.572564812 \times 10^{10} \times 2m^* = m \times 2\pi \times 137.036$ (41)

$41492115.16 \times 2m^* \approx m$ Photon masses from (35) (42)

Charge squared = m × R where R = delta d/2 See (51), (79) (43)

Ether of 11m = $1.48127222 \times 10^{28}$ kg at v^2 (44)

by the ***Sun acceleration*** acting locally on the arm of an interferometer.

See (33)

Ether $M \times c^2 = 1.48127222 \times 10^{28} \times 0.067467114 = 9.993716173 \times 10^{26}$J (45)

Ether Energy = Ether Force, F × Delta d/2 $\mathbf{F} = 1.21 \times 10^{44}$ N See (90) (46)

Distribution of Ether is $1.346611109 \times 10^{27}$ Kg per radial meter. The ether force is that of Fernandes-186-ether at speed of light squared.

Mass = 1.86×10^{-9}Kg and Radius = 1.380668×10^{-36} m See (33)

E = **F** × r = Mass × Speed of light squared. (47)

Ether M = $1.111950886 \times 10^{10}$ Kg See (45) (52) (48)

M/Ether constant = Delta d/2 See (57) (68) (49)

$m = 3.108689304 \times 10^{-28}$ Kg R = Delta d/2 = $8.25745 \times 10^{-18} \times 10^{7}$ (50)

Charge squared = $m \times 8.25745 \times 10^{-18} \times 10^{7}$ See (37) (51)

Phi, $\varphi/2$ = M / Wavelength entrained ether Phi , $\varphi = 2.8 \times 10^{-11}$ (52)

Ether entrained in λ of a sodium photon = $7.945005543 \times 10^{20}$ Kg (53)

Sodium photon mass m = $3.746133578 \times 10^{-36}$ kg (54)

Ether $M \times c^2 = 1.48127222 \times 10^{28} \times 0.067467114$ see (31) (55)

Ether of 11m arm = $1.48127222 \times 10^{28}$ kg [Accelerating Sun Ether] (56)

R = Delta d/2 = $8.257401699 \times 10^{-18}$ m (57)

Delta d = 1.65149×10^{-17}m = 2R (58)

$41492115.16 \times 2m^* = m$ at the arm length of 11m (59)

Or 41492115.16 rotations by $2\pi \times 137.036$ produce delta d shift (60)

$41492115.16 \times 2\pi \times 137.036 = 1/\text{phi} = 3.572564812 \times 10^{10}$ (61)

The existence of Ether has been thus proved.

Ether produced the fringe observed. Acceleration due to ***ether*** *gravity is now fully understood as a local phenomenon about a radial length L.*

In the summary equalities shown below the true meaning of acceleration due to gravity, g is empirically obtained.

$$\frac{\varphi}{2} = \frac{\Delta R}{\lambda} = \frac{\Delta R}{h} = \frac{\Delta f}{f} = \frac{v^2}{c^2} = \frac{hv^2}{\lambda c^2} \qquad \frac{v^2}{h} = \frac{v^2}{\lambda} = g \tag{62}$$

The Cs Clock – The equivalence of Quantum Physics and GRT.

A GPS Cs clock in geostationary orbit at an altitude *h* above the surface of Earth experiences gravitational lensing of a photon by delta f = 0.77 Hz. Photon frequency of f1 = 9,191,631,770 Hz (at mean sea level on earth) changes to 9,191,631,769.23 Hz, the Cs clock tick (in GPS orbit).

Altitude above surface of Earth, *h*	*h* = 768226.1658 m
Emitted photon frequency on Earth, f1	f1 = 9,191,631,770 Hz

Gravitational lensing measured as delta f	$\Delta f = 0.77$ Hz
Speed of Light Squared, $c^2 = VRK \times FTL$	VRK = 25812.807 m/s FTL = 3,481,818,845,725.757915441 m/s
737 Aitheron	$7.372497321 \times 10^{-51}$ kg.s
Phase Shift, $\varphi/2$	8.377185×10^{-11}
Velocity Squared, $v^2 = FTL \times v^*$	7,528,616.42484 m^2/s^2
Velocity, $v^* = R \times \Delta f$	291.66205848282986 m/s
Distance, R	378.781 m
Emitted photon of mass, m = f1 × 737 Aitheron	$6.776528059994348817 \times 10^{-41}$ kg
Charge squared, $e^2 = m \times R$	$(1.602176537 \times 10^{-19})^2$ C^2
Acceleration due to Earth's gravity, $g = v^2 / h$	9.8 m/s^2
Photon mass at FTL = Δ f × 737 Aitheron	$5.67682293717 \times 10^{-51}$ kg
Photon wavelength of mass m, λ	0.032615803757890767734 m
De Broglie Equation, m × VRK × R = h Planck, h= m × c × λ	$6.62607015 \times 10^{-34}$ J.s
Conservation of Momentum	$5.67682293717 \times 10^{-51} \times$ FTL $= 6.77652806 \times 10^{-41} \times 291.662$ Kg.m/s

Phase Shift, $\frac{\varphi}{2} = \frac{\Delta d/2}{\lambda} = \frac{hv^2}{\lambda c^2}$ [MM EXP]	$\frac{\varphi}{2} = \frac{\Delta f}{f} = \frac{gh}{c^2} = \frac{v^2}{c^2} = \frac{v*}{FTL}$ $\frac{\varphi}{2} = 8.377185 \times 10^{-11}$ [GRT&ETHER]
737 Aitheron Frequency $\varphi/2 = \frac{\Delta f}{f}$ [QUANTUM & FERNANDES ETHER MODEL]	DOGMAS [FERNANDES ETHER MODEL]

$$\varphi = \frac{\Delta d}{\lambda} = 2\frac{hv^2}{\lambda c^2} \qquad \frac{\Delta R}{h} = \frac{\Delta f}{f} = \frac{gh}{c^2} = 8.377185 \times 10^{-11} \tag{63}$$

For h, $\emptyset/2 = 8.377185 \times 10^{-11}$ when $g \sim 9.8\,m/s^2$ (64)

For 11m, $\emptyset = 2.398873521 \times 10^{-15}$ when $g \sim 9.8\,m/s^2$ (65)

The mass of delta f = Phi × Photon mass of lambda

If L=11m is replaced by $h = 768226.1658$ m (GPS) $delta\,f = 0.77\ Hz$ (66)

For Na, $\lambda = 5.9 \times 10^{-7}$ $delta\,f = 1.218922355\ Hz$ (67)

The source photon frequency emissions from atoms such as sodium [Spectroscopy] or cesium [GPS] work for the equations above.

GRT produces the same outcome as the MM experiment in (62), (63) and Delta d/2 of the MM Experiment is shown to be that of an Ether fringe. Velocity squared of Ether is the source of acceleration due to gravity (45) (46).

4. Entrained Ether for Earth Gravity. Equation holds for other planets and stars in our solar system. [Ref. 1]

Field: $\frac{M}{R} = \frac{1.859222909 \times 10^{-9}}{1.380668038 \times 10^{-36}} = 1.346611109 \times 10^{27}$ kg/m [Ether Constant] (68)

Acceleration due to gravity as defined by convention is, $g = \frac{v^2}{r}$ (69)

The Ether Model:

$$M_{Earth} \times c^2 = M_{Ether} \times v^2 \text{ The reason for motion.} \quad (70)$$

Entrained Ether for Earth's Gravity

The acceleration of entrained ether produces an acceleration of 9.8 m/s^2

Radius of Earth, $r = 6.371 \times 10^6$ m (71)

Ether = $1.346611109 \times 10^{27} \times 6.371 \times 10^6 = 8.57926 \times 10^{33}$ kg (72)

Force of entrained ether F = ma (73)

$F = 8.57926 \times 10^{33} \times 9.82 \quad F = 8.42483332 \times 10^{34}$ N (74)

Force, F of earth mass, m oscillators, F = ma (75)

$$F = m \times \frac{c^2}{r} \quad F = 8.42483332 \times 10^{34} = m \times \frac{c^2}{6.371 \times 10^6} \quad (76)$$

$m = 5.9748 \times 10^{24}$ kg mass of earth (77)

5. Wave Particle Duality & Field: Particle ripple wave in the etheric field.

Charge Squared derived as follows:

$$F = k \times q \times q/R^2 = Mc^2/R \quad (78)$$

$$q^2 = M \times R \times 10^7 \quad (79)$$

The Compton Wavelength can be stated as an empirical equation.

$\lambda = (2\pi \times 137.036) \times R$ and $\lambda = 2\pi \times (R \times 137.036)$ which depict limits of radial expansion and contraction of a torus or toroid from *R* to $R \times 137.036$.

The number 137.036 represents a radial pulsation of a torus between radius R and $R \times 137.036$. This pulsation yields the wavelength of light photons and the Compton wavelength of particles in general.

At the upper limit of R × 137.036 the wavelength $\lambda = 2\pi$ [R × 137.036].

At the lower limit R the same wavelength $\lambda = [2\pi \times 137.036] \times R$

Wavelength of Light: $\alpha = \mu_0 \times c \times \frac{e^2}{2h}$ (80)

$$\alpha = 4\pi \times 10^{-7} \times c \times M \times R \times \frac{10^7}{2(M \times c \times \lambda)} = 2\pi R/\lambda \quad (81)$$

$$\lambda = 2\pi \times R \times 137.036 \quad (82)$$

6. Electric Charge of Ether

Ether as Elementary Charge Squared

$$q^2 = M \times R \times 10^7 \quad (83)$$

$$(1.602176537 \times 10^{-19})^2 = 1.859222909 \times 10^{-9} \times 1.380668031 \times 10^{-36} \times 10^7$$

5. Results and Discussions

Fernandes Scientific Dogmas

Graviton Mass: $7.372497321 \times 10^{-58}$ Kg

f1 = *10e7 Hz of a graviton produces an aitheron*

$$1.859222909 \times 10^{-9} \times VRK = 7.372497321 \times 10^{-58} \times \frac{c^2}{1.380668031 \times 10^{-36}} \times 1.0 \quad (84)$$

737 Aitheron Mass: $7.372497321 \times 10^{-51}$ Kg

The energy of 737 equals the Planck's constant times one second

$$7.372497321\times10^{-51}\times c^2=h\times1.0 \quad (85)$$

$$1.859222909\times10^{-9}\times VRK=7.372497321\times10^{-51}\times\frac{c^2}{1.380668031\times10^{-29}}\times1.0 \quad (86)$$

The imposed condition is 1 second for the wave-maker to exist

DOGMA – Graviton mass x f1[10e7] = Aitheron mass

DOGMA – Aitheron mass × f2[Codata] = anti-matter mass [photon, atoms, electrons, protons etc] *in one second*

DOGMA – anti-matter mass × f3 = 186-ether mass *in one second*

NOTE: f2 × f3 events are simultaneous because their product is a constant.

DOGMA – 186-ether × f3 =Toroid mass simultaneous in one second with f1 and f2 and f3

The Ether toroid mass = $4.688656088 \times 10^{39}$ kg

DOGMA – Basically $2.521836443 \times 10^{48}$ cycles are being reorganized into tori.

DOGMA – The source of wavelength is the ether toroid as depicted in the image below.

DOGMA – The acceleration, a of the ether toroid from f3 is the source of the measurement of eV where the symbol V is acceleration, a.

DOGMA – The force generated by the acceleration, a or eV/e of the ether toroid of mass m is 1.21e44N.

DOGMA – This force of 1.21e44N is exactly that of Fernandes 186-ether mass at speed of light squared by its radius B or r in the torus image below.

The Ether Force of Gravity

$$E = 1.859222909 \times 10^{-9} \times (2.99792458 \times 10^8)^2 \quad (87)$$

$$E = 1.670986218 \times 10^8 \text{ J} \quad (88)$$

$$E = F \times R \tag{89}$$

$$F = \frac{E}{R} = \frac{1.670986218 \times 10^{8}}{1.380668031 \times 10^{-36}} \tag{90}$$

$$F = 1.210273708 \times 10^{44}\ N$$

Ether Gravitational Force is the strongest of all forces

Figure 3: An image of a torus with major and minor axes. The fabric of the mass of space is toroidal at the atomic, galactic, and in the void of space.
Major Axis Radius, $R = 1.380668031 \times 10^{-29}$m [Note: symbol R is for this image only]
Minor Axis Radius, $r = 1.380668031 \times 10^{-36}$m [Note: symbol r is for this image only]

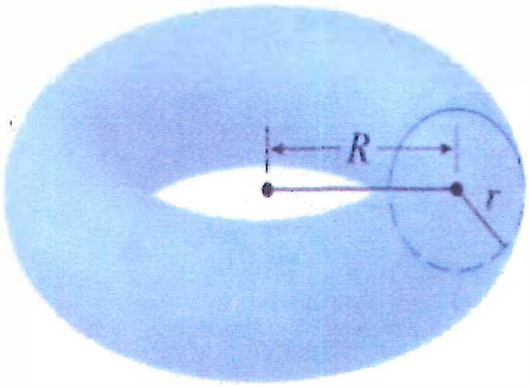

CYCLES OF ANTI-MATTER IN ONE SECOND INTERVAL OF TIME IS THE SCAFFOLD IN THE VOID [Note – A point graviton mass spirals creating the measures of mass we know as frequency and wavelength. A point cannot interact with itself.]

The Ether Toroid

Intervals of mass – As defined by Frequencies f1 x f2 x f3 x f3 define intervals of mass and length and time-period. The frequency f3 = f4 produces a toroid. The frequency f3 and f4 magnitudes are the same.

However, the mass outcomes are different. Frequency f3 produces 186-Ether whereas frequency f4 produces an ether toroid.

Figure 4: A depiction of an Ether Toroid the source of wavelength [Ether Dogmas]

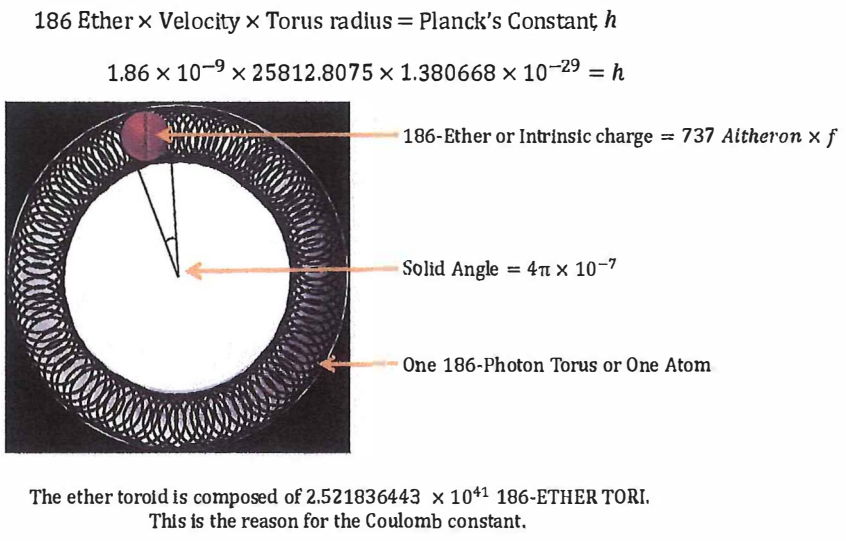
186 Ether × Velocity × Torus radius = Planck's Constant h
$1.86 \times 10^{-9} \times 25812.8075 \times 1.380668 \times 10^{-29} = h$
186-Ether or Intrinsic charge = 737 *Aitheron* × f
Solid Angle = $4\pi \times 10^{-7}$
One 186-Photon Torus or One Atom
The ether toroid is composed of $2.521836443 \times 10^{41}$ 186-ETHER TORI.
This is the reason for the Coulomb constant.

Data describing Ether:

186 Ether Mass $=1.859222909\times10^{-9}$ kg

Ether Force
$=1.210273708358125254544489963641 4\times10^{44}$ N ~ 1.21×10^{44} N

186 Ether Torus Radius $=1.380668031\times10^{-36}$ m

The Ether toroid radius = $1.380668031\times10^{-29}$ m

Ether Black Hole: Obeys the Ether Mass Constant described by the Schwarzschild radius

Schwarzschild Radius = $2\ G\ m\ /\ c^2$

Ether Mass Constant distribution ratio: 1.346611109×10^{27} Kg/m

VRK = 25812.807 m/s

The Ether Torus Radius is the reason for wavelength.

Wavelength = 2Pi x Torus Radius x 137.036

6. Conclusion

The entire math in algebraic form is based on dimensional homogeneity of empirical equations.

The Fernandes scientific dogmas define important structural hierarchy of the mass of the fabric of space. Frequency is the inverse of time period. The Fernandes Ether Model is a depiction of gravitons, 737 aitherons, photons/electrons/protons/atoms, 186-ether, ether toroid based on frequencies. It is an empirical model that explains wavelength based on a waving ether mass.

The force of gravity in standard Physics appears weak because the acceleration is that of ether on matter. In equations for planets the LHS represents matter mass and the RHS Ether.

Figure 5: Fernandes-186-Ether expands by 137.036 to Yield the Planck Ether.

Here is the solution of the Fine Structure Constant. The source of all measured phenomena in science.

$$m_{pl} \equiv \sqrt{\frac{\hbar c}{G}} = \text{Planck Mass} = 2.176450474 \times 10^{-8}\ \text{kg}$$

$$\text{or } \pi B^2 \times 137.036 = \pi \times (\text{Planck length})^2$$

I have discovered this correspondence in the dynamic living pulsation of ether

$$B = 1.380668031 \times 10^{-36}\text{m Torus radius}$$

$$\text{Planck length} = 1.616255(18) \times 10^{-35}\ \text{m}$$

TECHNOLOGICAL SIGNIFICANCE – In Physics

- Perpetual motion machines – By tapping into the reason for eV as acceleration of an ether toroid.
- Spectroscopy – By utilizing the equation equality in the MM Experiment.
- Imaging – By utilizing the clear understanding of magnetic field pressure.
- Nuclear remediation – By utilizing the ether scientific dogmas

References

[1] Francis V. Fernandes, The Hand of God Alpha Represents Radial Pulsation Limits of Fernandes-186 Ether to the Planck Ether Length, Sips23_70_407FS

[2] R. P. Feynman, (1985). *QED: The Strange Theory of Light and Matter. Princeton University Press*. ISBN 978-0-691-08388-9

[3] Arnold Sommerfeld, (1916), Zur Quantentheorie der Spektrallinien. Annalen der Physik. 4 (51): 51–52

HADRONIC JOURNAL 49, 95 - 111 (2026)
DOI 10.29083/HJ.49.01.2026/SC95

ON A LOGARITHMIC NONLINEAR SCHRÖDINGER EQUATION COMPATIBLE WITH HADRONIC MECHANICS AND ITS CONNECTION WITH OTHER APPROACHES FOR THE DESCRIPTION OF DISSIPATIVE SYSTEMS

Dieter Schuch
Institut für Theoretische Physik, J. W. Goethe-Univeristät
Robert-Mayer-Str. 8-10, D-60054 Frankfurt am Main, Germany
and Istituto per la Ricerca di Base, Castello Principe Pignatelli
I-86075 Monteroduni (IS), Molise, Italy

Abstract

The time-dependent approach of Caldirola and Kanai (CK) for dissipative systems can be traced back to the conventional system-plus-reservoir approach; however, it apparently violates the uncertainty principle. This discrepancy can be avoided by considering a consistent transition between the CK formalism and a logarithmic nonlinear Schrödinger equation (NLSE) which requires not only a transformation of the operators, but also a nonunitary transformation of the wave function. This procedure also shows the equivalence of three approaches - which, at first sight, seem to be incompatible with each other - for the description of dissipative quantum systems. In addition, the transition from the NLSE to the linear canonical CK-theory presents an explicit example of genolinearization, introduced by R.M. Santilli in the framework of hadronic mechanics.

Reprinted from: Gill, Tepper L., Editor, "*New Frontiers in Hadronic Mechanics*" Hadronic Press, ISBN 1-57485-016-4, p. 113-129 (1996)

Copyright © 2026 by Hadronic Press, Inc., Palm Harbor, FL 34684, USA

1. Introduction

Irreversibility and dissipation are not taken into account in the fundamental equations of motion - neither on the classical nor on the quantum mechanical level - they usually enter via some kind of course-graining arguments. Since irreversibility is the rule in the perceivable world, this discrepancy is considered unsatisfactory by an increasing number of scientists (see e.g. [1,2]). However, the question of how to modify the classical Lagrangian and Hamiltonian formalisms and the corresponding quantization methods, in order to include dissipation and irreversibility, has not yet been answered in a unique way that would be generally accepted. Different approaches exist in the literature which have their peculiar advantages and shortcomings and most of them seem to be incompatible with each other. In this paper three types of these apparently incompatible approaches which are frequently applied in the literature shall be discussed and it will be shown that they are actually intimately connected. These approaches are 1) the system-plus-reservoir model, 2) attempts to use explicitly time-dependent Lagrangians and Hamiltonians and 3) nonlinear Schrödinger equations (NLSE). The existence of a unique transformation between the latter two approaches will be explicitly shown and it will become clear how presumed shortcomings can be dispensed with if the problem is properly treated.

2. Problems with the Caldirola–Kanai Approach

The system-plus-reservoir ansatz is based on conventional conservative quantum mechanics. It couples the system of interest with a large number of environmental degrees of freedom. Subsequent elimination of these degrees of freedom reduces the entire conservative system to a "relevant" dissipative system. A well-known model of this kind has been proposed by Caldeira and Leggett [3]. Similar models and their interrelations, essentially via unitary transformations, are discussed by Ford et al [4]. However, the "consideration of a large number of degrees of freedom, each of which is governed by a partial differential equation" [5] might, in certain cases, e.g. for the study of the quantum limit of chaotic dissipative systems, exhaust or even go beyond the power of the largest and fastest computers.

Since the main interest is usually focused only on a few degrees of freedom,

more phenomenologically motivated approaches have been proposed which do not take the environmental degrees of freedom explicitly into account, but try to describe the system of interest with the help of some kind of effective Hamiltonian (see e.g. [6] and refs. cited therein). These Hamiltonians can be either explicitly time-dependent or they may contain additional nonlinear friction terms, thus leading to NLSEs.

The historically first and most frequently used time-dependent Hamiltonian was proposed by Caldirola [7] and Kanai [8]; a similar approach, using an expanding coordinate system and a Hamiltonian that is a time-dependent invariant, has been discussed by us [9]. Both models can be connected on the classical level, via a canonical transformation. The application of (linear) time-dependent Hamiltonians would permit the direct use of standard schemes of quantization. Although the classical Hamiltonian function of Caldirola and Kanai (CK),

$$H_{CK} \;=\; \frac{1}{2m} e^{-\gamma t}\, \tilde{p}_{CK}^{2} + e^{\gamma t} V(x) \quad . \tag{1}$$

with friction constant γ, yields the proper equation of motion for a system under the influence of a linear velocity (or momentum) dependent frictional force

$$m\ddot{x} + m\gamma\dot{x} + \frac{\partial}{\partial x}\, V(x) \;=\; 0 \quad , \tag{2}$$

a problem arises after canonical quantization. Since the canonical momentum

$$\tilde{p}_{CK} \;=\; m\dot{x}e^{\gamma t} \;=\; pe^{\gamma t} \quad , \tag{3}$$

which corresponds to the operator $\tilde{p}_{op} = \frac{\hbar}{i}\frac{\partial}{\partial x}$, differs from the physical kinetic momentum $p = m\dot{x}$, the commutator of physical momentum and position, and hence the uncertainty product, decay exponentially. This apparent violation of the uncertainty principle gave rise to serious criticisms [10-12] as well as attempts to avoid [13-14] or explain [15] this peculiarity of the CK model. (For a review, see also [16].)

Studying the literature carefully, one is under the impression that the explanations given for the violation of the uncertainty principle are not totally convincing and that the critics might be correct. However, a new aspect was recently added, when Sun and Yu [17-18] were able to show that it is possible to obtain the CK Hamiltonian *operator*, starting with the conventional

system-plus-reservoir approach. This leads to the paradoxical situation where a Hamiltonian operator, which can be traced back to conventional quantum mechanics, apparently causes violation of one of the most fundamental principles of this theory, the uncertainty principle! After a brief discussion of the third type of approaches, the NLSEs, it will be shown how this paradox can be eliminated.

3. Problems with some Nonlinear Approaches

A way to circumvent the problem of finding a classical Hamiltonian for dissipative systems that can be canonically quantized is to add a friction term directly to the Hamiltonian operator,

$$H_{NL} \;=\; -\frac{\hbar^2}{2m}\,\frac{\partial^2}{\partial x^2} + V(x) + W \;=\; H_L + W \quad . \tag{4}$$

There are several attempts of this kind in the literature (see e.g. [6,19-21]). Most of them use as a guideline to finding the proper form of W, that Ehrenfest's Theorem in the form

$$\frac{d}{dt}\;<p> + \gamma <p> + <\frac{\partial}{\partial x}V> \;=\; 0 \tag{5}$$

has to be fulfilled. From the Heisenberg equations of motion it follows then that the additional term W is defined via

$$<\frac{\partial}{\partial x}W> \;=\; \gamma <p> \quad . \tag{6}$$

This definition, however, is by far not unique as it contains 1) only the derivative of W, 2)in fact, only the mean value of this derivative, and 3) also only the mean value of the momentum p. Problems that could arise from 1) and 2) are obvious, but 3) is also a source of confusion, as different definitions of momenta (or velocities) occur in quantum mechanics, all of which have the same mean value.

In Schrödinger's first communication on wave mechanics [22] he starts with the Hamilton–Jacobi (HJ) equation

$$\frac{\partial}{\partial t}S_C + H\left(x, \frac{\partial}{\partial x}S_C, t\right) \;=\; 0 \tag{7}$$

with the action function S_C and the momentum $p_C = \frac{\partial}{\partial x} S_C$. He introduces the wave function $\Psi(x,t)$ through $S_C = \frac{\hbar}{i} ln \Psi$ (where he erroneously forgot the imaginary unit $i = \sqrt{-1}$ in his first paper) and arrives, via a variational ansatz, at the Hamiltonian operator H_L. With his definition of S_C, the momentum reads

$$p_C \;=\; \frac{\hbar}{i}\,\frac{\partial}{\partial x}\,\ell n\;\Psi \;=\; \frac{\hbar}{i}\frac{\frac{\partial}{\partial x}\Psi}{\Psi} \quad , \tag{8}$$

which is a *complex* quantity, if Ψ is complex, i.e. $S_C = S_R + S_I$! Obviously the mean value of p_C is identical with that of the quantum mechanical momentum operator $p_{op} = \frac{\hbar}{i}\frac{\partial}{\partial x}$, $< p_C > = < \frac{\hbar}{i}\,\frac{\partial}{\partial x} >$. The density $\varrho = \Psi^* \Psi$ obeys the Continuity Equation (CE)

$$\frac{\partial}{\partial t}\varrho \;+\; \frac{1}{m}\,\frac{\partial}{\partial x}(\varrho\, p_-) \;=\; 0 \quad , \tag{9}$$

where only the *real* part of p_C, namely $p_R = \frac{\hbar}{2mi}\frac{\partial}{\partial x} ln \frac{\Psi}{\Psi^*}$, occurs. Comparison shows, however, that p_R also has the same mean value as p_C and p_{op}, since the mean value of the imaginary part $p_I = \frac{\hbar}{2mi}\frac{\partial}{\partial x} ln \varrho$ always vanishes (for quadratically integrable functions).

In the most-often discussed and 'rederived' nonlinear approach, Kostin [19] clearly uses only the real part p_R, thus arriving at the real friction term

$$W_K \;=\; \gamma \frac{\hbar}{2i}\left(\ell n \frac{\Psi}{\Psi^*} - < \ell n \frac{\Psi}{\Psi^*} >\right) \quad , \tag{10}$$

where the occurring mean value guarantees that $< W_K > = 0$, and thus $< E > = < H_L > = < T > \;+\; < V >$ is still valid. As stated in the literature [6], this term leads to results that are difficult to explain in physical terms: 1) stationary solutions of the undamped Harmonic Oscillator (HO) (which are real functions) are also solutions to the problem including damping; 2) the solutions of the damped HO contain the undamped frequency ω instead of the reduced frequency $\Omega \;=\; (\omega^2 - \gamma^2/4)^{1/2}$; 3) the density $\varrho(x,t)$ fulfils the *reversible* CE, although the system displays *irreversible dynamics.*

4. A Logarithmic NLSE 'Derived' from an Irreversible Fokker–Planck-type Equation

It has been shown [23-24] that all these problems can be solved or avoided by modifying a separation method, which was introduced by Madelung [25] and Mrowka [26], to 'rederive' the conventional linear SE, without applying Hamilton's form of classical mechanics, but only Newton's form. In the following, the method shall be outlined only to the extent necessary for showing how irreversibility can be included; for further details see Refs. [23-26]. (The extension to three dimensions is straightforward.)

The axiomatic basis of the method is given by three principles taken from experimental evidence:

1. the uncertainty principle;
2. the occurrence of interference phenomena in experiments with material systems and
3. the correspondence principle, specified in the form of Ehrenfest's theorem.

The first axiom implies that exact initial conditions in the sense of classical mechanics cannot be given. Therefore, it is only possible to develop a theory which considers mean values of physical qauantities Q (such as position, momentum, etc.), $\overline{Q} = \int \varrho Q \, dx$, evaluated with the help of a distribution function $\varrho(x,t)$ that fulfils a conservation law, which, in this case, is assumed to be the CE (9) with the convection current density $j_- = \varrho v_- = \frac{1}{m}\varrho p_-$.

By analogy with optics, where the intensity is a quadratic function of the amplitudes, the second axiom requires a bilinear ansatz for the density ϱ, i.e.

$$\varrho(x,t) = \alpha(x,t) \cdot \beta(x,t) \geq 0 \tag{11}$$

with complex field amplitudes α and β, and similarly for the current density

$$j_- = \varrho v_- = C\left(\beta \frac{\partial}{\partial x}\alpha - \alpha \frac{\partial}{\partial x}\beta\right) , \tag{12}$$

or the velocity field

$$v_- = C \frac{\partial}{\partial x} \ell n \frac{\alpha}{\beta} = C\left(\frac{\frac{\partial}{\partial x}\alpha}{\alpha} - \frac{\frac{\partial}{\partial x}\beta}{\beta}\right) \tag{13}$$

with C being constant or, at most, purely time-dependent.

In order to solve the CE for ϱ, the phase of the complex field amplitudes which enter via j_-, also has to be determined. For this purpose, the definitions of ϱ and j_- are inserted into the CE(9). By introducing a function $f(x,t)$ which is independent of α and β, it is possible to separate this CE into two equations containing only α or β, exclusively:

$$\frac{\partial}{\partial t}\alpha + C\frac{\partial^2}{\partial x^2}\alpha + f\alpha = 0 \tag{14}$$

$$\frac{\partial}{\partial t}\beta - C\frac{\partial^2}{\partial x^2}\beta - f\beta = 0 \ . \tag{15}$$

The physical meaning of the separation function $f(x,t)$ becomes obvious when the third axiom is applied in considering the mean value of Newton's equation of motion:

$$\begin{aligned}\int \varrho\, F\, dx = m\frac{d}{dt}\int \varrho v_- dx &= m\int 2C\left(\frac{\partial}{\partial t}\beta\frac{\partial}{\partial x}\alpha - \frac{\partial}{\partial t}\alpha\frac{\partial}{\partial x}\beta\right)dx \\ &= \int \varrho[-\frac{\partial}{\partial x}(2mCf)]dx \end{aligned} \tag{16}$$

where Eqs.(14) and (15) have been used to replace the time-derivatives of α and β. The separation function f is obviously proportional to the potential $V(x)$,

$$f = \frac{1}{2mC}\,V(x) \ . \tag{17}$$

By replacing $\alpha(x,t)$ by $\Psi(x,t)$ and choosing $C = \hbar/2mi$, Eq.(14) becomes the well-known time-dependent SE

$$i\hbar\,\frac{\partial}{\partial t}\,\Psi\,(x,t) = \{-\frac{\hbar^2}{2m}\frac{\partial^2}{\partial x^2} + V(x)\}\Psi(x,t) = H_L\Psi(x,t) \ . \tag{18}$$

In aiming at describing irreversible dymamics, the CE has to be modified in a way that the new conservation law is no longer invariant under time-reversal. Diffusion processes represent an important class of irreversible processes with a simple, structurally similar equation of motion for the distribution function. Therefore, the addition of a diffusion current density

$$j_d = -D\frac{\partial}{\partial x}\varrho = -D\left(\beta\frac{\partial}{\partial x}\alpha + \alpha\frac{\partial}{\partial x}\beta\right) \tag{19}$$

(with diffusion coefficient D) to the convection current density (12) turns the CE into the irreversible Fokker–Planck-type equation (FPE)

$$\frac{\partial}{\partial t}\varrho + \frac{1}{m}\frac{\partial}{\partial x}(\varrho\, p_-) - D\frac{\partial^2}{\partial x^2}\varrho = 0 \ . \tag{20}$$

The inclusion of a diffusion current density was later supported by group theoretical arguments [27]. Due to the structure of the additional diffusion term

$$-D\frac{\partial^2}{\partial x^2}\varrho = -D\{\alpha\frac{\partial^2}{\partial x^2}\beta + \beta\frac{\partial^2}{\partial x^2}\alpha + 2\left(\frac{\partial}{\partial x}\alpha\right)\left(\frac{\partial}{\partial x}\beta\right)\} \tag{21}$$

separation of the FPE (20) is, in general, not possible, but can at least be achieved in special cases. In the context of this investigation, the additional condition

$$-D\frac{\frac{\partial^2}{\partial x^2}\varrho}{\varrho} = \gamma\,(\ell n\varrho - <\ell n\varrho>) \tag{22}$$

has to be fulfilled, where the mean value on the rhs guarantees normalizability. After separation, the SE contains an additional logarithmic nonlinear term (log NLSE):

$$i\hbar\frac{\partial}{\partial t}\Psi = \{H_L + \gamma\frac{\hbar}{i}(\ell n\Psi - <\ell n\Psi>)\}\Psi \ . \tag{23}$$

When Ehrenfest's theorem is considered, the physical meaning of the NL term becomes obvious, as the logarithmic term gives rise to the additional friction term $\gamma < p >$ in the classical equation of motion. Here, however, the NL term in the NLSE is not 'derived' from the classical friction term but, to the contrary, the correct classical friction term results from the additional irreversible diffusion term in connection with the separation condition (22). (This NL term is in agreement with the complex momentum p_C, where the imaginary part is responsible for the break of time symmetry in the density equation.) For further details see [23-24].

5. Connection Between the log NLSE and the Caldirola–Kanai Approach

The connection between our log NLSE and the time-dependent CK approach shall now be elucidated. For this purpose, we reverse the procedure of Schrödinger's original quantization method, divide the NLSE by Ψ and use the definition of action S_C, yielding

$$\left(\frac{\partial}{\partial t} + \gamma\right) S_C + H \;=\; -\gamma < S_C > \quad . \tag{24}$$

This is, of course, as little rigorous as Schrödinger's first attempt was; however, it follows his way of thinking of how to connect the classical HJ theory with a wave (mechanical) equation. The term $-\gamma < S_C >$ is necessary mainly for normalization purposes and shall be neglected for the moment. Eq.(24) now shows some similarity to an approach used by Razavy [28] and also discussed by Wagner [29]. However, in agreement with Kostin, these Authors also use only the *real* part S_R of the complex action function S_C. S_R enters a (real) HJ-type equation (with an additional so-called "quantum potential"), if Madelung's hydrodynamical form of quantum mechanics is used. The imaginary part is ignored, as it would yield an additional term to the CE and might thus violate the normalizability of the wave functions. The above-mentioned FPE shows that this is not necessarily the case as it still allows normalization. Multiplying the remaining lhs of Eq.(24) by $e^{\gamma t}$ and using the definitions

$$\tilde{S}_C \;=\; e^{\gamma t} S_C \quad \text{and} \quad \tilde{H} \;=\; e^{\gamma t} H \tag{25}$$

finally yields the HJ equation

$$\frac{\partial}{\partial t}\tilde{S}_C + \tilde{H} \;=\; 0 \quad . \tag{26}$$

From the definitions of the action functions, it follows that the wave function $\tilde{\Psi}$ in the transformed system is connected with the wave function Ψ in the physical system via

$$\ell n \tilde{\Psi} \;=\; e^{\gamma t} \ell n \Psi \quad . \tag{27}$$

Consequently, the complex momenta in the two systems are connected via

$$\tilde{p}_C \;=\; \frac{\hbar}{i}\frac{\partial}{\partial x}\,\ell n \tilde{\Psi} \;=\; e^{\gamma t}\,\frac{\hbar}{i}\,\frac{\partial}{\partial x}\,\ell n \Psi \;=\; e^{\gamma t} p_C \quad , \tag{28}$$

which is equivalent to the connection between canonical and kinetic momentum in the CK theory. The *non-canonical* connection between the classical variables (x,p) and $(x,\tilde{p}_{CK})$ corresponds to the *non-unitary* connection between Ψ and $\tilde{\Psi}$. Although Ψ and $\tilde{\Psi}$ both depend explicitly only on x and t, the connection between the momentum and $ln\Psi$ has the consequence that $\tilde{\Psi}(x,t)$ in the transformed system is *different* from $\Psi(x,t)$ in the physical system.

Expressing $\tilde{H}$ in terms of the canonical momentum $\tilde{p}_C$,

$$\tilde{H}(x,\tilde{p}_C,t) \;=\; e^{-\gamma t}\frac{\tilde{p}_C^2}{2m} + e^{\gamma t}\; V(x) \tag{29}$$

and following Schrödinger's quantization procedure, but now using the canonical momentum $\tilde{p}_C$, finally yields

$$i\hbar\frac{\partial}{\partial t}\;\tilde{\Psi}(x,t) = \tilde{H}_{op}\;\tilde{\Psi}(x,t) = \{e^{-\gamma t}\left(-\frac{\hbar^2}{2m}\frac{\partial^2}{\partial x^2}\right) + e^{\gamma t}V\}\tilde{\Psi} = H_{CK,op}\tilde{\Psi}\;, \tag{30}$$

where the Hamiltonian *operator* $\tilde{H}_{op}$ is identical with the one of CK and $\tilde{p}_{op} = \frac{\hbar}{i}\frac{\partial}{\partial x}$.

Remark: $\tilde{p}_C^2$ in Eq.(29) would actually lead to a term proportional to $\left(\frac{\partial}{\partial x}\tilde{\Psi}/\tilde{\Psi}\right)^2$ which differs from $\frac{\partial^2}{\partial x^2}\tilde{\Psi}$ by a term proportional to $\frac{\partial}{\partial x}\tilde{p}_C = \frac{\partial}{\partial x}\left(\frac{\partial}{\partial x}\tilde{\Psi}/\tilde{\Psi}\right)$. Following Schrödinger's variational ansatz, this term disappears. Further details will be discussed in forthcoming publications.

N.B.: The major difference between Eq.(30) and the CK-theory is that in the latter, the operator $H_{CK,op}$ acts on the wave function $\Psi(x,t)$ in physical space, instead of acting on $\tilde{\Psi}(x,t)$ in the transformed system! However, for consistency reasons it is necessary, if the momentum is transformed according to $p_C \rightarrow \tilde{p}_C$, that the wave function also has to be transformed accordingly, $\Psi \rightarrow \tilde{\Psi}$, since $p_C = \frac{\hbar}{i}\frac{\partial}{\partial x}ln\Psi \rightarrow \tilde{p}_C = \frac{\hbar}{i}\frac{\partial}{\partial x}ln\tilde{\Psi}$, where Ψ and $\tilde{\Psi}$ are connected via Eq.(27).

Since the connection between Ψ and $\tilde{\Psi}$ is not unitary, it follows that: if the solution $\tilde{\Psi}$ of Eq.(30) is normalized, the solution Ψ after transformation, i.e. the solution of the log NLSE without the term $\gamma < S_C >$, is not normalized. So, for normalization purposes, $\gamma < S_C >$ has to be subtracted from the rhs of the equation for Ψ, thus leading to the NLSE (23).

In Fig. 1 the connection between the different levels of description, classical (left) as well as quantum mechanical, is shown again schematically.

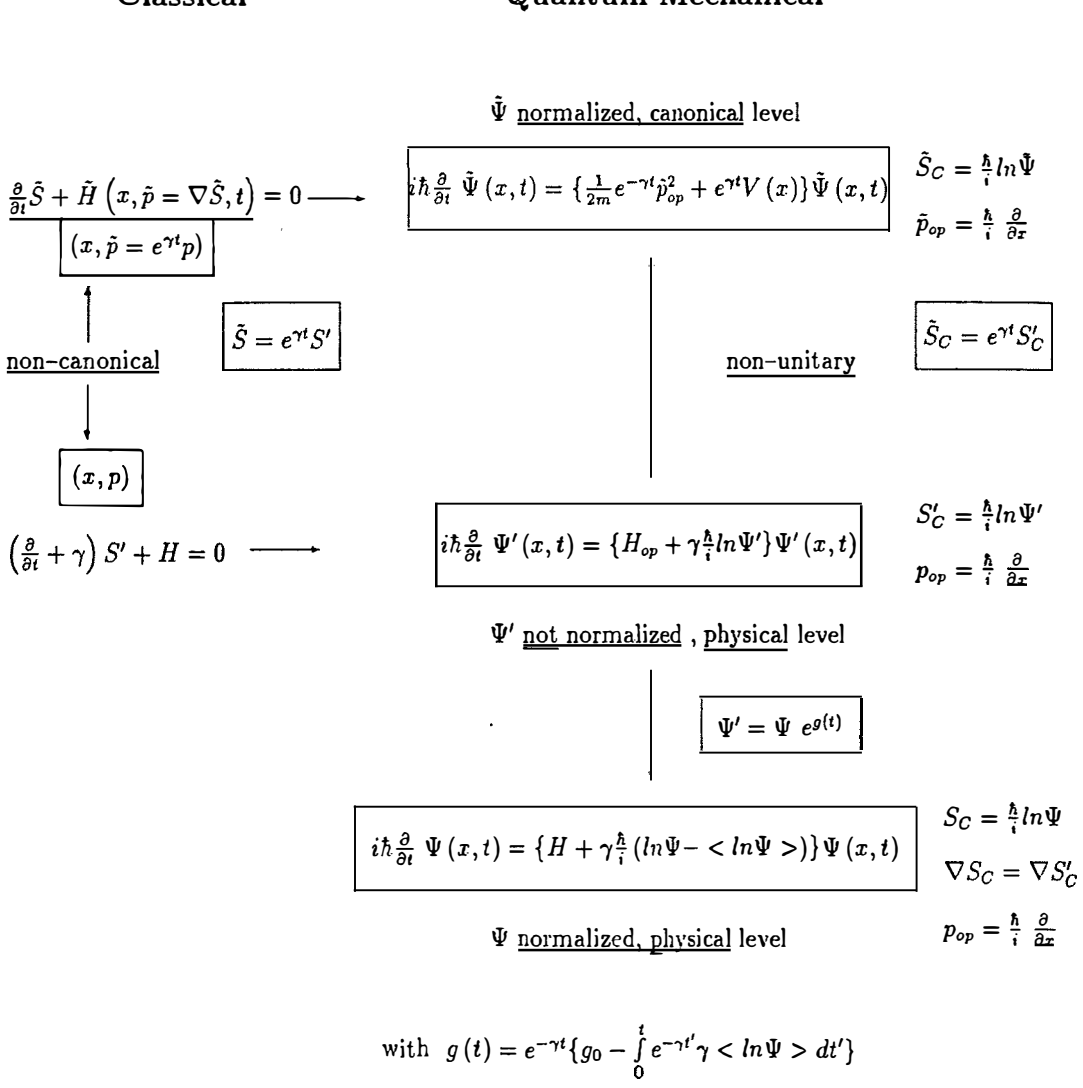
Classical
Quantum Mechanical
$\tilde{\Psi}$ normalized, canonical level
$\frac{\partial}{\partial t}\tilde{S} + \tilde{H}\left(x, \tilde{p} = \nabla\tilde{S}, t\right) = 0$
$(x, \tilde{p} = e^{\gamma t}p)$
$i\hbar\frac{\partial}{\partial t}\tilde{\Psi}(x,t) = \{\frac{1}{2m}e^{-\gamma t}\tilde{p}_{op}^2 + e^{\gamma t}V(x)\}\tilde{\Psi}(x,t)$
$\tilde{S}_C = \frac{\hbar}{i}ln\tilde{\Psi}$
$\tilde{p}_{op} = \frac{\hbar}{i}\frac{\partial}{\partial x}$
non-canonical
$\tilde{S} = e^{\gamma t}S'$
non-unitary
$\tilde{S}_C = e^{\gamma t}S'_C$
(x, p)
$\left(\frac{\partial}{\partial t} + \gamma\right)S' + H = 0$
$i\hbar\frac{\partial}{\partial t}\Psi'(x,t) = \{H_{op} + \gamma\frac{\hbar}{i}ln\Psi'\}\Psi'(x,t)$
$S'_C = \frac{\hbar}{i}ln\Psi'$
$p_{op} = \frac{\hbar}{i}\frac{\partial}{\partial x}$
Ψ' not normalized , physical level
$\Psi' = \Psi\ e^{g(t)}$
$i\hbar\frac{\partial}{\partial t}\Psi(x,t) = \{H + \gamma\frac{\hbar}{i}(ln\Psi - < ln\Psi >)\}\Psi(x,t)$
$S_C = \frac{\hbar}{i}ln\Psi$
$\nabla S_C = \nabla S'_C$
$p_{op} = \frac{\hbar}{i}\frac{\partial}{\partial x}$
Ψ normalized, physical level
with $g(t) = e^{-\gamma t}\{g_0 - \int_0^t e^{-\gamma t'}\gamma < ln\Psi > dt'\}$

Fig. 1: Connections between the canonical and the physical level in classical as well as in quantum mechanics.

Considering effective Hamiltonians for dissipative systems, one has to distinguish between two levels of description: 1) the physical level with physical coordinate x and kinetic momentum p (and wave function $\Psi(x,t)$), and 2) the canonical level with canonical coordinate $\tilde{x}$ (which in our example is identical with the physical coordinate x) and canonical momentum $\tilde{p}$.

On the physical level, these dissipative systems cannot be described by the canonical formalism (and probably also not by a linear effective Hamiltonian operator). However, via a non-canonical transformation (connected with a non-unitary transformation of the wave function), a level can be reached where the description within the canonical formalism can be possible.

6. Uncertainty Products in Canonical and Physical Descriptions

As an example it shall be shown that the apparent violation of the uncertainty principle vanishes, if operators *and* wave functions are transformed consistently. For this purpose we consider exact analytic Gaussian wave packet (WP) solutions of the damped HO. On the canonical level, i.e. where the CK Hamiltonian is applied, the WP $\tilde{\Psi}_{CK}(x,t)$ is proportional to

$$\tilde{\Psi}_{CK}(x,t) \;\propto\; \exp\{i\tilde{y}\,(x- < x > (t))^2\} \quad , \tag{31}$$

where $\tilde{y}(t) = \tilde{y}_R(t) + i\tilde{y}_I(t)$ is complex and $< x >$ is the mean value of position.

Inserting $\tilde{\Psi}_{CK}(x,t)$ in Eq.(30) shows that $< x > (t)$ fulfills the classical equation of motion (2), including friction. The mean square deviation of position is inversely proportional to the imaginary part of $y(t)$,

$$\left(\overline{\Delta x^2}\right)_{CK} = < x^2 >_{CK} - < x >^2_{CK} = \frac{1}{4\tilde{y}_I} \quad , \tag{32}$$

where the subscript CK indicates that the mean values are calculated using $\tilde{\Psi}_{CK}$, i.e. $< \ldots >_{CK} = \int \tilde{\Psi}^*_{CK} \ldots \tilde{\Psi}_{CK} dx$. Similarly, the fluctuation of the *canonical* momentum is given by

$$\left(\overline{\Delta \tilde{p}^2_{op}}\right)_{CK} = < \tilde{p}^2_{op} >_{CK} - < \tilde{p}_{op} >^2_{CK} = \hbar^2 \left(\frac{\tilde{y}_R^2 + \tilde{y}_I^2}{\tilde{y}_I}\right) \quad , \tag{33}$$

hence the uncertainty product

$$U_{CK} = \left(\overline{\Delta x^2}\right)_{CK} \left(\overline{\Delta \tilde{p}_{op}^2}\right)_{CK} = \frac{\hbar^2}{4}\{1 + \left(\frac{\tilde{y}_R}{\tilde{y}_I}\right)^2\} \geq \frac{\hbar^2}{4} \qquad (34)$$

obviously does not violate Heisenberg's principle.

The violation seems to occur if the canonical momentum operator $\tilde{p}_{op} = \frac{\hbar}{i}\frac{\partial}{\partial x}$ is replaced by the kinetic momentum, according to $p_{op} = e^{-\gamma t}\tilde{p}_{op}$, and the momentum fluctuation is calculated using the *same* WPs $\tilde{\Psi}_{CK}$, as used for $\tilde{p}_{op}$, i.e. $\left(\overline{\Delta p_{op}^2}\right)_{CK} = e^{-2\gamma t}\left(\overline{\Delta \tilde{p}_{op}^2}\right)_{CK}$. However, the operator p_{op} is not defined on the space to which $\tilde{\Psi}_{CK}$ belongs, but on the physical space. Therefore, to be consistent, if the operators are transformed, the WPs have to be transformed accordingly. The WPs which apply to the physical level are, as shown above, the solutions of the log NLSE (23). These WPs can be written in a form equivalent to (31), but $\tilde{y}$ has to be replaced (because of Eq.(27)) by $y(t) = e^{-\gamma t}\tilde{y}(t)$. The fluctuations of position and *kinetic* momentum, calculated with $\Psi_{NL}(x,t)$, are now given by

$$\left(\overline{\Delta x^2}\right)_{NL} = \frac{1}{4y_I} = e^{\gamma t}\frac{1}{4\tilde{y}_I} = e^{\gamma t}\left(\overline{\Delta x^2}\right)_{CK} \qquad (35)$$

$$\left(\overline{\Delta p_{op}^2}\right)_{NL} = \hbar^2\left(\frac{y_R^2 + y_I^2}{y_I}\right) = e^{-\gamma t}\left(\frac{\tilde{y}_R^2 + \tilde{y}_I^2}{\tilde{y}_I}\right) = e^{-\gamma t}\left(\overline{\Delta \tilde{p}_{op}^2}\right)_{CK} . \qquad (36)$$

So, the uncertainty product does not violate Heisenberg's principle,

$$U_{NL} = \frac{\hbar^2}{4}\{1 + \left(\frac{y_R}{y_I}\right)^2\} = U_{CK} \geq \frac{\hbar^2}{4} , \qquad (37)$$

but is identical with the one on the canonical level, as only the ratio of y_R and y_I occurs.

7. Connections with Hadronic Mechanics

In hadronic mechanics a generalization of Schrödinger's quantization method, based on the classical HJ-theory, is given by the so-called isoquantization, using the following mapping of the isoaction $S\prime$:

$$\hat{S}(x,t) \rightarrow -i\hbar\,\hat{I}\,\ell n\hat{\Psi}(x,t) \qquad (38)$$

with the hermitean isounit $\hat{I} = T^{-1}$. (For details, see [1] §2.) Particularly for irreversible systems, this leads to the so-called genoquantization, where two (non-hermitean) units and two actions are necessary (one forward and one backward in time). The quantization method uses the mapping

$$\hat{S}^{>}(x,t) \to -i\hbar\, \hat{I}^{>}\, \ell n \hat{\Psi}^{>}(x,t) \tag{39}$$

with the non-hermitean genounit $\hat{I}^{>} = R = \left(^{<}\hat{I}\right)^{+}$. The resulting Schrödinger-admissible (or geno-Schrödinger) equation for forward in time is

$$\begin{aligned} i\hbar\, \hat{I}^{>} \frac{\partial}{\partial x} \hat{\Psi}^{>}(x,t) &= H^{eff}\, R\, \hat{\Psi}^{>}(x,t) \\ &= \{H - i\hbar \left(\frac{\partial^{>}}{\partial t} \hat{I}^{>}\right) T^{>} \ell n \hat{\Psi}^{>}\} \hat{\Psi}^{>} \quad . \end{aligned} \tag{40}$$

Using the relations

$$\Psi = R\, \hat{\Psi}^{>} \quad , \tag{41}$$

$$-i\hbar \frac{\gamma}{2} = -i\hbar \left(\frac{\partial^{>}}{\partial t} \hat{I}^{>}\right) T^{>} \quad , \tag{42}$$

$$i\hbar \frac{\gamma}{2} < \ell n \Psi > = -i\hbar \left(\frac{\partial^{>}}{\partial t} \hat{I}^{>}\right) T^{>} \ell n \hat{I}^{>} \quad , \tag{43}$$

the rhs of Eq.(40) assumes the structure of the log NLSE, i.e.

$$rhs = \{-\frac{\hbar^2}{2m} \frac{\partial^2}{\partial x^2} + V(x) + \gamma \frac{\hbar}{i} (\ell n \Psi - < \ell n \Psi >)\} \Psi(x,t) \quad . \tag{44}$$

The main difference between Eq.(40) and the NLSE (23) is that the former is defined on genofields, genospaces, etc., while the latter is defined on conventional fields, carrier spaces, etc.. (For further details, see [1].)

In this sense, the transition from the log NLSE (23) to the linear Eq.(30) represents an example for isolinearization, or here, to be more precise, genolinearization. Therefore, the transformed functions $\tilde{\Psi}$ belong to a genotopic space and not to the conventional space, to which Ψ_{NL} belongs. The problems in the CK approach are based on the fact that the occurring wave functions are interpreted in the conventional way instead of the genotopic way.

8. Conclusions

In conclusion, it can be stated: the many-body problem of a system dissipating energy due to contact with an environment can, at least in certain cases, be reduced to a description with the help of an effective Hamiltonian for the system of interest. This Hamiltonian can be explicitly time-dependent, like the one of CK, allowing canonical quantization to yield a *linear* effective Hamiltonian operator. In this case, the *canonical variables* are connected with the *physical* ones, classically, via a *non-canonical transformation.* Consequently, the wave functions which belong to the domain of definition of the canonical operators are connected with the wave functions of the physical operators via a *non-unitary transformation.* An equivalent description can be achieved by directly using the conventional operators corresponding to the *physical variables* and the respective wave functions. This advantage has as a consequence the disadvantage of the corresponding Hamiltonian operator being *nonlinear.* In any case, both descriptions do not yield unphysical results if operators *and* wave functions are both properly considered on the same level, either canonical or physical. A more detailed discussion will be given in forthcoming publications.

Acknowledgements

The Author would like to thank Professor R.J. Jelitto for his support of, and interest in this work and Professor R.M. Santilli for electing me as member of the Istituto per la Ricerca di Base (IRB), inviting me to participate in the IRB International Workshops 1995 and for stimulating discussions.

References

[1] R.M. Santilli, "Elements of Hadronic Mechanics, Vol. II", Naukova Dumka Publishers, Kiev (1994).

[2] I. Prigogine, "From Being to Becoming - Time and Complexity in Physical Sciences", Piper, München (1979), in German.

[3] A.O. Caldeira and A.J. Leggett, Ann. Phys. (N.Y.) **149**, 374 (1983); ibid **153**, 445(E) (1983); Physica **A 121**, 587 (1983).

[4] G.W. Ford, J.T. Lewis, and R.F. O'Connell, Phys. Rev. A**37**, 4419 (1988).

[5] A. Davidson, Phys. Rev. A**41**, 3395 (1990).

[6] R.W. Hasse, J. Math. Phys. **16**, 2005 (1975).

[7] P. Caldirola, Nuovo Cim. **18**, 393 (1941).

[8] E. Kanai, Progr. Theor. Phys. **3**, 440 (1948).

[9] D. Schuch, Int. J. Quantum Chem., Quantum Chem. Symp. **24**, 767 (1990).

[10] W.E. Brittin, Phys. Rev. **77**, 396 (1950).

[11] J.R. Ray, Lett. Nouvo Cim. **25**, 47 (1979).

[12] D.M. Greenberger, J. Math. Phys. **20**, 762 (1979).

[13] I.R. Svin'in, Teor. Mat. Fiz. **27**, 270 (1976).

[14] J. Messer, Acta Phys. Austriaca **50**, 75 (1979).

[15] P. Caldirola, Nouvo Cim. **77**, 241 (1983).

[16] H. Dekker, Phys. Rep. **80**, 1 (1981).

[17] L.H. Yu and C.P. Sun, Phys. Rev. A**49**, 592 (1994).

[18] C.P. Sun and L.H. Yu, Phys. Rev. A**51**, 1845 (1995).

[19] M.D. Kostin, J. Chem. Phys. **57**, 3589 (1972).

[20] K. Albrecht, Phys. Lett. **56 B**, 127 (1975).

[21] N. Gisin, J, Phys. A: Math. Gen. **14**, 2259 (1981).

[22] E. Schrödinger, Ann. d. Phys. **79**, 361 (1926).

[23] D. Schuch, K.-M. Chung, and H. Hartmann, J. Math. Phys. **24**, 1652 (1983), ibid. **25**, 3086 (1984).

[24] D. Schuch and K.-M. Chung, Int. J. Quantum Chem. **29**, 1561 (1986).

[25] E. Madelung, "Die mathematischen Hilfsmittel des Physikers", p.432, Springer, Berlin (1950).

[26] B. Mrowka, Z. Phys. **130**, 164 (1951).

[27] H.-D. Doebner and G.A. Goldin, Phys. Lett. **A 162**, 397 (1992).

[28] M. Razavy, Z. Phys. **B26**, 201 (1977).

[29] H.-J. Wagner, Z. Phys. **B95**, 261 (1994).

HADRONIC JOURNAL 49, 113 - 119 (2026)
DOI 10.29083/HJ.49.01.2026/SC113

EXPERIMENTAL VERIFICATION OF SANTILLI'S CLEAN, SUBNUCLEAR, HADRONIC ENERGY

N. F. Tsagas, A. Mystakidis, G. Bakos, L. Seftelis,
D. Koukoulis and S. Trassanidis
Laboratory of Nuclear Technology
Department of Electrical Engineering
Democritus University of Thrace
GR-67100 Xanthi, Greece

Abstract

The structure of the nucleus and its constituents still presents a challenge to both theoretical and experimental physicists. This paper deals mainly with the an experimental attempt for the verification of the new theory for neutron structure and its stimulated decay recently proposed by R. M. Santilli which would imply a new, clean, subnuclear energy. The experiment is carried out by the Laboratory of Nuclear Technology at the University of Thrace, Xanthi, Greece.

Reprinted from: Gill, Tepper L., Editor, "*New Frontiers in Hadronic Mechanics*" Hadronic Press, ISBN 1-57485-016-4, p. 281-287 (1996)

Copyright © 2026 by Hadronic Press, Inc., Palm Harbor, FL 34684, USA

1.THE MAIN THEORETICAL PREDICTION OF HADRONIC MECHANICS

Although according to the established view for the neutron it is not permissible to present it as a bounded state of a proton and an electron, a relative new generalisation of non relativistic and relativistic quantum mechanics, that was initiated by Prof. R. M. Santilli, allows such a neutron representation [1-2].

In that case an expected property of the neutron is its stimulated decay via scattering with gamma ray photons, $\hat{\gamma}$, of a particular resonating frequency $\hat{\omega}$ suitable to excite the electron, according to the reaction:

$$\hat{\gamma} + n \rightarrow p^{+} + e^{-} + \nu$$

The above reaction can take place even if the neutron is not isolated and considered as a member of a nuclear structure i.e. an (A,Z) isotope. In that case the reaction can be written in the following general form.:

$$\hat{\gamma}' + (A,Z) \rightarrow (A,Z+1) + e^{-} + \nu \qquad (1)$$

The resonating frequency of the gamma ray photons, $\hat{\gamma}'$, is different from the resonating frequency for the isolated case.

In most cases the (A,Z) $\longrightarrow$ (A,Z+1) transmutation releases energy as the neutron is heavier than the proton and therefore the atomic weight of the nucleus (A,Z) is generally bigger than that of (A,Z+1).

A convenient element for experimental verification of the above transmutations seems to be Zn-70, which occurs in natural Zn with an atomic percent abundance of 0.6%.

According to the general reaction (1), if a proper resonating frequency of gamma ray photons is used to bombard the Zn-70, the following equation holds:

$$\hat{\gamma}' + {}_{30}Zn^{70} \rightarrow {}_{31}Ga^{70} + e^{-} + \nu \qquad (2)$$

The products of this reaction are Ga-70 plus the expected electron and neutrino. Gallium 70 is a radioactive isotope that decays via beta minus (with meanlife of 21.1 minutes) to Ge-70 that is stable. So the final product Ge-70 is a stable element with atomic weight 69.924, thus smaller than the atomic weight of the initial element Zn-70 which is 69.925.

Hadronic Mechanics theory predicts that the electron from the neutron has 80% probability to have a 1.66 + 1.294 =2.954 MeV energy if gamma ray photons with energy of 1.294 MeV (Hadronic Mechanics calculations) are used for the bombardment and the following excitation. In the case that photons with energy

0.511 MeV are used (Quantum Mechanics calculations), the above energy becomes 1.66 + 0.511 = 2.171 MeV.

2. PROPOSED EXPERIMENTAL SET UP

For the investigation of the reaction (2), the following experiment is proposed :
The main idea is to bombard a Zn-70 foil with gamma ray photons of the proper energy, 1.294 or 0.511 MeV (at first place), and then try to detect electrons with energies 2.954 or 2.171 MeV respectively.

Schematically this idea can be presented as follows:

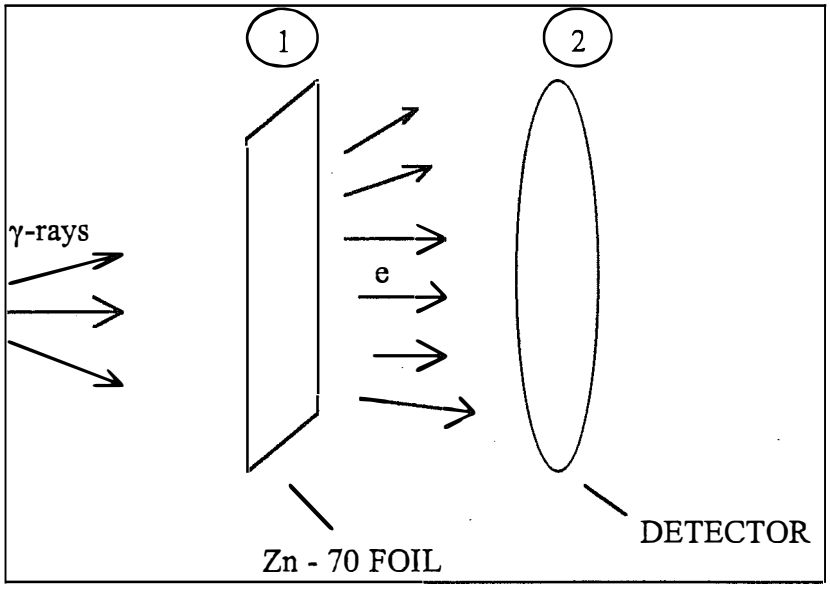

FIG.1

Two main procedures are taking place during such an experiment :

1. Interaction of gamma ray photons with Zn-70 foil and

2. Interaction of the produced electrons with detector's matter.

Concerning the first procedure the predominant mode of this interaction is Compton scattering.

The result of a Compton scattering interaction is the creation of a recoil electron and a scattered gamma ray photon, with the energy between the two dependent on the scattered angle. Under normal conditions a continuum of energies

can be transferred to the Compton electron, ranging from zero up to a maximum energy which can be easily calculated [3, p.290].

If gamma ray photons of 0.511 or 1.294 MeV are used, the maximum energies of Compton electrons will be :

0.340 MeV for hν=0.511 MeV
1.081 MeV for hν=1.294 MeV

So not only the expected neutron electrons will be produced (of course under the condition that the transmutation is going to take place) but also Compton electrons. As it can be noticed the Compton electrons will have energies that can easily be discriminated from the energies of the neutron electrons (2.954 MeV or 1.271 MeV for the Zn-70 case).

The second procedure is leading to the detection of the expected electrons. While the produced electrons are travelling through detector's active area they lose energy and are deflected from their original course: they are scattered. For the energies that we are interested in, the deflection of the electrons is due almost entirely to the elastic collisions with the atomic nuclei, while the energy loss, except that due to the breamsstrahlung, which is practically negligible, results from the interaction with the atomic electrons [4].

In order to detect the neutron electrons, it should be ensured that detector's thickness is sufficient for the complete absorption of these electrons. However there is a small possibility for complete absorption of an electron even if detector's depth is not enough for stopping the electron. This is due to the longer path length which can be caused by large angle and multiple scattering [5].

On the other hand, electrons are not the only events that will be presented to the detector. As the Zing foil must be thin enough to allow the produced neutron electrons to exit (or in other words to avoid self absorption), there will also be gamma ray photons that they won't be absorbed. A portion of these photons will reach the detector and Comtpton electrons together with few photoelectrons will be created. Photoelectrons have energies almost equal to the energy of the incident photons, so greater than the energy of Compton electrons. Even if a photoelectron is detected its energy is much smaller than the energy of the expected neutron electrons and therefore its presence is not a problem.

Finally, the electrons from beta decay of the, probably, produced Ga-70 should be taken into account.. These electrons have a continuous energy spectrum, (as it happens to every beta minus decay), and the endpoint energy of this spectrum is 1.66 MeV, so they can also be easily discriminated from the neutron electrons.

Therefore, at least in principle, an experiment based on these ideas could be valid.

There are three main points that someone is obliged to focus on, in order to conduct an experiment based on the previous ideas:

a) the sources used in order to have the desirable gamma ray photon energies,

b) the Zn foil characteristics and

c) the detector and counting system.

As it was mentioned before according to professor's Santilli calculations, gamma ray photons with energies 0.511 and 1.294 MeV are going to be used in the first place (sub multiples of these frequencies can also be used in a later stage). The 0.511 MeV energy is very common, due to annihilation process. Our laboratory has finally concluded that Na-22, with meanlife 2.502 y, is the preferable isotope for the required 0.511 MeV gamma ray photon energy, while Eu-152 with meanlife 13.33 y and gamma ray photon with 1.299 MeV energy is the preferable isotope for the 1.294 MeV energy.

The next consideration involves the Zn-70 foil that is going to be used. A compromise has to be done in the choice of foil's thickness. On the one hand a thick enough foil has to be used in order the necessary active material to be achieved, on the other hand self absorption must also be avoided. A main problem seems to be that Zn-70 is a very expensive isotope. An alternative solution is to use natural zing, but in that case the active material is minimised. By this time a 1.25 mm thick natural zing foil is used.

In future Mo(100,42) or Li(6,3) can also be used for the provment of the principle of Hadronic Transmutations, as there are similar reactions with the reaction (2) for these two elements.

The detector and the counting system is the third main point. After an extensive research, it was concluded that a semiconductor silicon detector appears to be the best solution. A silicon semiconductor detector whose active thickness exceeds the range of electrons of interest (in silicon), makes a very suitable spectrometer. Ion implanted passivated detectors are very reliable instruments with detection efficiency in electrons nearly 100% [6]. Their active thickness can reach 6mm, which means that up to 3 MeV electrons can be detected [7]. The detector used in our laboratory is an 1 mm active thickness ion implanted passivated detector with active area 100 mm^2 with energy resolution in beta particles 25 KeV. The detector is connected to a charge sensitive preamplifier and then to an amplifier and a multi channel analyser. A scheme of the counting system is given to figure 2.

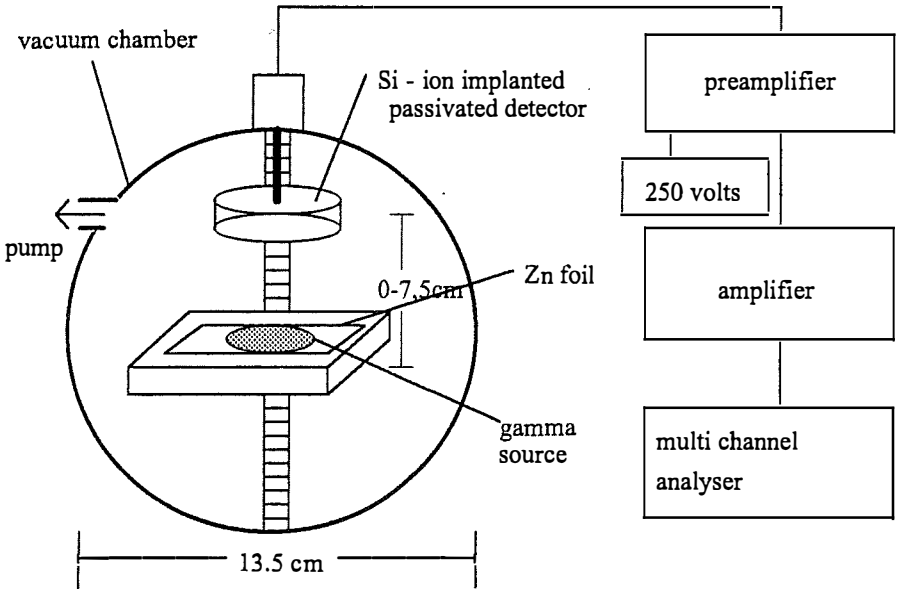

FIG.2

Every electron that enters the detector creates electron-hole pairs that are collected by a 250 V electric field, giving rise to a pulse whose height is proportional to the energy of the incident electron. After amplification the signal is driven to a 1024 channel computerised multi channel analyser. A full energy spectrum of the incident to the detector electrons can be taken. If counts appear to channels that correspond to the energies of the expected neutron electrons this could be sufficient to establish the principle of the Hadronic transmutation.

3. COMMENTS, SUGGESTIONS

A main problem of the experiment at present is that natural zing is used and therefore the expected events are only few per month (1-2). This number eliminates the efficiency of the experiment as the background contribution, due to intrinsic properties of the detector, in the energy range that we are interested in, is in the order of 2-3 counts/day [8].

Therefore the following points should be considered in order to maximise the efficiency of the experiment :

1. An exact theoretical calculation of the expected events by taking into account the quantity of the "active" material (Zn-70) and the activity of the gamma source.

2. The use of pure Zn-70.

3. The use of a thicker detector.

Due to the above facts the results taken in our laboratory by this time, can only be considered as preliminary. We believe that by realising the above points we will soon be in position to give reliable results.

Acknowledgement-The authors would like to thank Prof. R. M. Santilli for his continuous advice and valuable suggestions.

REFERENCES

1. R. M. Santilli, Hadronic Journal **17**, 311-348 (1994), R. M. Santilli, Chinese J. Syst. Eng. & Electr. **6**, issue no.4 (1995).

2. R. M. Santilli, Elements of Hadronic Mechanics, Vol. I, II, III, Academy of Sciences of Ukraine, Kiev.

3. Glenn F. Knoll, Radiation Detection and Measurement (Wiley, New York, 1979).

4. K. Siegbahn, Alpha-, Beta-, Gamma-Ray Spectroscopy (North-Holland, Amsterdam, 1966).

5. Th. Frommfold, W. Arnold, H. Friedrichs, R. Gobel, R. D. Heil, U. Kneissl, U. Seemann and F. Steiper, Nucl. Inst. and Meth. in Physics Research A310(1991)657-664.

6. M. J. Berger, S. M. Seltzer, S. E. Chappell, J. C. Huumphreys and J. W. Motz, Nucl. Instr. and Meth. 69 (1969) 181.

7. J. C. Blanknship IRE Trans. Vol. NS-7, Nos. 2-3, pp 190-195, June 1960.

8. Silicon charged particle radiation detector's instruction manual. EG & G Ortec, 100 Midland Road. Oak Ridge.

ISSN: 0162-5519

Established in 1978 by Prof. R. M. Santilli at Harvard University Hadronic Journal and Algebras, Groups and Geometries have been regularly published since 1978 without publication charges and are among the few remaining independent refereed journals.

This Journal publishes advances research papers and Ph. D. theses in any field of mathematics without publication charges.

For subscription, format and any other information please visit the website http://www.hadronicpress.com

HADRONIC PRESS INC.
35246 U. S. 19 North Suite 215
Palm Harbor, FL 34684, U.S.A.
http://www.hadronicpress.com
Email: info@hadronicpress.com
Phone: +1-727-946-0427

HADRONIC JOURNAL Volume 49, Number 1, March 2026

H/P HADRONIC PRESS, INC.